ENHANCED GEOTHERMAL ENERGY AND COGENERATION: DESIGN, TECHNOLOGY AND ECONOMICS

By

Shoa-Ollah Ehsani

B.Eng. Chemical Engineering
McGill University, Montreal, 1992

Submitted to the Engineering Systems Division and
the Department of Civil and Environmental Engineering
in Partial Fulfillment of the Requirements for the Degrees of

Master of Science in Technology and Policy
And
Master of Science in Civil and Environmental Engineering

At the
Massachusetts Institute of Technology
February 2003

Signature of Author.....
Technology and Policy Program, Engineering Systems Division
January, 17, 2002

Certified by.....
Jefferson W. Tester
H.P. Meissner Professor of Chemical Engineering
Thesis Supervisor

Certified by.....
H.J. Herzog
Research Engineer, Laboratory for Energy and the Environment

Certified by.....
David H. Marks
Morton & Claire Goulder Professor of Engineering Systems and Civil & Environmental Engineering
Director, Laboratory for Energy and the Environment
Thesis reader

Accepted by.....
Daniel Hastings
Professor of Aeronautics and Astronautics and Engineering Systems
Director, Technology and Policy Program
Chairman, Committee for Graduate Student

Accepted by.....
Oral Buyukozturk
Professor of Civil & Environmental Engineering
Chairman, Departmental Committee for Graduate Student

To My Parents and Grandparents as a Token of Love and Respect

ENHANCED GEOTHERMAL ENERGY AND COGENERATION: DESIGN, ECONOMICS AND TECHNOLOGY

by
Shoa-Ollah Ehsani

Submitted to the Engineering Systems Division & the Department of Civil and Environmental Engineering
on January 16, 2003 in Partial Fulfillment of the Requirements for the Degrees of
Master of Science in Technology and Policy and
Master of Science in Civil and Environmental Engineering

ABSTRACT

The search for and the development of new sources of energy continue to gather importance into the 21st century. One of the options at hand is mining heat from the earth's crust. The U.S. Department of Energy has supported research into Enhanced Geothermal Systems in Hot Dry Rock (HDR) since the mid seventies. Advances in drilling technology, reservoir management and power conversion cycles have all contributed to the further development of HDR geothermal energy schemes.

Apart from outlining and reviewing some of the specific characteristics of Enhanced Geothermal Energy Systems, this thesis investigates the possibility of using HDR technology for commercial scale combined heat and electric power applications. This is carried out through cogenerative design of current HDR electric power plant options with direct process heat capacity required in industrial production today. The MIT EGS Simulator was modified to accommodate cogeneration to assess the success of such designs in three separate, industrial case studies.

Overall system busbar cost for electricity produced and various thermodynamic efficiency measures will be used as metrics to access the effectiveness of cogeneration design in HDR power generation. Lastly, this research is used to qualitatively evaluate the performance of other low-temperature electric-power and direct use cogeneration designs; one of the important aspects in a move towards increased global energy efficiency.

Thesis Supervisor: Jefferson W. Tester
H.P. Meissner Professor of Chemical Engineering

ACKNOWLEDGMENT

My time at MIT has been instrumental to the reawakening of the joy of scientific learning and research, an aspect of my life that had been dormant for the decade before. Much of this is due to the brilliant and enthusiastic Professors and mentors at MIT and an able student body.

I would like to take this opportunity to thank the MIT staff as a whole and in particular my thesis advisors, Jeff Tester and Howard Herzog for their infinite patience, interest and encouragement; the US DOE for providing the funds to support part of this research into new geothermal energy opportunities.

I'd like to thank my parents Susan and Abbas for their never-ending support and love in all my ventures, academic and otherwise, and for having nurtured the love of learning in me. My siblings, Mehrdad and Ladan for their humor, faith and encouragement.

I'd also like to thank the Almighty for having bestowed me with a sound mind and the opportunity of studying at an institution of higher learning; a privilege that many of the more capable inhabitants of the planet do without.

"Knowledge is as wings to man's life, and a ladder for his ascent. Its acquisition is incumbent upon everyone..... In truth, knowledge is a véritable treasure for man, and a source of glory, of bounty, of joy, of exaltation, of cheer and gladness unto him. Thus hath the Tongue of Grandeur spoken in this Most Great Prison." -- Bahá'u'lláh

TABLE OF CONTENTS

CHAPTER 1: THESIS OBJECTIVES AND OVERVIEW 9

CHAPTER 2: INTRODUCTION TO GEOTHERMAL ENERGY 11

2.1 Introduction and History of Use of Geothermal Energy 11
2.2 Geothermal Resource Types 13
2.2.1 Hydrothermal Resources 13
2.2.2 Magma 14
2.2.3 Geopressured Resources 15
2.2.4 Hot Dry Rock (HDR) 16
2.3 Geothermal Resource Base and Distribution 18
2.4 Cogeneration 20
2.5 Sustainability and Environmental Characteristics of Geothermal Energy 21
2.6 The Growth of the Geothermal Industry 25

CHAPTER 3: TECHNICAL ASPECTS OF GEOTHERMAL ENERGY AND POWER CONVERSION 27

3.1 Resource Exploration 27
3.2 Geothermal Drilling 29
3.3 Creating Permeability: Rock Fracturing 31
3.4 Energy Conversion Technologies 32
3.4.1 Direct Use 32
3.4.2 Single and Multistage Flash Systems 33
3.4.3 Binary Systems 36
3.4.4 The Stirling Cycle 37
3.4.5 Total Flow Concepts 38
3.4.6 Hybrid Cycles 39
3.4.7 Combined Cycles 40
3.5 Turbines 41
3.6 Thermal Drawdown 43

CHAPTER 4: ECONOMIC ASPECTS OF GEOTHERMAL ENERGY SYSTEMS 45

4.1 Introduction 45
4.2 HDR Costs by Component 46
4.1.1 Exploration & Land Cost 47
4.1.2 Drilling and Simulation Costs 48
4.1.3 Power Plant Equipment Cost 50
4.3 Competition and Finance 52
4.4 Inflation and Cost Indicies 56

CHAPTER 5: HDR COGENERATION CASE STUDIES 61

5.1 Introduction to Case Studies 61
5.2 Tropical Fish Farming in California 62
5.2.1 Fish Farm's Heating Requirements 64
5.2.2 Design of Power Plant 67
5.2.3 Cost Savings from Fish Farm Cogeneration 74
5.2.4 EGS Modeling and Optimization 77
5.2.5 Results of Analysis 78
5.3 Pulp & Paper Mill in New Zealand 83
5.31 The Electrical and Geothermal Industries in New Zealand 84
5.3.2 Steam Requirements at the Fletcher Paper Mill, Kawerau, NZ 86
5.3.3 EGS Modeling and Optimization 87
5.3.4 Cost Savings from Pulp & Paper Cogeneration 90
5.3.5 Results and Analysis 92
5.4 District Heating in Macedonia 98
5.4.1 The Geothermal Field at Kocani and District Heating Requirements 99
5.4.2 Cost Savings from District Heating Cogeneration 103
5.4.3 EGS Modeling and Optimization 104
5.4.4 Results and Analysis 105
5.5 Multiple Case Analysis 109

CHAPTER 6: CONCLUSION AND RECOMMENDATIONS 112

REFERENCES 114

APPENDIX 117

By Chapter:

Chapter 4 118
Chapter 5 118-130
Chapter 6 130

LIST OF FIGURES

Figure 2.1	Geothermal heat transfer and resource development	12
Figure 2.2	Hot Dry Rock concept of Heat Mining	17
Figure 2.3	World Resource base estimate	18
Figure 2.4	Geothermal Resource by Region	19
Figure 2.5	Growth of installed geothermal capacity in the world since 1980	25
Figure 3.1	Double-Flash Power Conversion Scheme	34
Figure 3.2	Organic Rankine Cycle Power Conversion Scheme	37
Figure 3.3	Hybrid Organic Rankine Cycle Power Conversion Scheme	39
Figure 3.4	Approximate Multistage Steam Turbine Efficiency	42
Figure 3.5	Reservoir Temperature Drop Due to Drawdown	45
Figure 4.1	Generalized effect of production temperature on electricity busbar cost	47
Figure 4.2	Projected HDR individual well drilling and completion costs	49
Figure 4.3	Initial Capital investment cost of power plants for different technologies	51
Figure 4.4	MIT Composite Plant Cost Index, 1965-2002	60
Figure 5.1	Normal Annual Temperatures for Imperial Valley, CA	66
Figure 5.2	Design Schematic of a Dual-Flash 600 °F Geothermal Power Plant	76
Figure 5.3	Electricity Busbar Costs for Fish Farm Cogeneration Case	80
Figure 5.4	Map of New Zealand showing Kawerau	85
Figure 5.5	Electricity Busbar Costs for Pulp & Paper Cogeneration Case	94
Figure 5.6	Diagram of Kocani Geothermal District Heating Scheme	102
Figure 5.7	Electricity Busbar Costs for Space Heating Cogeneration Case	107
Figure 5.8	Electricity Busbar Costs for District Heating Cogeneration Case	107
Figure 5.9	Graph of Busbar vs Cogenerative Power Showing Outlier	109
Figure 5.10	Graph of Busbar vs Cogenerative Power for all Cases Studied	110
Figure 5.11	Increase in Cycle Efficiency vs Cogenerative Power for Cases	110

LIST OF TABLES

Table 4.1	Economic Characteristics of different power technologies	54
Table 4.2	Producer Price Index- Electric Power, Pacific Region	59
Table 4.3	PPI Commodities: Fuels & related products, #2 diesel fuel	59
Table 4.4	MIT Composite Plant Cost Index	60
Table 5.1	Heat Load required for a 130-Ton Fish Farm in Imperial Valley, CA	67
Table 5.2	EGS Simulator design parameters for Fish Farm Cogeneration	78
Table 5.3	EGS Simulator Results with and without Fish Farm Cogeneration	79
Table 5.4	Thermodynamic Efficiency for Fish Farm Cogeneration Case	82
Table 5.5	Mean Air Temperatures for New Zealand's East Coast 1961-1998, °C	88
Table 5.6	EGS Simulator design parameters for Pulp & Paper Cogeneration	89
Table 5.6.1	Annual Fuel Savings Equivalent for Pulp & Paper Mill using Cogeneration	91
Table 5.6.2	NPV Fuel Savings Equivalent for Pulp & Paper Mill using Cogeneration	92
Table 5.7	EGS Simulator Results with and without Pulp & Paper Cogeneration	93
Table 5.8	Thermodynamic Efficiencies for Pulp & Paper Cogeneration Case	96
Table 5.9	Annual Energy Consumption of the Largest District Heating Systems	98
Table 5.10	Thermal Power Requirements of Kocani Distict Heating	101
Table 5.11	Thermal Power Requirements of Subunits of Kocani Space Heating	102
Table 5.11.1	Fuel Savings Equivalent for District and Space Heating Cogeneration	103
Table 5.12	EGS design parameters for District & Space Heating Cogeneration	105
Table 5.13	EGS Simulator Results with and without Space Heating Cogeneration	106
Table 5.14	EGS Simulator Results with and without District Heating Cogeneration	106
Table 5.15	Thermodynamic Efficiencies for Space Heating Cogeneration Case	108
Table 5.16	Thermodynamic Efficiencies for District Heating Cogeneration Case	108

CHAPTER 1

THESIS OBJECTIVES AND OVERVIEW

The search for new energy technologies in the late seventies and eighties as a result of the Arab oil embargo resulted in several major research and development efforts aimed at exploring ways to extract energy from Hot Dry Rock (HDR) or Enhanced Geothermal Systems (EGS), funded by the US government amongst other options(Tester, Brown, Potter, 1989). While there was a realization of the vast magnitude of a Hot Dry Rock (HDR) resource, its technical and economic viability is still in question, particularly with respect to its universal applicability in today's energy markets. Research and development of improved drilling technologies, reservoir creation and management have decreased the cost of HDR by increasing resource productivity and lowering drilling costs. Nevertheless, thirty years of research and development into HDR energy technology has yet give rise to a commercial niche (Brown, D., 1995).

This thesis is an attempt to look and perhaps further the economic viability of HDR schemes by way of plant design: namely the use of cogeneration in the production of electricity. It is hoped that the bringing together of direct heat schemes and electricity generation, the overall efficiency of the system would improve yielding a lower levelized energy cost in comparison to a scheme that produces only electricity from a HDR source.

To aid this investigation, the thesis looks at three case studies employing different grades (temperature and enthalpy) and scales of thermal power. Such direct thermal power, normally supplied via the combustion of fossil fuels, is now supplied by the geofluid stream from the HDR resource; as such there is a displacement of fossil fuels and hence an operational cost saving that is used to offset capital cost of the geothermal system.

The cogeneration cases being considered include power generation coupled with the fish farming of tilapia, a pulp and paper mill in New Zealand and lastly, a district heating scheme in Macedonia. These cogenerative uses were chosen in such a way as to investigate a broad thermal power space that is used in the respective operations. The fish farm represents a low-temperature, low-flow rate heat use, the pulp mill is an example of a high-temperature, high-flow rate load and the district heating design employed a medium-temperature fluid at high and low flow rates. All three cases represent mainstream industrial and commercial uses of direct heat.

In a narrow sense then, the questions that this thesis attempts to answer are:

1. Are there cogenarative schemes that are compatible with HDR power production technologies? If so what are these initial designs.

2. What are the financial benefits in the displacement of fossil fuel in these designs and for different grades of a HDR resource? The metric used to measure this will be the busbar cost of electricity production.

This thesis is divided into six chapters. Chapter 2 is an introduction to geothermal energy, the different grades, types and distribution, environmental and industrial growth characteristics. Chapter 3 looks at current and futuristic energy conversion schemes for geothermal energy, high-efficiency and combined cycles and steam turbine efficiencies. In Chapter 4, the economics of HDR geothermal energy are explained and explored, attention is also given to costing indices and industry inflation; the EGS Simulator that was modified and used is also introduced. The design and analysis of the three case studies that were selected to fulfill the objectives of the thesis are tackled in chapter 5. These preliminary cogenerative designs are analyzed and the benefits, if any, are communicated. Chapter 6 summarizes the findings of the thesis and discusses this author's take on cogenerational design in enhanced geothermal power production; it also includes conclusions and recommendations.

CHAPTER 2

INTRODUCTION TO GEOTHERMAL ENERGY

2.1 INTRODUCTION AND HISTORY OF USE OF GEOTHERMAL ENERGY

"Geothermal energy is the natural heat of the earth that is trapped close enough to the surface as to be extracted economically"(L.M. Edwards *et al*, 1982). This statement implies that geothermal energy is mined from the earth's crust, comprising of thin layer no more than 35 kilometers depth at its thickest point, albeit that with today's drilling technology this is limited to roughly the upper 14 km of the crust. The subsistent use of geothermal energy for cooking and bathing via natural springs and spas has been in practice for centuries, its commercial deployment however, did not occur until the early 1900s where electricity production from steam was introduced in Larderello, Italy.

Geothermal energy is distributed unevenly in the host rock and fluids found in the earth's crust. Pockets of high-grade energy, where the thermal energy concentration and rock and fluid temperatures are highest exist only in a few regions in a similar way that fossil fuels tend to be found in concentrated zones. These high-grade resources have water or steam in reservoirs relatively near the surface, typically 1 to 2 km deep. The magnitude of geothermal energy tends to be greatest along young fault and plate lines experiencing tectonics; an example would be "the Ring of Fire" in the Pacific that includes a chain of islands such as New Zealand and certain southern pacific nations that reside on a plate line; interestingly, these areas have had good, albeit limited development of their geothermal resources. Geothermal energy is attributed to two natural occurring phenomena in the earth's crust: first, the intrusion of bodies of magma at high temperature into the crust of the earth from the underlying mantle; and secondly, the radioactive decay of elemental isotopes such as potassium, uranium and thorium in the earth's crust. This heat is transferred upward into the shallower regions of the crust by the process of conduction, convection and mass transfer. Figure 2.1 illustrates these phenomena:

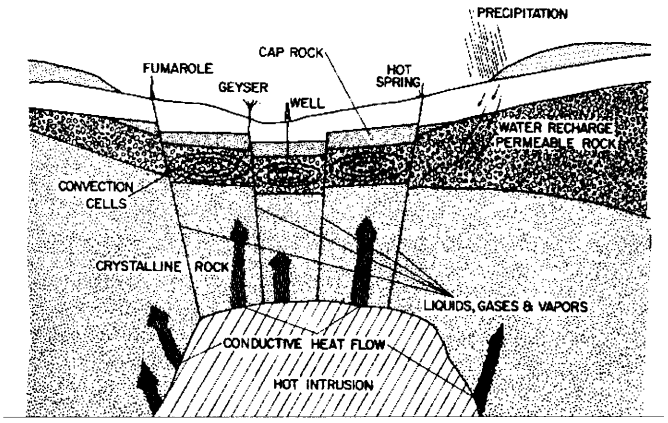

Figure 2.1 Geothermal heat transfer and resource development

Source: L.M. Edwards et al., 1982, Handbook of Geothermal Energy, Gulf Pub. Co., Chapter 2

There are various ways in which geothermal energy presents itself. Categorized in the next section, these resources have characteristics that allow further classification into hot igneous, conduction-dominated and hydrothermal systems. While the first two systems contain the most energy and are much more ubiquitous, it is the hydrothermal systems that have so far received the most attention and been in use commercially.

The quality or grade of the particular resource depends on various characteristics: first and foremost of these is the temperature of the resource or in dynamic terms, the temperature gradient (The change in temperature with depth, expressed in ^{o}C/ Km). The permeability of the rock structure that houses the resource determines to a large extent the natural production rate of the geothermal system. In fluid dominated systems, the salinity and chemical makeup of the geothermal fluid would be important aspect in operational planning, as corrosion and fouling can become an issue. Like many other energy sources, geothermal energy can only be transported efficiently for long distances via its conversion to electricity and subsequent transmission. In some cases, transporting hot water and / or steam for short distances has been used in municipal district heating systems. Chapter 3 of this thesis reviews these features in more detail.

2.2 GEOTHERMAL RESOURCE TYPES

There are four subtypes of geothermal energy: hydrothermal, magma, geopressured and hot dry rock (HDR). This thesis focuses mostly on hydrothermal and hot dry rock systems, the case studies are based exclusively on HDR systems.

2.2.1 Hydrothermal Resources

Comprised of high temperature water and /or steam, hydrothermal resources are found in a permeable, porous reservoir rock. The hot fluid is convectively circulated to the shallower regions of the rock through faults and fractures, being driven up by the buoyancy of the hot fluid through seeping colder fluid supplied from water tables and reservoirs accumulated by precipitation and rainfall.

Hydrothermal resources typically appear at depths of 1-2 kms and can contain hot aqueous fluids of up to 350 ^{o}C in temperature. The highest grade, containing steam vapor is rare; liquid-dominated resources are much more common. If in liquid form, the effluent is often flashed to produce steam or is used in the vaporization of a working fluid to operate turbines in the production electricity. Nearly all the commercial geothermal instillations in the world are of this type. There are possibilities of depleting this resource if the fluid used is not replaced or if in the longer run the surrounding conducting region cools. An example of this depletion is The Geysers in Northern California, where production rates have dropped. With depletion, a dry hydrothermal well as well as empty oil wells maybe rejuvenated by further drilling in some cases and be used in HDR heat mining.

High quality fields have been identified in several regions: Western US, Central and South America, Iceland, New Zealand, Indonesia, China and the Philippines, to name a few.

2.2.2 Magma

Magma chambers often occur by the intrusion of molten rock from deep within the crust to accessible depths of 7 kms or less (L.M. Edwards, 1982). Such protrusions occur near the surface in Hawaii's volcanoes or the Yellowstone National Park. Magma is a "hot-igneous" system as is its solidified form, hot dry rock. Because temperatures of magma range between 650 and 1200 ^{o}C, it can in principle, make for a very efficient source of electricity production. However, the extremely high temperatures pose technological barriers: current drilling technology cannot withstand such temperatures and has difficulty creating stable drilling in a plastic magma medium. The US Department of Energy (US DOE) did fund two separate phases of the Magma Energy Program in the late eighties and early nineties (Kitsou, O., 2000). Projects have been able to drill to a depth of 33 feet in stagnant surface lava in Hawaii, using a cooling jet of water that stabilized the sides of the drilled hole (the walls would revert to a plastic state if the coolant flow stops).

The extraction of useful heat from such a high temperature resource poses significant problems; consequently further government-funded initiatives in this area have been postponed. While the use of magma as an energy source is seen as a possibility, it nevertheless exhibits a high risk and is technically very challenging to harness. Other indirect magma energy schemes have been considered and if developed, could be a source of great benefit. The first of these is the production of hydrogen gas by the injection of water into hot magma containing ferrous oxide; the latter acts as a reducing agent and produces hydrogen from the water while forming a ferric oxide. Many believe that we are on the threshold of a hydrogen economy; where hydrogen would become the fuel of choice for transportation and distributed generation. The other scheme involves the use of water superheated by underwater magma at the ocean's depth; the high water pressure raises the boiling point of water resulting in a high temperature resource which may be brought to the surface using insulated pipes and the buoyancy gradient available. These schemes are challenging and costly; they have not been applied yet.

2.2.3 Geopressured Resources

As the name implies, this resource consists of brine under high pressure (4,000 to 6,000 psig)(Tanenbaum, 1999) containing dissolved methane (CH_4) gas. Often found in sedimentary rock at depths of between 3 to 6 km and temperatures ranging from 80 to 250 ^{o}C, this resource manifests thermal, mechanical and chemical energy. Drilling and completion technologies employed in the oil and gas industries may be used to access geopressured rock structure.

While the majority of the energy is held in thermal and chemical form, the great fluid pressures apart from providing a possible power source, eliminates the need for pumping the geofluid. In Hungry, the newly explored Pannonian Basin area has revealed the presence of geopressuerd resources, the best of the three wells drilled features a temperature of 190 ^{o}C at depth and pressures of 70 MPa: twice the fluid static pressure of the reservoir at its deepest point (Arpasi, Lorberer, Pap, 2000). Another advantage of the geopressured system is the low thermal conductivity of the neogene sediments casing the fluid; this results in minimal temperature drops in the fluids journey to the surface. The cascade use of this resource's different energies, to produce electricity and to heat directly, are in the planning and research stage. The processing of the brine for useful salts is also being considered. Closer to home, the US DOE's efforts have yielded fruit in the identification of geopressured fields Louisiana, Mississippi and offshore in the Gulf of Mexico.

The geopressured resource will become an attractive energy source when economical technologies to obtain useful energy from all three of its energy forms are perfected.

2.2.4 Hot Dry Rock (HDR)

Hot Dry Rock or HDR refers to geothermal resources that contain thermal energy but have very little natural permeability and consequently, minimal amounts of *in situ* fluids. HDR can be viewed as a hydrothermal system with little permeability or a hot-igneous system such as magma in solid state, governed by conduction-dominated heat transfer process because of its lack of fluid mobility. Hot Dry Rock resources are considered technically accessible for commercial exploitation technically accessible depths to 10 km and is the most prevalent and ubiquitous of all geothermal resources and ranks foremost in the magnitude of its stored energy.

The HDR resource grade is determined by its temperature gradient: the rise in temperature with increasing depth. Tester and Herzog (1990) define three grades of HDR on this basis: "High", with the temperature gradient $\nabla T = 80\ ^{o}C/km$; "Mid": with the temperature gradient $\nabla T = 50\ ^{o}C/km$ and "Low" with the temperature gradient $\nabla T = 30\ ^{o}C/km$. The global average is thought to be approximately 25 $^{o}C/km$. It should be noted that geothermal gradients do not have to be constant and in reality will vary with depth. Thus, this HDR grade classification is based on average gradients. The higher the average gradient, the more economically attractive (lower drilling costs per kw) and more efficient (lower plant costs/kw) the power generating scheme using this resource at a specific depth will be.

With low permeability, HDR systems need to have closed/sealed natural joints stimulated or artificial fractures created to allow for fluid flow and heat transfer. An injection well is drilled to the desired depth (and therefore temperature) and the rock fractured at depth. Production wells are then drilled to capture and return to the surface the hot working fluid that is pumped under immense pressure through this new permeable geometry. The working fluid is almost always water, although experiments with gaseous carbon dioxide have been attempted; the cost of make-up fluid as result of seepage in the reservoir is much lower for water. The hot water from the production wells are then piped to the particular application of interest and once expelled, pumped back in the reservoir, making

a closed operating loop, ensuring little or no emissions into the environment. Figure 2.2 provides a schematic of the HDR extraction process.

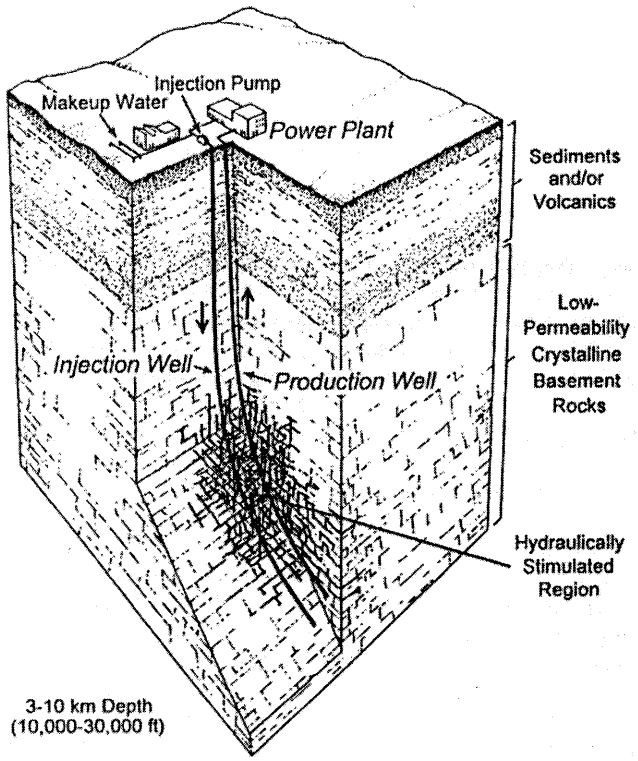

Figure 2.2 Hot Dry Rock concept of Heat Mining

Source: Geothermal energy from the earth: Its potential impact as an environmentally sustainable resource, Mock, Tester, Wright, 1997

The development and experimentation of HDR resources in the United States has happened exclusively at Fenton Hill, New Mexico. Funded by the US DOE, the Los Alamos Laboratories has drilled to temperatures of 250 °C to 300 °C, enough for commercial power production. In order for HDR energy to be employed ubiquitously, the technology for the viable use of the low grade resources have to be developed.

2.3 GEOTHERMAL RESOURCE BASE AND DISTRIBUTION

In order to get a sense for the energy content of geothermal energy at a micro level, it would be useful to demonstrate the heat stored by a block of granite of known volume for an example. A cubic kilometer of granite with a density of 2.7 g/cm^3 and a heat capacitance of 0.19 cal/g-^{o}C; if brought from resource temperature of 250 ^{o}C to 50^{o}C would release:

$$Q = \rho C V \Delta T$$
$$= 4.275 \times 10^{15} \text{ cal} \quad \text{or} \quad 1.791 \times 10^{8} \text{ GJ}$$

If we consider that a barrel of oil (42 gallons) has an energy value of 5.486 GJs, then the heat energy stored in a cubic kilometer of granite would be equivalent to roughly 8 million barrels of oil: this is substantial.

On a global scale, the total HDR, hydrothermal, and geopressured geothermal energy resources for the upper 10 km crust of the earth are estimated by Armstead and Tester: (1987).

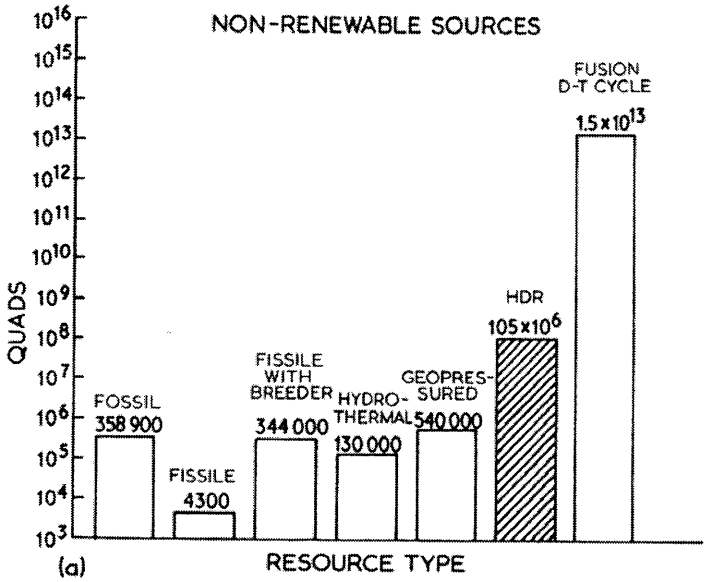

Figure 2.3 World Resource base estimates

Source: Heat Mining, Armstead, Tester, Wright, 1987

The figure on the last page has a logarithmic scale, so the HDR resource estimate is actually one to two orders of magnitude greater than the estimated fossil fuel resource base. It should be noted that some 75 % of the HDR resource estimated are low-grade.[1] The only estimated resource base that out-sizes geothermal energy is fission which continues to be the energy of the future!

In terms of distribution of geothermal resources, the globe diagram below shows the regions of high-grade activity in dark. Notable among these regions is The Geysers resource in California. Although there has been a decline in production due to depletion of *in situ* fluids, the resource has a very high temperature gradient and is regarded as one of the richest geothermal deposits on the planet. Other areas such as the Great Rift Valley that spans across several countries in East Africa, and the tectonic regions of the Pacific and Asia are also contain sizeable resources of high quality. The term "Heat Flow" in the diagram refers to the flux of energy from an area of high temperature to that of low temperature, the rate of this flow is proportional to this temperature difference expressed and hence ∇T, the temperature difference per unit depth also known as the temperature gradient.

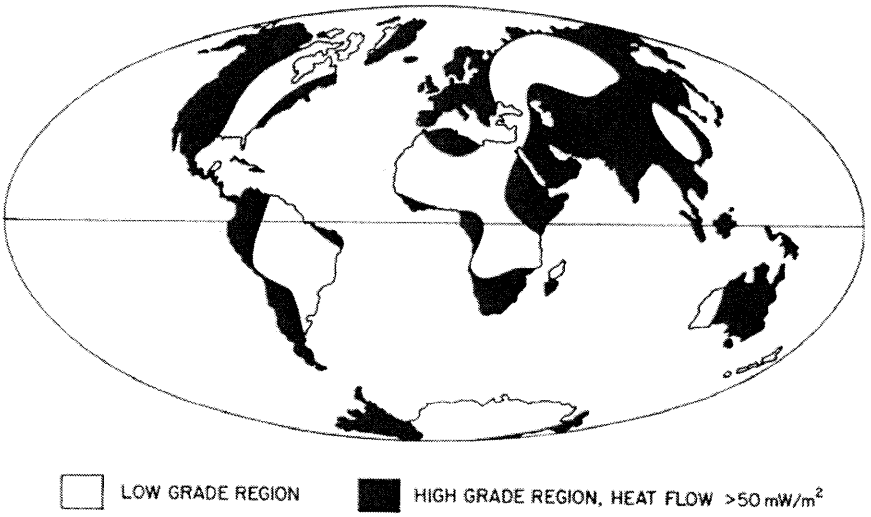

Figure 2.4 Geothermal resource by region

Source: Handbook of Geothermal Energy, 1984

[1] This estimate includes rock temperatures that range between 40 to 85 °C.

2.4 COGENERATION

Cogeneration is defined as the combined production of electrical, mechanical or useable thermal energy from the same fuel source. Combined heat and power (CHP) can occur in a parallel or sequential mode. Sequential cogeneration systems fall into two general categories: those involving topping power cycles for electricity production and those that produce power as a bottoming process after some useful heat has been drawn for mechanical or direct heating purposes initially.

In the early 1900s, many industrial plants produced their own electricity. A large portion of these implemented cogeneration by using the exhaust steam from the power plant for their processes. However, as centrally produced electricity became cheaper due to the impact of the economies of scale, many plants could buy electricity cheaper than they could produce it themselves and this factor led to the decline of cogenerative design. By 1979 on-site generation of electricity accounted for only four percent of U.S. power output. In more recent times, there has been a relatively significant increase in the price of purchased electricity. The advancement of technology has reduced the effect of the economies of scale and with the recent lack of availability and high peak prices in some areas, a move back towards operating one's own power plant is being seen in some industries. Additionally, the conservation promoting energy legislation starting in 1978 as a result of the Arab oil embargo of the seventies, provided important economic benefits including tax breaks to cogenerators and small power producers who satisfy certain qualifying criteria.

The general advantage of cogenerative power systems over conventional systems that produce thermal and electric power separately is the energy savings experienced that results in some 10 to 30 percent less fuel being consumed. This is particularly attractive in an industrial setting where the plant, already producing heat for its manufacturing needs, does not have to buy additional electricity from a utility. As such, cogeneration can offer significant overall energy and cost savings for an industry as well as a nation if implemented as policy and practiced widely: Malaysia's energy plan is a case in point.

Special cogenerative designs that consider seasonal variations are in existence today. For example, a cascade system that produces electricity and as a bottoming cycle supplies district heating during the winter when the demand exists; in the summer; a secondary power cycle with low boiling point organic working fluid can be used as an alternative bottoming cycle in the summer months when the demand for electricity is often higher due to the use of compressor-operated air-conditioning systems. Other ingenious cogenerative systems that accommodate load variations exist. In Neubrandenburg, for example, the exhaust stream of a combined gas and steam turbine process are used to supplement the geothermal district heating unit in the winter; in the summers this stream is fed into the geothermal aquifers which raises its temperature to 80 ^{o}C, this stores some of the heat needed for the cold winter months in a cogenerative fashion (Zenke, Seibit, Kabus, 2000). Heat Pumps employing the subterranean temperatures (warmer than ambient air temperatures in winter and cooler in the summer) provide substantial opportunities for the use of HDR for building heating in residential and industrial applications.

The case studies in this thesis will further demonstrate the preliminary design and economics of such (CHP) ventures, using HDR as the energy source.

2.5 SUSATAINABILITY AND ENVIRONMENTAL CHARACTERISTICS OF GEOTHERMAL ENERGY

There are many definitions of sustainability, in the broadest sense it implies development that "meets the needs of the present generation without compromising the needs of future generations" (The World Commission on the Environment and Development, 1987). The many dimensions associated with geothermal energy and sustainability need to be addressed in order to get a better feel for its possible contribution to a sustainable global energy policy. These characteristics are most meaningful when compared to other presently available energy forms (as opposed to a perfect form) as all options tend to have weaknesses and strengths.

In the recent past, the fear of depletion of fossil fuels, the staple of the world energy supply, was the driving force behind the search for alternatives. As it appears, the current rate of discovery of fossil reservoirs out paces our rate of consumption of fossil fuels. Furthermore, fossil resources that are not economically and technically viable today may become as with the forward movement of technology and/or higher prices for energy as a commodity. The main consideration for the continued use of fossil fuels is now an environmental one.

The environmental concern over the impact of energy use is an important aspect of sustainability as it implies the maintenance of the global habitat for humans and other life forms. In order to get the holistic picture of environmental impacts associated with the different modes of energy production, it is important to look at the lifecycle and supply-chain activities involved in the particular process. With nuclear power for example, the major challenge is in the disposing of the spent fuel: there are currently no safe or feasible means to achieve this. Fossil fuel applications involve the mining and transport of the resource; the possibility of large scale and grave impacts on the environment are very real; sad examples of such mishaps particularly from the transportation of fossil fuels are now more frequent. The other negative impact of fossil fuel usage is emission of the combustion gases. While the curtailment and control of sulfur and nitrogen oxides (responsible for acid rain) have to a large extent been successful, less progress has been made with carbon dioxide emissions. The possibility of anthropogenic global warming is very likely according to studies conducted by the IPCC (Intergovernmental Panel on Climate Change)(Watson, R.T., 2001). Greenhouse gases such as carbon dioxide, emitted into the atmosphere from the combustion of fossil fuels, are thought to be responsible for this phenomenon. Global efforts to harmonize the cut back of such emissions have thus far failed: the Kyoto Protocol has not been ratified. While research into carbon dioxide sequestration is being carried out, this option tends to be expensive and power consuming at present (H.J. Herzog Ed., 1988). The use of green energies to avoid harmful gaseous emissions is another possibility.

Hydrothermal systems are commonly characterized by trace emissions of hydrogen sulfide, low emissions of carbon dioxide and minute amounts of water-born toxins. Hydrothermal power schemes emit a fair amount of water vapor and heat; although water vapor is a greenhouse gas, its concentration in the atmosphere is dictated by regional temperatures: excess water vapor precipitates. There are possibilities of local climate changes in the vicinity of the power plant, these are minor at best and generally not detrimental. All the minor emission aspects discussed are not a factor in the operation of HDR systems that operate in a closed-loop mode; as such, HDR energy can be considered a "non-emitting" technology. Problems of silica scaling and heat pollution are also less pronounced in HDR in comparison to hydrothermal and geopressured systems containing brine and emitting a plume of vapor.

Geothermal schemes can produce a fair amount of noise; the initial drilling can and the emission of unused steam can be loud, then there is the sound of the operating power station. Noise abatement technologies and scheduled drilling can work around these factors; steam emission is not a problem with HDR systems. The footprint and esthetic problems related to geothermal systems are minimal at the surface as the resource is mainly at depth and in comparison to open-pit coal mines which have large footprint. The mining of heat from a mass of rock results in a drop in temperature of this mass which also coincides with the physical shrinkage or "subsidence" of the land; this phenomenon while seemingly dangerous happens at such a slow rate that it's magnitude is no more than the shrinkage by natural cooling of tectonic behavior; furthermore, the pumping of large volumes of water into the rock tends to counter this shrinkage by providing a slight bloating of the rock mass. Finally, there have been concerns about heat mining and fracturing of rock at depth causing seismic activity and/or subsidence. Although there are not much data and what does exist is very site specific, experimental field testing at Fenton Hill, USA, have shown no subsidence or changeless levels of induced seismisity.

Having dealt with some of the environmental characteristics of geothermal energy, it would be important to look at its initial availability and the possible rate of consumption and regeneration of this resource. In terms of the resource size, geothermal energy would

be able to sustain at least five hundred years of global energy supply, if it were to displace fossil fuel use completely (an unlikely scenario[2]). This projection is based on the consumption rates at the end of the twentieth century. In addition, when left unused, depleted HDR reserves recover all their thermal energy, typically in 100 to 200 years.

One drawback of HDR geothermal energy may be its inability to supply basic-load energy to high population density, energy-intense areas. If a major North American city was to be supplied solely from HDR resources from an area in its locality, land as much as 50 times the local area may be needed to supply this energy (i.e. the heat concentration would not be enough in the local). In the case of Manhattan for example, the immediate area could not provide more than about two months supply of energy (from HDR resources) due the high energy consumption rate in associated with the city (Armstead H.C.H, J.W. Tester, 1987).

Another aspect to consider is the geopolitical forces at play in today's world; many countries export energy in the form of oil, LNG and electricity. Large cartels such as OPEC can collude and exert tremendous influence on the supply and price of fossil fuels, a complete embargo resulting in some instances. Such moves can cause stresses and shocks to the economies of energy importing countries and are often a threat to short term sustainability and can precipitate military intervention at times. Countries not blessed with a wealth of fossil fuels are then at the mercy of others. The US has tried to counter this possible problem by creating oil reserves stored in mined salt caverns (The Strategic Petroleum Resource (CSPR), by carrying out research on non-fossil forms of energy, and under the current administration by exploring for and expanding domestic oil production. While the deployment of a self-sufficient energy policy looks far off for the US and many other countries; it is however of strategic consideration in a politically immature and disunited world. The development of indigenous renewables, including geothermal energy should in my opinion be part of such a strategy.

---

[2] Some regions have the potential of relying solely on geothermal energy. Iceland for example claims that it can forego the use of fossil fuels for energy, if it developed its geothermal potential and implemented fuel-cell transportation systems replenished by geothermal electric power.

2.6 THE GROWTH OF THE GEOTHERMAL INDUSTRY

While geothermal fluids have been used for centuries by humanity for its heating and possible medicinal benefits, the production of electricity from geothermal energy started at the turn of the 20th century in Laderello, Italy. This experimental scheme was soon replaced by a 250 KW power plant built and operated during the First World War. There was almost no growth in the industry until after the Second World War after which countries with high-grade hydrothermal fields started implementing the technology. Such fields often fell near fault lines or along tectonic plate edges, examples of such development include The Geysers Field in Carlifornia in Western United States and Wairakei on the "Ring of Fire" in New Zealand.

Substantial growth and advancement of geothermal power production followed the OPEC oil embargo of the 1970s that incentivized the search for non-fossil power alternatives. This created major industries in the United States, New Zealand, Italy and Japan who are now the main suppliers of the commercial geothermal technology. Further growth in recent times in Asia, Latin America and Africa have brought world installed geothermal capacity to about 10 GW_e by 2002. Figure 2.5 shows the dynamics of this growth since the 1980:

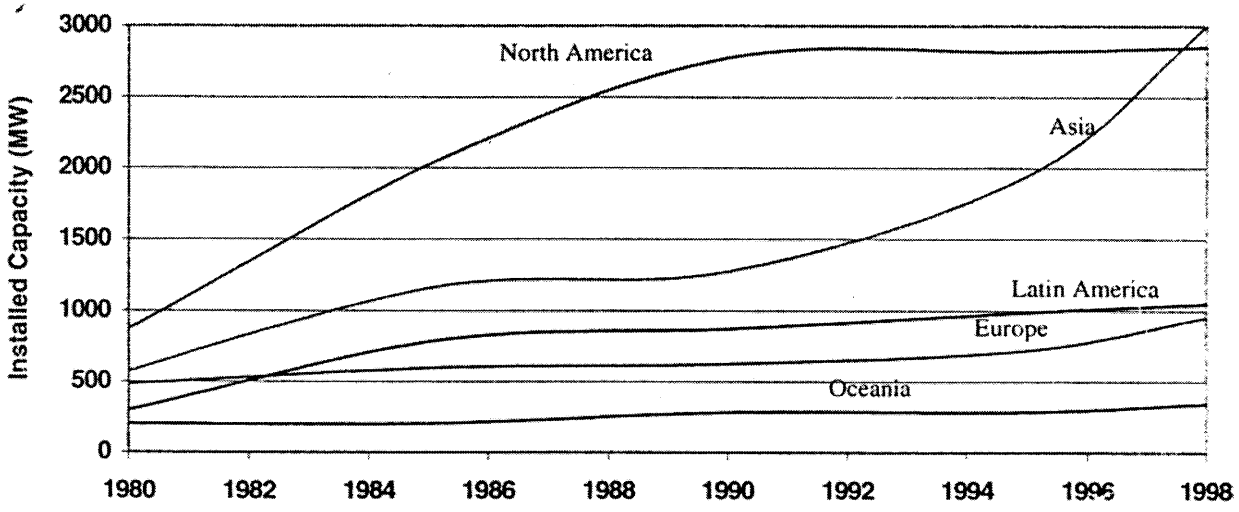

Figure 2.5 Growth of installed geothermal capacity in the world since 1980

Sources: Goodman (1980), Huttrer (1995); International Geothermal Association (1988)

Most recently, new developments in the Philippines and Kenya are adding additional capacity. In Kenya, a 60 MW_e hydrothermal power plant constructed by Mitsubishi Corp, Japan just came on line in 2001; this pushes the portion of power produced by geothermal energy to 8 %. The goal is further reliance on geothermal energy in Kenya in the future, some 25 % of national capacity by 2010.

Closer to home, the Geysers arguably the largest hydrothermal reservoir in the world has run into trouble. The rate of fluid extraction has resulted in reduced output; while it is important to manage this resource properly, it is imaginable that after fluid exhaustion this site will become ripe for HDR mining of heat for power.

The HDR effort is has been some 20 years in the making. As of today there are still no commercial or industrial applications of this technology. In France, work at the Soultz-sous-Forets field have yielded deep granite wells of 1800-2200 meters depth boasting well-bottom temperatures of 270 ^{o}C. Efforts in the U.S. date back to 1977 and have focused on the Fenton-Hill site. In Japan and the United Kingdom the Ogachi and Rosemorrowes fields have been researched, the former being a crystalline granite field with a very healthy temperature gradient (a temperature of 230 ^{o}C at a depth of 1 km). The data from these sites vary greatly as HDR's viability tends to be very site specific.

The growth of conventional geothermal energy, especially in developing countries, shows a healthy trend. For HDR and other more exotic alternative technologies to develop beyond the testing phase, some or all of these scenarios need to occur: ratification of a carbon-dioxide emissions treaty that would result in the internalization of the cost of carbon emissions and accounting for the economic advantage of non-emitting energy technologies; Governmental support and subsidies in research and development and the initial phases of commercial development (some argue that this is actually to the detriment of real growth and is only a crutch); lastly, the continued rise in fossil fuel prices which may include larger governmental taxation.

CHAPTER 3

TECHNICAL ASPECTS OF GEOTHERMAL ENERGY AND POWER CONVERSION

3.1 RESOURCE EXPLORATION

Commercial geothermal systems are relatively few in number worldwide, as such, xact procedures and practices for resource exploration and development are not as well defined as in other energy industries. The lack of knowledge in this field is further affected by the propensity, when investigations have been thorough, to consider the results and techniques as proprietary information and not make them readily available. Consequently, there is much debate about what methods are best suited for efficient and successful exploration and development of geothermal resources.

The methods in existence today focus mainly on three characteristics of the resource in question: the geological, geochemical and geophysical nature of the area and the underlying / surrounding rock. The general approach tends to first use inexpensive, regional methods of exploration that are not necessarily very accurate: these are followed by more technical and quantitative options available as the exploration effort zeros –in on a possible high-grade resource.

Before all else, a literature search into available data on the site is recommended. Data and information from state and federal agencies, geothermal data banks, universities and research institutions may provide leads. This is often followed by geological mapping, considered as the foundation of all exploration efforts, satellite and air photography is typically used for this purpose. The object of this exercise is to find young igneous rock, likely to harbor the most heat; fault lines and natural fractures are also used to further understand the site in question. Simple petrological and seismic studies can confirm mapping techniques. Fracture studies are important to learn about the permeability of the

resource: in fluid-dominated systems, the natural permeability (known as secondary permeability) dictates to a large extent the production from bored wells; in HDR systems, it is important to try and drill around major fractures that can not be incorporated into the artificial fracturing scheme in order to stop working fluid loss.

Geochemical exploration techniques include the study of chemical geothermometers and trace-element investigations. The former concentrates on the temperature of the below ground fluid that contains silicon cations; while the latter looks at the concentration of several trace elements, including noble gases, to verify the presence of young volcanic rock. These methods, if coupled, can be fairly accurate and do not require the drilling of expensive exploratory holes. These techniques were used in the preliminary geothermal energy exploration in Arizona in the late 1970s (Edwards, L.M. *et al*, 1982).

Two of the more popular geophysical exploration techniques are those that use gravity and electromagnetic signature of the site. Gravity measurements are used to primarily in defining the extent of the heat source by exploring the presence of young igneous rock and possible magma intrusions. Aeromagnetic measurements provide minimum reservoir temperatures based on the fact that certain magnetic minerals loose their magnetism when they reach certain temperatures known as the Curie point.

Apart from these methods already described, a host of other techniques are used and are in development. The surest method in practice today is the use of exploratory drilling. This method is expensive and possibilities of hitting a "dry-hole" are high; it should be used once adequate positive information about a site are present. Research into cheaper exploratory holes with smaller diameters ("slim hole" drilling) has been promising.

Once the exploration has identified a potential site, it is important to model the resource and determine the geometry and characteristics that will effect heat mining. Various numerical techniques, including the finite-elements method could be used to simulate the reservoir.

3.2 GEOTHERMAL DRILLING

The technology harnessed for the drilling of geothermal wells is not that different from that which is used in the oil and gas industry. As such, any country that has an oil and gas exploration industry, can with some technical modifications, enter the geothermal industry. The marked differences are that in geothermal drilling, little underlying pressure from fluids exist (apart from geopressured resources) and higher well temperatures are experienced. The type of rocks being drilled in the two industries are often different: oil and gas often being trapped in sedimentary strata of rock, and a good grade geothermal resource is often found in metamorphic or igneous rock. These harder rocks often lend to more expensive drilling, but tend to be more stable at depth.

Conventional drilling practices employ rotary drilling technology with a drill bit made of a hard substance such as tungsten carbide. The drill head rotates at 30 to 300 rpm with sufficient weight to crush the underlying rocks into chips it is supported by a string of drill pipe and a rig and is powered by a diesel or electric engine of some 1500-3000 hp. A drilling fluid is pumped down the drill string, apart from cooling the drill bit and stabilizing the well by providing hydraulic pressure, this fluid pumps out the drilled rock chips. A special fluid circuit with its own pump is designed for this function. In cases where more stability is required, drilling muds that cake the walls of the well are used, special attention should be given to the drilling temperature as water based muds can degenerate at temperatures exceeding 150 ^{o}C and may need pre-cooling, oil based muds can withstand temperatures of about 200 ^{o}C. Blowout preventers are used to stop the mud or geothermal fluid from shooting out through the well-head.

The instillation of production casing after drilling is important to provide further stability to the structure. Steel pipe cemented into place is used to line the walls of the well. Casing sections are of various thickness and diameters, both decreasing with depth; the thickest, the anchor casing is set near the well foundation. Apart from providing stability, the lining may have to withstand high fracturing and operating pressures for HDR systems, high temperatures and the thermal expansions and contractions associated with

shutdown and possible corrosive brines in the case of drilling hydrothermal resources. Downhole drilling motors are often used in difficult drilling scenarios caused by depth and directional requirements, which can be far from simple in a geothermal project.

Drilling techniques and procedures in HDR reservoirs are similar to the aforementioned description but with some notable exceptions. First, well depths tend to be deeper, measuring some 3- 6 km. The type of rock being mined in HDR systems is often hard crystalline rock with minimal stresses occurring along the horizontal rock plane at depth. This requires the hardest of material to be used in a drill bit; and as a consequence of the insitu stress orientation, HDR wells may need to be slanted off vertical and as such require down-hole directional drilling control. Some of the directional wells drilled in Takigami, Japan for example have an extreme slant of about 50^{o}, this has allowed for the exact directional bypass of a geological fault and an area of high permeability (Jotaki, H. 2000). One problem posed by such extreme angles is the difficulty in removing drill cuttings.

New innovations in drilling technology are being researched. Some, if brought to fruition might well provide for a quantum-leap in drilling practices: these include efforts that focus on melting and vaporizing rock, thermal spallation and chemically induced rock removal. The current changes that are reaching the market, however, are incremental and represent variations on current drilling practices. New Advanced Geothermal Drilling Systems (AGDS) such as percussion drilling for example can solve the problem of lost circulation considerably and hence be a more cost effective technology for drilling hard rock. This technique coupled with the use of new muds can increase penetration rates by 10- 15 %: in the case of a 3 km long well for example, this translates to about 40 days of drilling as opposed to 65 days with conventional drilling practices. Real-time feedback drilling systems such as the MWD are being engineered to withstand temperatures of over 200 ^{o}C, once again improving speed and well completion times. Another recent advance being tested by Royal Dutch Shell for their oil and gas practice, is the mono-diameter drilling technology (Watts, P, 2002). Apart from less earth removal and enhanced speed, substantial cost reductions are expected using this technique.

3.3 CREATING PERMEABILITY: ROCK FRACTURING

In order to be able to mine the heat present in a rock structure, sufficient heat-transfer area to permit the passage of a working fluid is required. Most rocks have some degree of natural permeability, however, this may not be enough for economic heat mining and so the structure needs to be further stimulated if there are natural blockages to this permeability or further fractured to allow for heat mining. In some cases considerable natural permeability may exist in the structure, this is not always good: if the fractures are not properly configured and aligned within the reservoir excessive working fluid and heat losses may result. The overall reservoir impedance is also of importance as this and the pressure differential in the reservoir will determine the rate of working fluid flow; high impedance would require high operating pressures and result in increased cost.

While the oil industry has been employing fracturing techniques for the past 60 years, these have not been successfully transferred to the HDR geothermal industry. The types of rocks manipulated in the two industries have very different permeability structures. A word must be said about the types of rock that are mined for heat: these are known as *competent* (as opposed to *incompetent*) and have a natural rigidity and little permeability, these can resist a fair amount of stress while keeping their structure once permeability has been created. The other, *incompeten*t rock, such as unconsolidated sand or clay, degenerates under shear and direct stresses and as such is unsuitable for being fractured for heat transfer (Armstead, Tester, 1987).

There are four basic modes by which fracturing of rock is achieved. Hydraulic pressurization achieves this by the high pressure pumping of water or other fluids downhole. Thermal stressing of the rock based on a temperature differential between the drilled rock and a hot or cold fracturing fluid is another possible method. Rapid gas pressurization, which occurs by the ignition and the expansion of a gaseous or liquid propellant downhole holds special future promise. Explosive fracturing involves the detonation of a charge underground; the resulting shockwaves produce radial fractures around the drilled well that can be used for heat transfer. Out of the methods above,

hydraulic and explosive fracturing are receiving the most research time. It is important that fracturing occur at specified depth, otherwise, fractures near the borehole can result in a working fluid short-circuiting and create inefficient reservoir operation (Armstead, Tester, 1987).

3.4 ENERGY CONVERSION TECHNOLOGIES

Geothermal energy is very much a site dependent phenomenon with limited possibilities for the transport of the heat via pipelines; albeit that with the advent of HDR mining the advantages of an ubiquitous resource are now at hand. Nevertheless, the need of conversion of this resource into a transportable commodity such as electricity is obvious. HDR resources are characterized by temperatures ranging from 100 to 300 ^{o}C; this spread is below working temperatures common for fossil fuel and nuclear energy technologies. Considering the second law of thermodynamics which dictates limits of efficiency (Carnot-type efficiencies) for the production of useful work (mechanical and electrical energy) from the heat of these resources, HDR like other geothermal system suffer from relatively low heat to electrical work conversion efficiencies. For HDR resources efficiency range from 10-25 %, in comparison, fossil fuels and nuclear technologies operate at 35-50 % efficiency with new generator combined gas turbine/steam Rankin cycle power plants approaching efficiencies of 60 % (Tester, Brown, Potter, 1989).

3.4.1 Direct Use

The more efficient application of geothermal energy has historically been found in its direct use in heating, cooling and a wide variety of agricultural and industrial applications. These have included district heating, cement drying, food processing and use in spas, to name a few applications. In most industrial countries, a great portion of the energy use is at lower temperatures; the current production of this low temperature energy by fossil fuels using a much higher operating temperature makes this process inherently less efficient. In the U.S. alone some 30 % of the energy use (30 quads) has

been for resources operating below 250 °C, of this a substantial portion consists of industrial and residential space heating utilizing temperatures in the range of 50-80 °C (Tester, Edwards, Chilingar, Rieke III, Fertl, 1984). An obvious advantage of geothermal heating use is the displacement of carbon dioxide emitting fossil fuels; a HDR heating system can be economically competitive with natural gas or oil fired space heating systems in large enough applications. There is however no direct-heat geothermal industry or infrastructure in the way that there is an electric power generation industry with ready made, off-the-shelf products. Direct-use systems have to be designed and built from scratch, which lends to relatively more expensive schemes and longer implementation periods, although a major attraction of direct use systems is their lower capital requirements in comparison to electric power production from the same source. Another challenge in direct use applications is that the heat load often varies with season; this would then require control of the heat input in terms of flow rate of heating fluid. As such it is difficult to estimate the total worldwide magnitude of direct use; estimates of 40,000 to 70,000 MW_t today would put this utilization above that of electricity production of geothermal energy. This development owes its growth to the existence of more numerous low-temperature geothermal reservoirs available for direct use near demand centers, the simplicity of such systems and their demonstrated efficacy.

There are several ways in which HDR energy can be converted to electricity. The grade and makeup of the geothermal resource affects the choice of method. Some of these power generation cycles and their characteristics are described below on the following pages. While some such as the Flash and Binary systems have been tried and tested, others like the Stirling cycle have not had widespread use in the geothermal industry as yet.

3.4.2 Single and Multistage Flash Systems

In HDR systems, hot water is received from the reservoir at high pressure. The reduction in pressure in a separator, known as "Flashing" creates two streams of hot water and steam. The steam is then run into a condensing turbine, unless large volumes of non-

condensable gases are in the stream. The additional hot water from the first separator maybe further flashed to produce steam of a lower pressure that can be fed into a multistage turbine for additional power; this procedure may be repeated, however, it is very rare that more than two flash stages are used.

Noncondensable gases at Kizildere for example, a 20 MW_e Geothermal Power Plant in Turkey (10-20 % by weight non-condensable gases in the steam stream that leads to the turbine) has required the use of gas compressors to remove this unwanted gaseous matter, but this draws some 18 % of the power generated (Gunerhan, Coury 2000). The use of an upstream reboiler can be implemented to remove a large portion of these non-condensable gases from the stream in this specific case. The figure below is a schematic of a typical dual flash cycle.

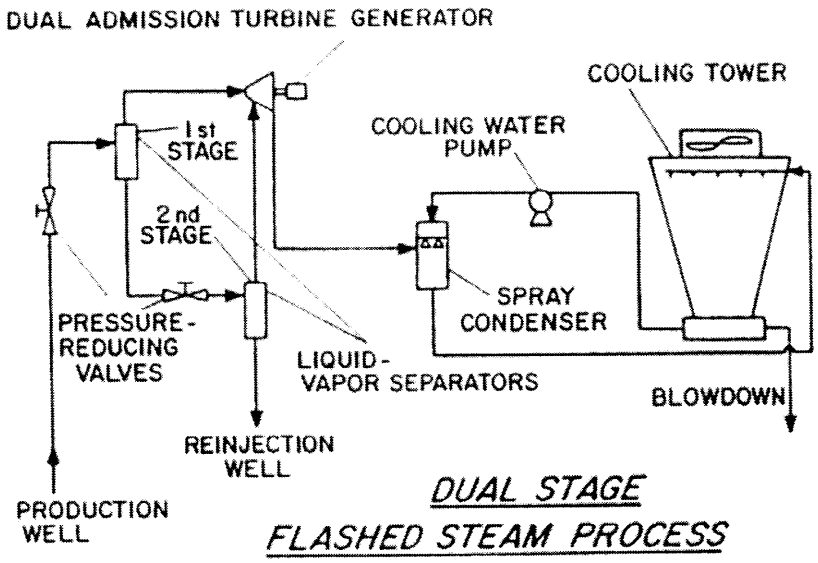

Figure 3.1 Double-Flash Power Conversion Scheme

Source: Heat Mining, Armstead, Tester,1987

Direct steam systems are another power generation option used in vapor-dominated geothermal resources; this rarely, if ever occurs in HDR systems due to high operating pressures through the reservoir outlet (although some phase separation does occur at the outlet). The issuing vapor from the reservoir is passed through separators to strip the stream from particulate matter and condensate that can erode equipment and the resulting effluent is fed directly into a turbine. This is essentially the same as the flash steam systems with the exception that the resource is already in vapor phase and requires no further flashing.

The advantage of flash systems is their simplicity and relatively smaller capital requirements in comparison to say the Organic Rankine Cycle (ORC) schemes discussed further on. The need for large and expensive heat exchange areas, feed pumps and additional condensers are avoided. Furthermore, the addition of second separator is of minimal cost, but can substantially increase the power output from the additional steam production in a high-grade geothermal resource.

The exhaust stream from the turbine needs to be cooled and condensed using cooling towers and a condenser if a condensing turbine is not used. If water availability is a constraint, dry towers and condensers using air-cooling techniques have to be employed. In high ambient temperatures this can lead to additional heat exchange surface costs and lower efficiencies due to a higher temperature of the exhaust gas from the turbine. This condensed water, together with the liquid effluent from the last separator is then reinjected into the reservoir or discarded. The considerably large sensible heat available in this effluent, in particular due to the above-ambient operating temperature of the last separator is the subject of cogenerative analysis in a case presented in chapter 5.

The main disadvantages of a flash system is the need for large expensive steam turbines that can consume a large part of the power plant capital and their susceptibility to steam corrosion and droplet impingement. Scaling problems due to silica deposition on the internal surfaces of the equipment is another aspect that requires attention and regular maintenance.

3.4.3 Binary Systems

Also referred to as Organic Rankine Cycles (closed loop), binary systems use a working fluid that extracts the heat from the geothermal source fluid by means of a heat exchanger. The working fluid is typically a volatile, low molecular weight organic hydrocarbon such as ammonia, isobutene and chlorinated hydrocarbons, although the use of CFCs in new projects is controversial because of their negative environmental impact. A recent 25 MW_e binary plant built by Mitsubishi in Takigami, Japan which was commissioned in 1997, uses Freon (HCFC-123) as binary fluid to make use of low temperature geothermal fluid for power production. These fluids often have relatively low boiling points, heat capacitances and vapor densities; this characteristic lends itself to high pressure operation of the vaporized fluid through the turbine, which tends to be much smaller and operate at higher revolutions than the large, low-pressure steam turbines. The turbine exhaust is then condensed using a condenser / cooling tower and pumped into the heat exchanger for a repeat of the cycle.

There are certain advantages of the binary cycle: the first amongst these is the ability to use low-grade geothermal resources to produce electricity; this is due to the low boiling point of the working fluid: geothermal fluids flashed in the range of 90- 150 ^{o}C produce power inefficiently. The second advantage is the ability to isolate excessively corrosive brines and dissolved matter in the source fluid from the turbine; streams with large portions of noncondensable gases may also be isolated from the energy loop.

One of the challenges of binary fluid systems is the high maintenance and capital costs of heat exchanger equipment, due mainly to fouling and scaling of dissolved minerals contained in the geofluid. Research into special polymer-based coating to be employed on carbon-steel tubing is hopeful and will make the use of expensive stainless steel shell and tube heat exchanger construction redundant (Gawlik, Kelly, 2000). Another solution is the use of the multistage flash-organic binary cycle, essentially a hybrid between the flash steam and ORC systems: the steam produced after flashing is used to vaporize a secondary fluid to operate an ORC.

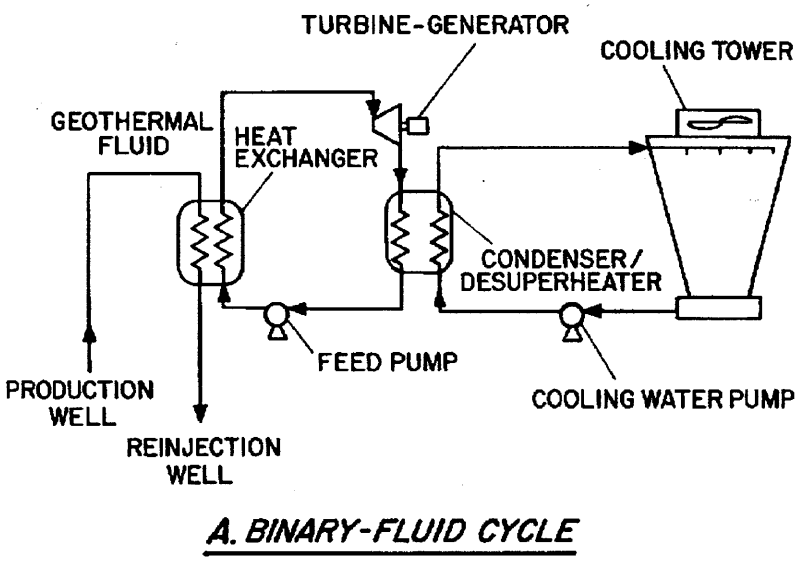

Figure 3.2 Organic Rankine Cycle Power Conversion Scheme

Source: Heat Mining, Armstead, Tester,1987

3.4.4 The Stirling Cycle

The Stirling cycle is another option for low temperature operations. It works on the principle of the difference in enthalpy in the compression of cold gaseous matter and its hot expansion. Traditionally employed in low temperature solar applications, this cheap piston-operated engine has the advantage of simplicity requiring no compressors, turbines or expensive heat exchange surfaces; the engine unit is exposed to the heating source externally and requires no internal working fluid flow, this further reduces fouling and erosive problems. A further advantage of this cycle, invented in 1815 by Reverend Stirling is its extreme efficiency, reaching the theoretical second law Carnot-efficiency (Kolin, Koscak-Kolin, Golub, 2000).

The wide-spread global use of this engine since the 1980s especially in remote regions is encouraging. This development is also challenging the presumption that low temperature geothermal resources are only fit for direct-use applications; commercial electricity production from low temperature geothermal resources are being considered in Mladost,

Zagreb(Kolin, Koscak-Kolin, Golub, 2000). An estimated low resource temperature of 80 ^{o}C in the Croatian winter, in the month of January when ambient temperatures are just above 0 ^{o}C, would yield an impressive Carnot efficiency of 22.5 % (conversion to mechanical energy). With hot fluid supplied at say 60 kg/s, taking the heat capacitance, temperature differential and efficiency into consideration, a theoretical power production of some 4.4 MW results.

The main drawback with the Stirling engine is the magnitude of the power produced from low-temperature resources, typically the engines of today produce no more than 1 kW_e (concentrating solar applications have been developed at 100 kW_e) while this may be sufficient for some remote applications, further enhancements are required to use this engine in a sizable commercial application for low-temperature resources.

3.4.5 Total Flow Concepts

Examples of such systems include the helical screw expander and the biphase turbine. Hot geothermal fluid is pumped into these devices that allow for expansion and hence vaporization of the geothermal fluid while in the device. This increase in volume then causes a displacement or rotation of a screw like portion of the device connected to a shaft allowing for the transfer of mechanical work produced. The advantage of such systems is their ability to interact with hot, high-salinity geothermal fluids. Unlike flash systems in which a substantial amount of the resource remains in the liquid state and is discarded, total flow devices use almost all the liquid available for expansion; their technical simplicity is also attractive, albeit very high efficiencies are required for them to compete with steam flash systems.

3.4.6 Hybrid Geothermal-Fossil Cycles

The use of geothermal heat in hybrid schemes with fossil fuels can result in much higher power generation efficiencies (40-45 %) and reduce the amount of fossil fuel required. The initial heating of the working fluid is carried out by the lower temperature geothermal fluid from the reservoir. Fossil fuel combustion is then utilized to superheat and vaporize the working fluid; in the case of steam generation, geothermal heat is used to replace initial feedwater heaters. It is estimated that in a 500 MW_e hybrid steam cycle power plant utilizing a HDR resource at 200 °C to replace some 5 feedwater heaters, some 10 % fuel savings would be realized (Tester, Brown, Potter, 1989). Although this is not substantial, if implemented as policy in a country, it can have major fuel displacement ramifications. Figure 3.3 below shows a hybrid cycle of geothermal preheat and fossil fuel boiler for power production:

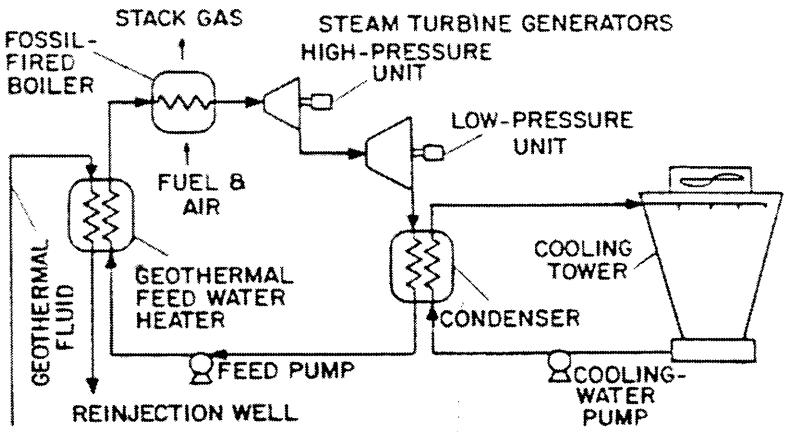

Figure 3.3 Hybrid Organic Rankine Cycle Power Conversion Scheme

Source: Heat Mining, Armstead, Tester,1987

3.4.7 Combined Cycles

Other combined cycles such as that with the presently popular combustion gas turbines are also possible. The gaseous exhaust from the turbine is at some 600 ^{o}C. The use of HDR heating to produce a low-temperature working fluid can be further augmented by the gas- turbine exhaust to create an efficient bottoming cycle.

Apart from fossil fuel hybrids, combinations exist with cycle types such as hybrids of flashed steam and binary systems, as previously described. Often times, the temperature of the geofluid resource in the second flash stage is low and this leads to an inefficient conversion to a additional power; the use of a binary cycle in place of a second flash would be more efficient, but more expensive.

Dual cycle design employ separate schemes that are used when needed and shunted at other times. For example, a district heating loop fed as a bottoming cycle in an electrical production scheme would be online in winter; but in the summer months, when heating is not required it would be bypassed and the effluent fed into a binary fluid power plant to produce more electricity for air conditioning. The requirements of the heating load often determine the order of electrical and direct heat use in design. In a pulp mill for example, high pressure steam is need, as such, this use may form the topping cycle and the electrical production using a low-temperature scheme would be designed in parallel or as a bottoming cycle.

Advances in low-temperature conversion technologies will further enhance the efficiency of geothermal energy conversion. Already, the Kalina Cycle, which employs the advantages of an ammonia-water working fluid mixtures has been shown to be useful in low temperature geothermal power conversions. The lower boiling point ammonia allows for high pressure and lower temperature expansion through steam turbines: hopes for 40 % cycle efficiencies due to this are not uncommon.

3.5 TURBINES

The operation of the turbine at high efficiency is paramount to an energy efficient power plant; furthermore the choice of system design and working fluid has capital and economic ramifications that must be considered. Turbines employed with steam as the operating fluid as in direct flash systems tend to be large and expensive, whereas those used with organic binary-fluid cycles are more compact due to the higher density of the working fluid at typical exhaust conditions. This creates a tradeoff between binary-fluid systems that require large expensive heat exchange surfaces and employs lower cost, smaller turbines and the steam flashing systems that use large expensive turbines but require little or no heat exchange equipment for operation.

Turbines for steam systems larger than 50 MW_e are commercially available; for lower power outputs specifically designed units may need to be manufactured. Turbines for binary-fluid systems rarely get larger than 1 MW_e. There are currently a huge backorders for custom made turbines and specifically gas turbines used in power generation due in part to the shortfall of power supply in California and a move towards power deregulation resulting in a larger number of producers. In early 2001 for example, there was a 2 year back log of orders at General Electric for gas turbines; as they have quickly become the most popular method for electricity generation systems.

Turbine efficiencies depend on four parameters expressed in dimensionless terms as functions of Reynolds and Mach numbers (parameters include: pitch diameter, flow rate, RPM, and enthalpy drop per stage). The exact science of these concepts is beyond the scope of this thesis, in its place a generalized correlation for multistage steam turbine efficiencies with operational pressure and horsepower as independent variables is used. This is reproduced on the next page in graphical form. While somewhat outdated dating back to 1984, it provides for ballpark efficiency figures of multistage steam turbines and is sufficient for the purposes of initial design and the work in this thesis.

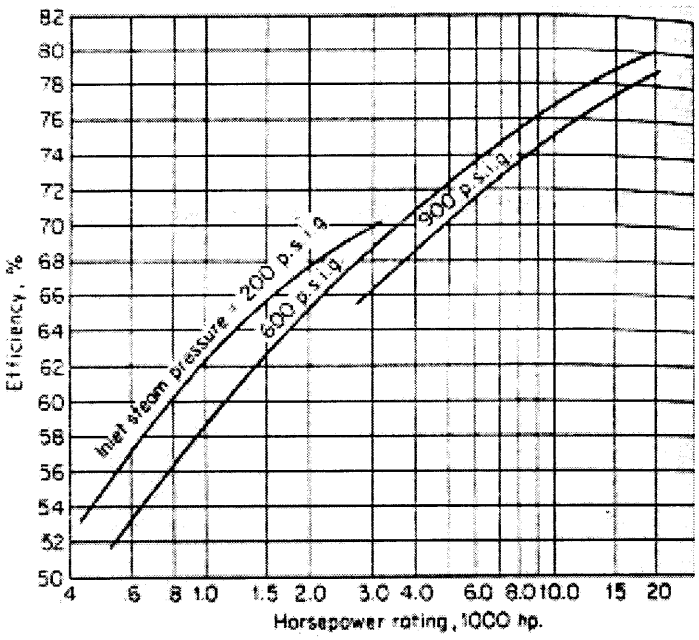

Figure 3.4 Approximate Multistage Steam Turbine Efficiency

Source: Perry's Chemical Engineers' Handbook, 1984, p 14-14

While many arrangements and types of turbines are in use today, a multistage condensing turbine was chosen for use in the fish-farm cogeneration scheme presented later. The advantage of a multistage system is the flexibility and better efficiency in part-load scenarios; furthermore the design of the plant requires the use of two flash separators producing steam at two different pressures and temperatures, this is handled best by a multistage turbine system. A condensing turbine receives steam at a single pressure per stage and exhausts at a pressure at just below or below atmospheric, this is advantageous as it limits the need of condensing systems and cooling towers.

Geothermal systems have their own particular challenges; wet expansions in flashing systems can produce liquid droplets that drastically reduce efficiency in steam turbines and can also result in the erosion of turbines resulting in large repair or replacement costs. As such, geothermal turbines commonly use moisture separators between each turbine stage to offset this effect. Turbines employing organic working fluids in a binary fashion can generally avoid this problem by careful choice of working fluid and operating conditions outside the liquid-vapor region.

3.6 THERMAL DRAWDOWN

The thermal drawdown of a HDR reservoir is a measure of the drop in temperature of the reservoir rock and circulating fluid as heat is mined. Many economic studies omit this factor. Proper projection of the technical and economic sustainability of a HDR geothermal scheme depends to a large extent on how fast drawdown occurs. The dynamic temperature drop of the reservoir is very much a site-specific phenomenon although operational parameters have a bearing on the rate of drawdown, which is asymptotic in nature, dropping fastest initially. The reservoir at the Reihen for example, a doublet HDR project, is used for district heating and operates at low flow rates and production temperatures and experiences little drawdown: which is estimated at some 0.7 K over 10 years (Megel, 2000). For commercial exploitation, no more than five to ten percent reservoir temperature decline over a 10 year period is acceptable: under conditions of greater drawdown, redrilling the reservoir or increasing the flow rate through the reservoir would be required to maintain a sustainable power output.

Several models for the study of this effect exist and depend on factors including the heat capacity of the rock mined, flow rates through the rock, the rock's thermal conductivity, fracture structure and type, to name a few. The results are often presented as a percentage temperature drop of the reservoir to measures of power loss or decreased flow rate of the working fluid as a result of the drawdown. A "Drawdown Parameter" given by the mass flow rate divided by the heat transfer surface area in kg / m^2-s, is employed to quantify this effect in modeling scenarios.

While there are formula and diagrams that providing a nondimentional temperature change with time for a mined reservoir; the diagram provided on the next page shows the loss of power associated with a thermal drawdown parameter over time. This will give the reader a feel for the output loss in case studies undertaken in Chapter 5, where the EGS Simulator package calculates busbar energy prices having already incorporated the applicable drawdown parameter for the case in question.

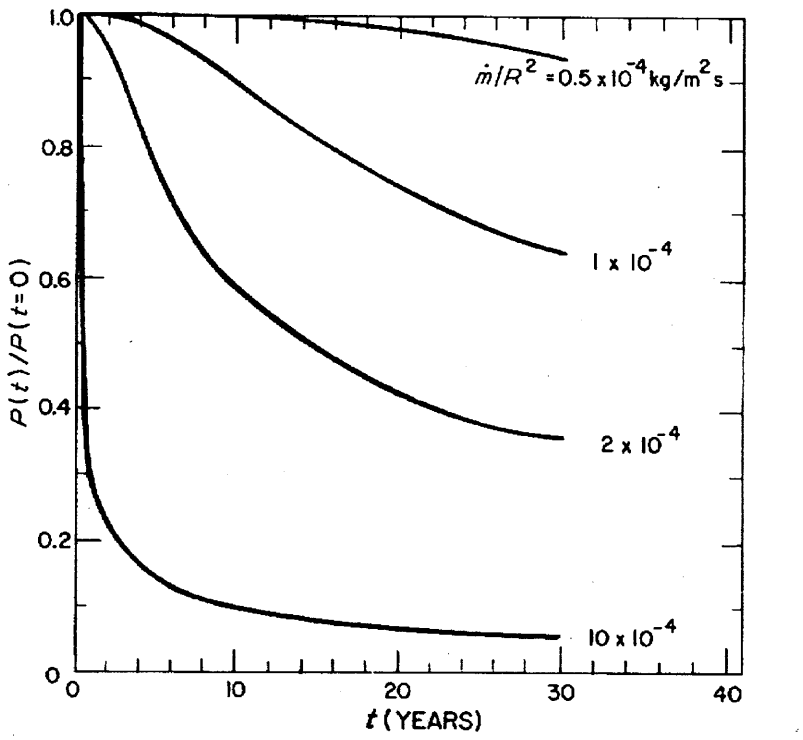

Figure 3.5 Reservoir Temperature Drop Due to Drawdown

Source: Economic predictions for Heat Mining, Tester, Herzog, 1990

CHAPTER 4

ECONOMIC ASPECTS OF GEOTHERMAL ENERGY SYSTEMS

4.1 INTRODUCTION

There are four general factors that affect the economics and viability of HDR power projects. These are:

1. The Resource Grade- As discussed in Chapter 1, the temperature gradient (^{o}C/km) of a geothermal resource defines its quality. Higher gradients would require relatively less drilling for reaching a set temperature translating into a reduction in costs; or put another way, higher temperatures for a given depth would result in more efficient power plant energy conversion.

2. Cost Components- This includes drilling, simulation and formation of the reservoir as well as the cost of the power plant. These factors can vary greatly from project to project depending on requirements.

3. Reservoir Performance- The total available thermal energy in the rock being mined, the water-loss rate and drawdown rate provide metrics to determine the long-term fortunes of project and its longevity. Careful operation and maintenance of the plant and subsurface reservoir also play important roles in this matter.

4. Economic Conditions- The breakeven electricity production cost depends in a large measure on how the project is financed and what incentives and inducements the local government is willing to provide. This is discussed in further detail.

4.2 HDR COSTS BY COMPONENT

While geothermal energy use has been in practice for centuries, its commercial application really commenced at the beginning of the twentieth century in the harnessing of high-grade hydrothermal resources for power production. Other enhanced geothermal systems including HDR, are still in the experimental stage of development in various countries and no active industry employing these systems exists as yet. The lack of commercial experience translates into uncertainty in arriving at costs associated with schemes of enhanced geothermal systems: nevertheless the breakdown of costs by segment and comparison with like activities in the hydrothermal and various other analogous industries allows for cost prediction.

The greatest uncertainties in HDR schemes are attributed to the drilling and simulation phases of the project; while in HDR drilling there is no possibility of hitting a "dry-hole", there are nevertheless financial risks and uncertainties associated with snagged and trouble-burdened drilling and simulation. The lifespan of the reservoir is also an uncertain quantity due to inexact understanding of heat flows and drawdown characteristics in the reservoir and its vicinity. Any one of these factors can seriously affect the viability of the project.

In HDR power schemes there is generally a trade-off between the component cost associated with the power plant and that for drilling. Deeper wells result in higher operating temperatures that increase efficiency and lower power plant costs; this, however, is achieved at the detriment to the cost of drilling that rises exponentially with depth. Illustrated in Figure 4.1, These factors effectively translate into parabolic shaped family of curves, exhibiting the highest electricity busbar costs at very low and very high temperatures. The optimal is the point with the lowest busbar cost as shown by the figure on the next page, other optima for different temperature grades of HDR resource provide a locus of optima for any temperature resource.

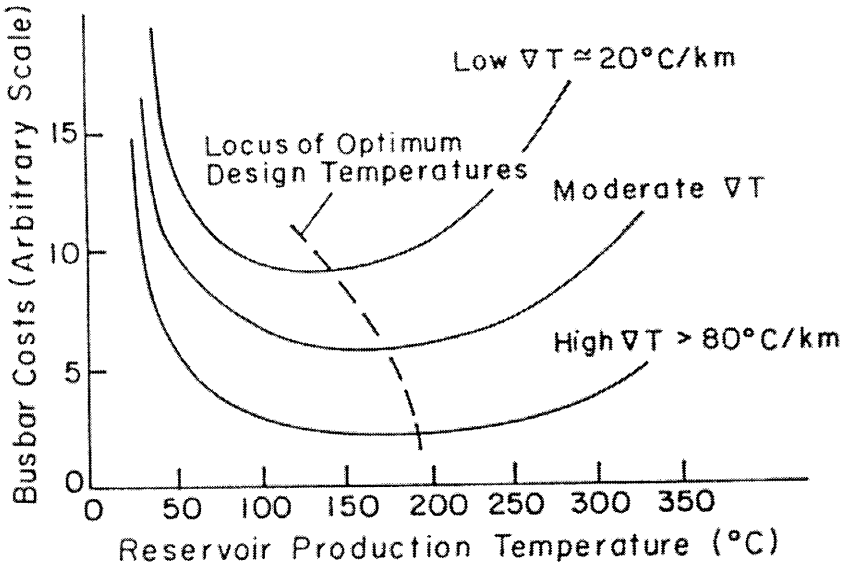

Figure 4.1 Generalized effect of production temperature on electricity busbar cost

Source: The Economics of Heat Mining: An Analysis of Design Options and Preformance Requirements of HDR Geothermal Power Systems, Tester, Herzog, 1991

4.2.1 Exploration & Land Cost

Finding the right conditions in a site for the possible introduction of a geothermal power project is key. Various techniques involving aerial photography, geophysical, geochemical and tithographic measures that manifest the physical, chemical and thermal characteristics at depth (all described in Chapter 2) are used to determine the suitability of a proposed site. The costs associated with this phase of the project can be significant especially as they occur substantially before the possible generation of revenue. More reliable tests such as core drilling are expensive, but would seem prudent ahead of a multi-million dollar investment in a commercial system. In HDR systems the deployment of a pilot plant on site is the surest means of determining viability; reservoir performance can thereby be ascertained accurately, this is obviously very expensive and the test phase can take many months, but given the relative youth of the HDR industry and lack of commercial experience, this route may be a requirement for the cautious investor. Again a balance exists between burdening a project with too high exploratory costs, which may in the end prove fruitless versus charging into a project without adequate exploration subjecting the venture to undue risk.

Land rights are required for the set up of a power plant and the creation of the reservoir. The costs can vary greatly depending on the location of the proposed project. Options for direct acquisition, amphetutic leases (long term lease / ownership- the property and any improvements revert back to original owner after periods typically from 60 to 99 years) and shorter term leases generally exist. It is also important that mineral and water rights for the property also be obtained; the first would allow for the processing of brines for product the second is vital to the operation of hydrothermal projects or for the injection of water as a heat transfer fluid in HDR ventures.

4.2.2 Drilling and Simulation Costs

While data on the completion costs of hydrothermal wells up to 3 km depth exists, commercial information on deeper HDR wells is not available. However, information from a score of experimental HDR wells in the US, UK, France and Japan provide adequate knowledge for depths of up to 6 km. Comparison with other drilling industries such as that for oil and gas is also useful and provide a possible lower limit for HDR drilling technology once commercially mature. At present, geothermal wells cost two to three times that of their oil and gas counterparts; apart from the larger bore of geothermal wells (8 to 10 inches) that would require larger bits, more earth removal and larger diameter well casing, harder rock and lost circulation associated with geothermal reservoirs are responsible for this difference. Ironically, at depths of over 8 km drilling a harder rock is projected to may be more advantageous because of the inherent stability it manifests; drilling in sandstone for example, would be technically challenging at such depths. Figure 4.2 on the next page exhibits these different well completion costs with depth. "Commercially Mature" technology refers to problem-free rotary drilling considered as the optimal HDR drilling scenario. Note the logarithmic scale on the vertical axis: the linear lines testify to the exponential increase in well cost with drilled depth.

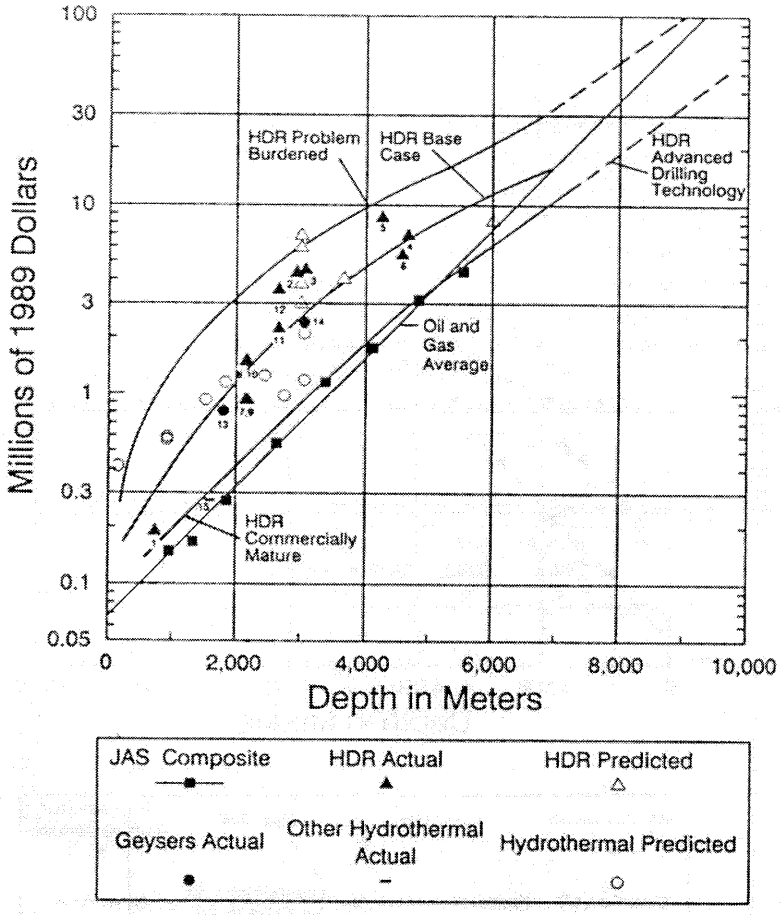

Figure 4.2 Projected HDR individual well drilling and completion costs

Source: The Economics of Heat Mining: An Analysis of Design Options and Preformance Requirements of HDR Geothermal Power Systems, Tester, Herzog, 1991, with updates.

Stimulation costs depend on the type and volume of rock that is being fractured. Fracturing has only occurred for small pilot plant ventures thus far and uncertainty from the lack of commercial-sized reservoir experience exists. The technique essentially involves the pumping of water or a fracturing fluid with special rheological properties at high pressure through the reservoir. The resulting fractures are diagnosed for size (area and volume) and flow characteristics. The cost of this procedure increases with depth, requiring platforms, large pumps and pipes. Reservoir costs can be significant ranging from some USD 200 to 700 per kW_e installed of the intended power project.

4.2.3 Power Plant Equipment Costs

The nature of the geothermal resource often dictates technological power plant decisions: in the case of hydrothermal resources with corrosive brines a binary cycle plant or specially designed multi-stage flash plants maybe advantageous for example. These costs include the equipment such as turbines, condensers, cooling towers, pumps (downhole and surface) and large heat exchange surfaces (for some options). The actual installation cost is roughly 2.7 times the equipment cost (Armstead, Tester, 1987), this accounts for the buildings and structures, piping, insulation, engineering and legal fees. Again, these costs vary greatly depending on the scheme, land cost and plant footprint and availability of cooling water for condensation or the deployment of large and expensive cooling towers; in some cases it might be advantageous to pipe the reservoir effluent horizontally at some distance to a different site. The exact costs of individual pieces of equipment (uninstalled) can be arrived at using costing correlations and formula after the equipment is sized during the design phase.

The actual plant cost depends on the geofluid temperature; this decreases almost linearly with a unit increase in fluid temperature. Apart from increased power conversion efficiencies in the operational phase, the higher temperatures would translate into less heat exchange requirements. While some economies of scale in power plant costs exists (discussed in the next section) these are moderate and exist for plant sizes below 50 MW_e. It is the norm to give this cost in a $\$/kW_e$ basis, for a 50 MW_e instillation this can cost as much as \$ 1800 /kW_e (2001 Dollars) for a plant designed for 100 ^oC; this figure drops to about \$ 900/ kW_e for a fluid design temperature of 300 ^oC. These costs compare well with other renewable energy sources, but are more capital cost intensive than conventional fossil fuel power plants. The following figure shows this more accurately, note that the white bar shows a range of values for a technology depending on site-specific conditions; "CCT" for the gas technology refers to Conventional Combustion Turbine:

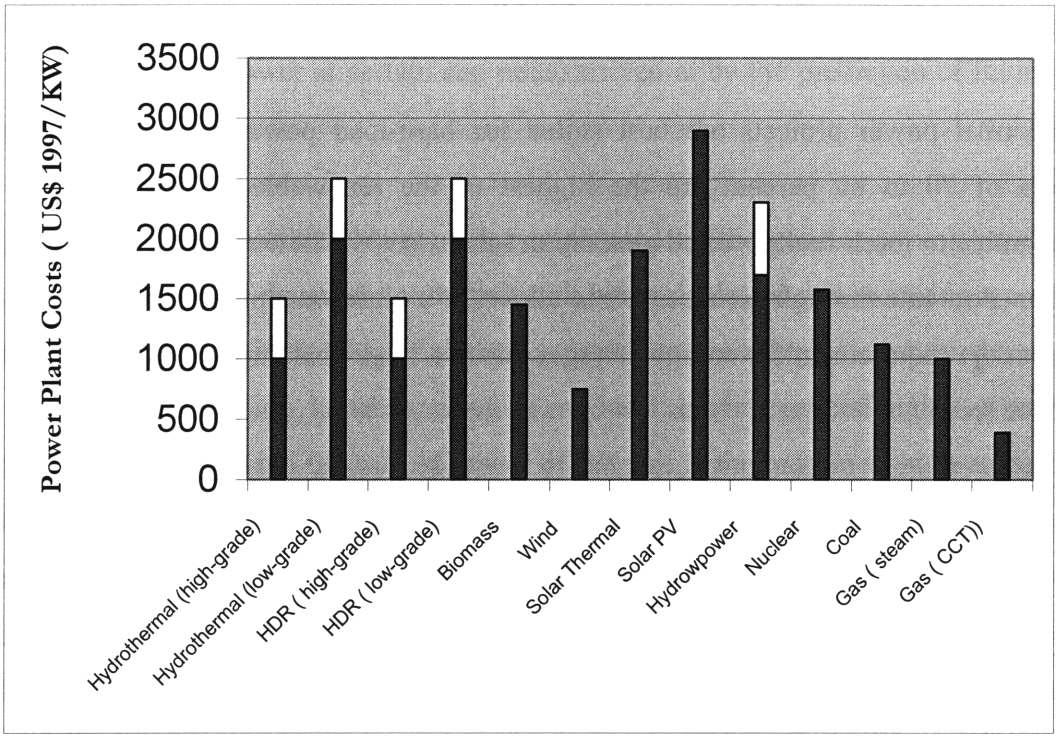

Figure 4.3 Initial Capital investment cost of power plants for different technologies

Source: EIA (1998), DOE (1998), Mock *et al.* (1997)

Finally, a brief word about operation and maintenance of a HDR project: these costs tend to be minimal typically only .03 to 0.4 ¢/kWh for high-grade HDR and hydrothermal schemes. HDR systems have a lesser problem with corrosion and fouling in comparison to hydrothermal power projects. In low impedance HDR systems, fluid pumping needs are greatly reduced and can be further assisted as a buoyancy gradient drives the hot water at the bottom of the reservoir to the top, however, it is important to manage reservoir throughput to minimize parasitic heat losses. There may well be a need for redrilling of the wells to obtain optimal reservoir performance as the cooling of the mass of rock being mined for heat would result in lower conversion efficiency; this requirement is more pronounced in low-grade HDR systems and can be costly.

4.3 COMPETITION AND FINANCE

Geothermal power projects are best suited for base-load power production; capacity factors of 70 to 80 percent are the highest of the renewable / green energies and comparable to fossil fuel powered generation schemes. It is however possible to vary the coolant flow rate through the reservoir to allow for a closer mapping of the demand load without the requirement for energy storage; this is a huge challenge in the electric utility practice today.

The availability of geothermal energy for direct heat use in industrial applications reach as high as 95 %; space heating applications have much lower availability rates due to the seasonal variation in the heat requirement and are typically at 50 % (this is very much dependent on the local temperatures, colder climes having higher rates). In direct heating applications, geothermal sources are generally more cost effective fossil fuels; at $ 30 per barrel, fuel oil, the equivalent energy cost is around $ 5.45/ 10^6 BTU. For the same heating value the cost is estimated at $ 1 to $ 2/ 10^6 BTU using HDR resources (Armstead, Tester, 1987).

Further flexibility exists in HDR systems in which actual operating temperatures can be chosen with depth to suit the particular application and increase the overall operating efficiencies. At times wells of differing depth can be drilled to allow for multiple uses if cogenerative design is not employed, apart from allowing for streams of differing temperature, this method also allows for heat mining from differing depths, better utilizing the reservoir.

The electricity produced is often sold to state utilities with the mandate of distribution of this commodity to end-users. The price of this transaction could be agreed upon ahead of time in a Power Purchase Agreement (PPA) or could be determined by real-time bids in a deregulated free market scenario in which the daily demand is accessed and power producers bid to supply the required energy. In the former case, geothermal power production may be at an advantage: not being affected by variations or instabilities in

fuel price. The recent power fiasco in California was caused by the utilities entering into an agreement to sell power at certain cap rates, arrived at by the prediction of future fuel costs which were erroneous.

In a free market, the market-clearing price is dictated by the generation unit producing power at the margin of demand, i.e. the last unit being deployed and receiving a contract for the day. This price is equal to or slightly greater than the marginal cost to operate this last unit. The exception happens when a producer having several units of varying marginal costs, tries to bid the sale of power of the unit at the margin as high as possible to affect a high market clearing price (N.B. in a power pool all units get paid this price) to reap enormous benefits on the units with substantially lower marginal costs of operation.

Alternatively, a lack of supply could mean that the expensive units used only for peak demand ("peakers") would set the price. The marginal cost (busbar cost, also known as break-even cost shown further on for different generation methods) of geothermal power is fairly well placed among the various generation technologies so as to allow a profit even in real-time bidding markets.

Table 4.1 provides ranges of levelized costs (essentially marginal costs of production), capacity factors and other possible annualized costs for a number of energy sources. Note that a discount rate of 15 % was used for these data; with single digit discount rates, geothermal energy would be much more competitive. All values are in 1997 US$ and all levelized costs are provided in ¢/kWh.

TECHNOLOGY	CAPACITY FACTOR %	capital cost ¢/kwh	O & M ¢/kwh	FUEL COST/ ANNULIZED WELL DRILLING	BUSBAR COST ¢/kWh
Coal (scrubbed)	60	3.1	0.4	0.7-4.5	4.2-8.0
Coal (IGCC)	65	2.9	0.1	0.6-3.5	3.6-6.5
Gas (Steam)	40	4.3	0.1	1.0-2.9	5.4-7.3
Gas (CCT)	65	0.9	0.1	1.1-3.2	2.1-4.2
Hydropower	45	6.5-8.8	0.2	0	6.7-9.0
Nuclear	65	4.1	0.1	0.8	5.0
Biomass (IGCC)	60	4.1	0.6	1.6	6.3
Hydrothermal (Low-grade)	75	2.3-3.4	0.3	2.0-3.0	4.6-6.7
Hydrothermal (High-grade)	75	4.6-5.7	0.4	4.0-10.0	9.0-16.1
HDR (Low-grade)	75	2.3-3.4	0.3	3.0-4.0	5.6-7.7
HDR (High-grade)	75	4.6-5.7	0.4	20.0	25.0
Wind	30	4.4	0.1	0	4.5
Solar Thermal	40	8.2	0.2	0	8.4
Solar PV	26	19.1	0.1	0	19.2

Table 4.1 Economic Characteristics of different power technologies[1]

Source: EIA (1998), DOE (1998), Mock *et al.* (1997)

Geothermal projects exhibit some economies of scale. Apart from the industrial user-operators who generally require in the region of say 5 MW_e and 30 MW_t (this mode of power supply has particular attraction in remote locations, kindly see the case studies); most suppliers to the grid tend to be 30-60 MW_e in size. Smaller projects experience a diseconomies of scale as the cost of drilling (especially in HDR systems) tends to be forbidding and larger projects absorb this in their per kW costs that tend to be in the $1000/kW and $1500-2500 / kW-built range for hydrothermal and HDR projects

[1] IGCC- Injected Gas Combustion Cycle.
CCT- Conventional Combustion Turbine

respectively. Above 50 MW_e there seems to be no more economies of scale as multiple and large turbines, as well as complex geo-fluid distribution networks, control systems and equipment need to be used; this gives rise to multiple units of power plants to be built side by side as in the case of the Geysers in California. Modularity provides additional advantages, such as better control and failure risk management.

Geothermal power projects have the disadvantage of requiring large initial capital investment. As such, the need for an institutional financier is almost always there. To obtain finance, it is often important to have a proof of the concept as well as a healthy long-term PPA with escalations to allow for inflation. There being little operational cost due to the absence of fuel purchase; the economic success of a geothermal project is then dictated to a large extent by the capital discount rate available and by the speed at which power can be drawn from the system: earlier sale of power being worth more to a t otal net present value. A problem with high throughput rates used to enhance early and larger cash flows for heat mining, is the need to further stimulate the reservoir and increasing the cross sectional areas of the fractures: while this can allow for a higher flow rate of heat exchange fluid at lower pressures, it can also lead to an underutilization of the reservoir and greater parasitic heat losses and adversely affect the projects vitality. The projects financial outcome then, apart from depending greatly on a high-grade, snag-free reservoir, is determined by long-term operational procedures and the local financing mechanism available. The large financial duration of the project (defined by and proportional to the sum of the magnitude of the required payments each multiplied by their time out from the origin or "fulcrum") means that geothermal projects can be most susceptible to volatility in capital financing rates and sometimes unviable in countries with double digit rates of interest exist.

These problems can be dealt with by creative financing. These can include issuing of long-term bonds, governmental subsidies, tax incentives and careful and prudent reservoir management. The use of back-to-back loans is an option and can result in minimal rates of interest; this option however requires even more capital. While the rate of the capital interest rate can be dictated by the currency choice, this would be suitable

for operation in countries with high interest rates, but results in a net exposure to fluctuations in the local currency which is often prone to devaluation.

Finally, there are externality benefits to the use of geothermal energy which can not at present be estimated. The first is the lack of carbon emissions, relative to fossil fuel combustion; the cost associated with carbon removal and sequestration is likely to play a part in the choice of fuel in transitioning to alternative fuels and energy sources with lower carbon emissions. (See Chapter 2). The second is the strategic advantage gained by utilizing indigenous energy, weaning the country from imported foreign oil, a commodity that has been used as a bargaining instrument for policy or be rendered expensive in collusions of international cartels.

4.4 INFLATION AND COST INDICIES

In order to account for the inflationary and technological dynamics in the geothermal industry, MIT has created two indices. The first, "The MIT Drilling Cost Index" is based on the JAS (Joint Association Survey) published data on the completion costs of drilling oil and geothermal wells, and stretching from 1965 to 1989, with 1965 being the base year at an index value of 100. The second is the MIT Composite Plant Cost Index, created from the average of four other indices: the Chemical Engineering Plant Cost Index, The Marshall & Swift Equipment Cost Index, The Nelson Refinery Cost Index (Capital cost) and the ENR General Cost Index.

The need to evaluate economic results from various years on a level, constant dollar basis then requires the expansion of this index to cover the years from 1989 to the present. Another very popular method to allow for inflation is the use of the Producer Price Indices (PPIs) described in the next section. The PPI for electricity generation in the Pacific states of the U.S. was available and compared well to the MIT Composite Plant Cost Index also produced. The PPI has a distinct advantage over other inflation-accounting systems as shall be explained.

The Producer Price Index is a family of indexes that measures the average change over time in selling prices received by domestic producers of goods and services. PPIs measure price change from the perspective of the seller. This contrasts with other measures, such as the Consumer Price Index, (CPI), that measure price change from the purchaser's perspective, as such it is more in line with the escalation of costs faced by an owner/producer of a geothermal power plant. Sellers and purchasers prices may differ due to government subsidies, sales and excise taxes, and distribution costs.

There are three main PPI categories, the two main important ones used in this theses are:

- Industry-based: The PPI publishes over 500 industry price indexes in combination with over 10,000 specific product line and product category sub-indexes. In this case the price of electricity production for Western US States on the Pacific. (without seasonal variability i.e. variability of the index in the same year)

- Commodity-based: The PPI publishes over 3,200 commodity price indexes organized by type of product and end use. This in important as in the application of a geothermal cogenerative system we will be displacing the cost of fossil fuel normally employed. The exact fuel in question is isolated and its PPI looked at; in the case analysis in Chapter 5, data on diesel fuel or Oil No. 2, a heavy, cheap industrial oil with high caloric value is considered as the energy source being displaced.

PPI data are used in escalating purchase and sale agreements. These agreements sometimes specify dollar amounts to be paid at some point in the future. Hence, it is desirable to include an increase clause that accounts for changes in input prices for the producer. PPI's also indicate price movement before to the retail level. Therefore, they may allow for the prediction of future price changes for business and consumers. The President, Congress, and the Federal Reserve use these data in formulating fiscal and

monetary policies. PPIs are also used to adjust other timer series for price changes and to translate those prices inflation-free dollars, this is of import in this thesis. Other uses include the Comparison of input and output costs, measure of price movement for specific industries and products. The abridged PPI data for electricity generation and diesel fuel, also known as "Industrial Oil No.2" are produced in Tables on the next page.

So much for the PPI, on the last page of this chapter the normalized MIT Composite Plant Index Cost Index is produced from the year 1989 to 2001. Dates preceding 1989 can be found in the July, 1990 MIT Energy Laboratory Report for the US DOE titled: "Economic Predictions for Heat Mining: A Review and Analysis of Hot Dry Rock (HDR) Geothermal Energy Technology" (Tester and Herzog, 1990). In order to correctly apply these indices, it is necessary to ascertain how much of the total HDR project cost is due to drilling and what portion represents the plant cost, the MIT Drilling and Composite Plant Cost Indices would then be used on these separate cost portions respectively to arrive at comparable pricing today.

The MIT Composite Plant Cost Index (provided on the last page of this chapter) is composed of the average of four other cost indices, namely: the Chemical Engineering Plant Cost Index, the Marshall & Swift Equipment Cost Index, the Nelson-Fara Refinery Cost Index and the ENR General Cost Index; all were normalized to 100 in 1965 for this procedure. These indices are reviewed from time to time and revisions may be made; the Chemical Engineering Plant Cost index for example had an additional productivity subcategory added to its makeup in the 1980s; in 2000 the weight ratio of some categories were revised, labor supervision, administration, engineering and executive costs were up, typist / draftsman category was removed and a CAD designer was added. The actual (not normalized) aforementioned four indices are provided in the appendix.

Table 4.2 Producer Price Index-Electric Power, Pacific Region

1988	74.7
1989	81.2
1990	89.6
1991	113.8
1992	116.2
1993	116.9
1994	117.0
1995	118.9
1996	115.4
1997	114.4
1998	113.8
1999	114.0
2000	118.8
2001	114.8*

* Based on January to June 2001, of which last 4 months were predictions

Source: Bureau of Labor Statistics, US Government, http://stats.bls.gov/blshome.htm

NASA and Johnson Space Center
http://www.jsc.nasa.gov/bu2/inflate.html

Table 4.3 Producer Price Index Commodities

Group: Fuels & related products and power
Series Id: WPU057303
Item: #2 diesel fuel

1991	65.6
1992	61.9
1993	60.5
1994	56.0
1995	57.0
1996	70.0
1997	64.5
1998	47.4
1999	57.3
2000	93.3
2001	89.2^{+}

+ Based on January to July 2001, of which last months were predictions

YEAR	CE PLANT COST INDEX	M&S EQUIPMENT COST INDEX	NELSON REFINERY COST INDEX	ENR GENERAL COST INDEX	MIT COMPOSITE PLANT COST INDEX
1989	341.7	365.3	458.2	494.0	414.8
1990	343.8	373.5	469.6	506.5	423.4
1991	347.4	379.8	480.0	517.5	431.2
1992	344.4	384.9	489.4	533.6	438.1
1993	345.4	393.5	502.2	557.7	449.7
1994	353.9	405.4	517.1	578.9	463.8
1995	366.4	419.3	533.4	585.6	476.2
1996	367.0	424.1	543.6	601.6	484.1
1997	371.6	431.3	555.2	623.5	495.4
1998	374.5	433.4	566.1	633.7	501.9
1999	375.5	436.0	573.6	648.7	508.5
2000	378.9	444.4	591.1	665.9	520.1
2001	379.1	446.4	605.2	678.9	527.4
2002	376.4	445.7	619.2	696.0	534.3

Table 4.4 MIT Composite Plant Cost Index

Derived from Tester and Herzog, (1990) and various indexes as shown above.

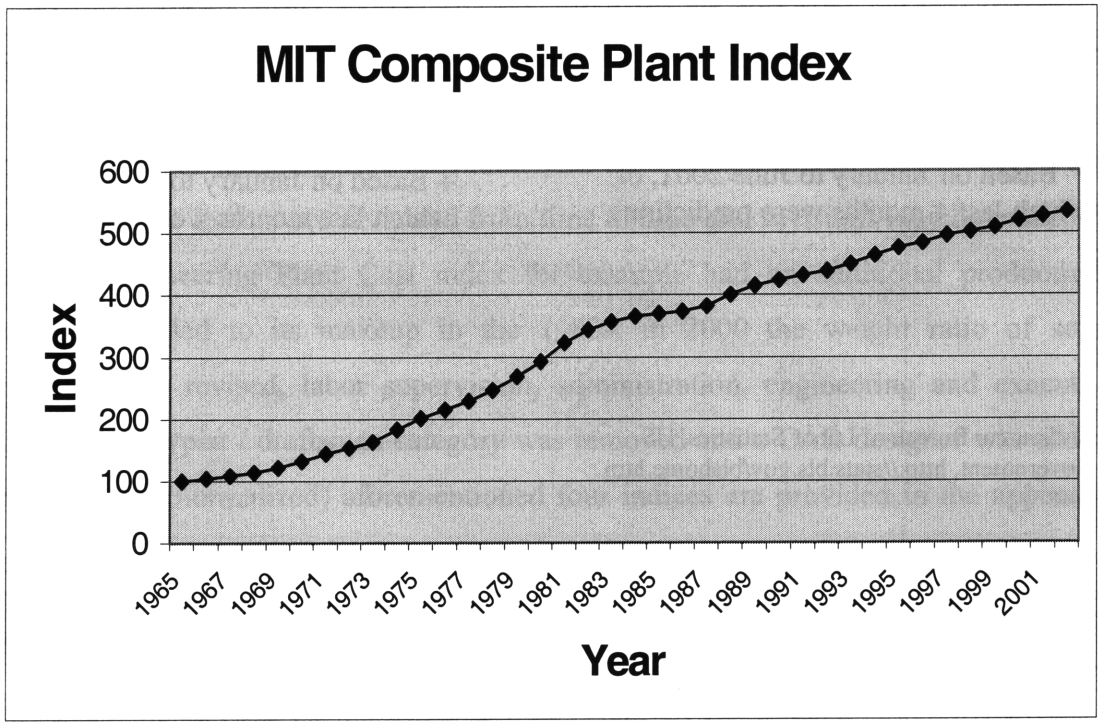

Figure 4.4 MIT Composite Plant Cost Index, 1965-2002

CHAPTER 5

HDR COGENERATION CASE STUDIES

5.1 INTRODUCTION TO CASE STUDIES

The size and seasonal variability of a heating load determine the energy and possible financial savings produced by a geothermal heating system. The variability of the heat load is rarely known from practical experience; it is often determined by models of heat transfer and physics that predict and allow for design taking environmental conditions into account.

The three cases being studied in this thesis will be approached using cogeneration designs with the analysis of their thermodynamic and economic aspects in mind. The first involves the heat requirements of a tropical fish farm in southern California, apart from the seasonal variability; this system is characterized by its large demand for low-temperature geothermal fluid and its low electric power requirement. The second case looks at the steam requirements by a pulp and paper plant; while this load may more or less be characterized as constant employing a high temperature fluid, the electric power requirements will vary greatly depending on the design of the system and the question of whether the system is a primarily a power plant with a cascade type heat load making use of the exhaust heat stream, or if in fact it's mainly a heat load with the power plant being an afterthought will arise. While this distinction seems of little import, it shades the analysis on the effectiveness of the scheme as this analysis is essentially based on a kWh cost of electricity produced less the savings that is associated with the displaced heating cost of the (secondary) load. Finally, a cogenerative district heating system is studied. While the use of space heating is seasonal, this load can be characterized as large and low to medium temperature; it is estimated that this scheme will benefit from the economics of scale more than the other examples and would therefore yield the most competitive energy costs.

5.2 TROPICAL FISH FARMING IN CALIFORNIA

In the past half century, the world's demand for seafood has steadily increased. While global demand continues to rise, supply from indigenous, wild stocks have reached the maximum sustainable output limit and in some cases over fishing has resulted in the decline of these stocks. The destruction of marine natural habitat and increased pollution are also threatening wild fish stocks as never before.

The above scenario has lead to the rapid growth of aquaculture: since 1984 aquaculture and in particular fish farming have been the fastest growing food production system globally. Today aquaculture provides 29 % of the seafood used for human consumption and according to estimates of the Food and Agricultural Organization of the United Nations; this proportion will rise to 50% by 2020 (FAO, 2000).

The subject of the first cogeneration case is the farming of tilapia, a fresh water fish native to Africa and the Middle East, using the waste heat of a geothermal power plant. Nile tilapia is a popular choice for culture conditions because of its high yield, rapid growth and mild taste. Tilapia is a warm water fish and requires water with temperatures of 25 to 30 °C, provided by heat exchange with the spent geothermal fluid or its direct introduction into the fish tanks.[2] As water quality and disease control are very important in fish farming, the use of geothermal fluids that have inherently low bacterial counts are a distinct advantage (alkalinity and salinity permitting). Controlled use of warm geothermal fluids has been known to increase aquaculture growth rates by 50-100% (Mock, Tester, Wright,1997); a by requirement is however to provide adequate aeration of the incoming fluids by agitation and air entrainment as geothermal fluids have low levels of dissolved oxygen.

---

[2] This direct use of spent geothermal fluid in the fish tanks depends on the quality and salinity of water. The California Desert Fish Farm of the Imperial Valley in Southern California pumps geothermal fluid directly into their fish tanks. The new cogeneration HDR projects in Animas Valley, New Mexico, which includes a fish farm will be looking at direct fluid introduction thanks to a layer of fresh ground water above the hot rock to be stimulated.

In order to determine heating and water load requirements for the design of an HDR cascade system involving a power plant and a 130 ton per year fish farm, some farms in the Imperial and Coachella Valleys of southern California were studied. These farms consist of installations utilizing 100-ft (30.5 m) and 30-ft diameter concrete tanks with a depth of 6 ft (1.83 m) and 4 ft (1.22 m) respectively, to produce tilapia; supply of water and heat is achieved through tapping geothermal aquifers. Geothermal fluids, after sedimentation and particulate separation, are introduced into cooling reservoirs and then directly into the fish-tanks.

Fish yields for a 100 ft diameter tank of 6 ft depth is typically 2,600 kg/ month. This would amount to a specific yield of:

$$\frac{\text{Output rate}}{\text{Volume}} = \frac{2600 \text{ kg /month}}{(100/2)^2 \pi (1.8)} = 0.184 \text{ kg/ft}^3\text{/month} \qquad \textbf{(5.1)}$$

$$= 1.98 \text{ kg/m}^3\text{/month}$$

Data from a 130-ton operation California Desert Fish Farm Inc, indicates that for this level of production two 60-ft by 15-ft rectangular tanks, eight 30 ft diameter tanks and another eight 100-ft diameter tanks are required. Yields are lower than expected in this specific case because of the limited geofluid flow rate, although using airlifting techniques the flow rate can be enhanced.

5.2.1 Fish Farm's Heating Requirements

A fish farm's energy requirements are dependent on the ambient temperatures that vary with season: hence the variability of this load. In order to estimate this load monthly, some calculations based on data available for the heat use in the coldest month is utilized, this essentially equal to the flow rate of hot fluid multiplied by its heat capacitance and the temperature differential between the tank and the hot fluid. This single reference point is equal to the heat loss by the tank at equilibrium and could be used to yield an average heat transfer coefficient that may then be used for the calculation of heat loads in other months, having the respective ambient temperatures at hand. It should be noted that some assumptions are made to allow for the employment of this method. First it is assumed that this heat transfer coefficient is invariant with temperature; for the range of operation and ambient temperatures considered this is acceptable. Second: although the fish tanks have a slight slope at the bottom forming a shallow cone and allowing for easier drainage, surface areas are calculated based on the assumption that these tanks are cylindrical and include an open top; the error in calculating the surface area from this approximation is minimal, the fact that one face of the tank is open to the air and the other surfaces are partially underground means that the former surface will experience heat loss via convection and conduction while the latter losses heat to the earth via conduction, barring big changes in seasonal wind speeds at the surface (fish farms in colder climes are housed in an enclosed greenhouse like environment) there should be minimal variation on the heat transfer coefficient, furthermore since we are only concerned with an "average" heat transfer coefficient for the whole farm, differences in ambient conditions should not matter.

Lastly it is assumed that the fluid in the tanks is homogeneous and that the sink temperatures are the same as the ambient air temperatures and the system operates at steady state; after the direct introduction of geothermal water into the tanks, motorized paddles are used to mix the fresh water and create aeration in the vessels and so the condition of homogeneity is fulfilled, the tanks are no more than a few feet underground and hence there will be minimal variation of sink temperature with depth, a steady-state

operation means that there are no heat storage requirements and that the heat from the geothermal fluid is equal to the heat lost by the tank. This gives rise to the relationship on the next page:

Heat Lost = Heat provided by the geothermal fluid

$$\langle U \rangle \cdot A \cdot \Delta T_2 = F \cdot \rho \cdot C_p \cdot \Delta T_1 \quad \textbf{(5.2)}$$

Where:

$\langle U \rangle$ is the average specific coefficient of heat transfer, $Wm^{-2}K^{-1}$

A is the surface area of the all tanks, m^2

ΔT_2 is the difference in temperature between the water inside the tank, T_2 (77 °F, 25 °C) and the ambient air temperature in January, T_3 (54 °F, 12.2 °C), °C

ΔT_1 is the difference in temperature between the geothermal exhaust fluid from the power plant, T_1 (149 °F, 65 °C) and the water inside the tank, T_2 (77 °F, 25 °C), °C

F is the volumetric flow rate of geothermal fluid into the tank, 32.2 L / s

ρ is the density of the geothermal fluid roughly 1,000 kg/ m^3

C_p Heat capacity of geothermal fluid at constant pressure, 4,200 $Jkg^{-1}K^{-1}$

Heat provided by the geothermal fluid $= (32.2 \times 10^{-3}) \cdot (1000) \cdot (4{,}200) \cdot (65 - 25)$

$= 5.41$ MW

Also,

$A = (\pi R_1^2 + 2\pi R_1 H_1) \cdot 8 + (\pi R_2^2 + 2\pi R_2 H_2) \cdot 8 + 2 \cdot$ (surface area of rectangular pool)

$= 14{,}904\ m^2$

This gives the average specific coefficient of heat transfer, U as:

$$<U> = (5{,}410{,}000)/(14{,}904)\cdot(25\text{-}12.2) = 28.4\ Wm^{-2}K^{-1} \quad \textbf{(5.3)}$$

This value is about two orders of magnitude greater than low thermal conductivity walls used in extreme cold climes for housing (which is equivalent to 1.8 m thick ceramic wall k= 0.28 $Wm^{-2}K^{-1}$. But this is expected as, <U> is the average heat transfer coefficient which includes conduction and convention. While <U> will vary because the top surface of the tank is open to convention, it is calculated based on the coldest months when heat transfer at the surface is at a maximum; consequently heating needs calculated from <U> represent a maximum that nevertheless should be made available if required.

Using this value of the heat transfer coefficient and the average air temperatures for Imperial Valley in Figure 5.1, and the temperature of the tank (25 °C): the monthly variable heat load for the fish farm in Imperial Valley is arrived at, the result of these computations are provided in Table 5.1 on the following page. As an example, the average ambient temperature is 65 °F (18.3 °C) in Imperial Valley in the Spring. This means that the load required for this period is:

$$U \cdot A \cdot \Delta T_2 = 28.4 \cdot 14{,}904 \cdot (25 - 18.3) = 2.83\ MWt$$

Figure 5.1 Normal Annual Temperatures for Imperial Valley, CA
Source: www.weatherunderground.com

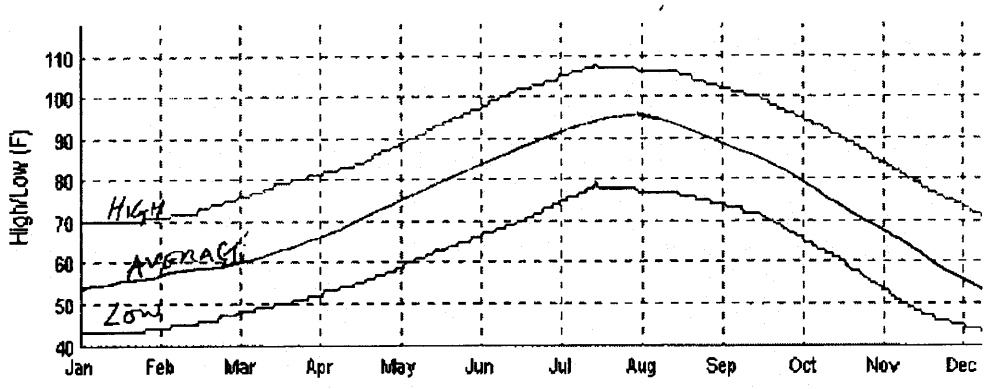

MONTH	AIR TEMPERATURE, °C	HEAT LOAD, MW	TOTAL ENERGY SUPPLIED, GJ
January	12.2	5.40	13,996
February	13.9	4.68	12,137
March	15.6	3.97	10,278
April	19.4	2.36	6,123
May	23.3	0.72	1,859
June	28.3	0.00	0
July	33.3	0.00	0
August	34.4	0.00	0
September	31.1	0.00	0
October	26.7	0.00	0
November	19.4	2.36	6,123
December	12.4	5.32	13,777
TOTAL			**64,292**

Table 5.1 Estimated heat load requirements for a 130-Ton Fish Farm in Imperial Valley, CA

5.2.2 Design of Power Plant

With the heat requirements of the fish farm identified, the design of the power plant can be undertaken. The constraint on this design is then for the exhaust streams of the power plant to meet the variable power needs of the farm, this requires an iterative approach to power design optimization that will be illustrated below.

In actuality, the design needs to be optimized for performance and economics, taking the drilling of HDR wells into account. This optimization would be a very involved and tedious if done by hand; thankfully the use of the EGS 1 (Enhanced Geothermal

Systems) simulator developed in the MIT Energy Laboraotory by Herzog, Tester and has automated the optimization. The inputs and dynamics of this tool are described later.

For the purposes of the thermodynamic design, it is assumed that hot water at 32.2 kg/s is available (this is the design flow rate from the fish farm) at 600 °F (315 °C) and a high pressure of 1550 psia (106 bar). These conditions are not unusual for closed-loop HDR systems that operate at high pressures and use circulation pumps (down-hole or surface) albeit the temperature is pushing the upper limit of viable operation for HDR systems. This high-grade liquid resource is then flashed to lower pressure to generate a saturated steam phase that is used to operate a turbine. Generally speaking, for high temperature (>250°C) operation, flashing is the most economic mode of energy transfer and in lower-temperature (<250°C) systems the use of organic Rankine cycles with low boiling point working fluids is favored.

At 600 °F, a single flash and separation stage does not yield the optimal steam production and flow rate; flashing the liquid effluent from the first separator yield further steam for input to the turbine. The exhaust temperature was set at 37.7 °C, this was done for two reasons: first, this would allow for a second flash stage at positive pressures due to the higher second phase flash and would therefore simplify matters by not requiring a compressor to pump out the steam produced; second, it was important that there be enough energy for the fish farm during this one iteration done by hand to demonstrate overall calculation approaches.

For maximum power output, the first partial derivates of the sum of total power obtainable from flashing stage 1 and stage 2 flash process with respect to the two flash temperatures T_1 and T_2 are set equal to zero and solved simultaneously to find the optimal flash temperatures (see Milora, Tester (1976), Appendix A for a full description of the terms and explanation of this method).

Then the below relationship satisfied and simplified yield the following solutions:

$$\partial(P_1 + P_2)/\partial T_1 = 0 \quad \text{and} \quad \partial(P_1 + P_2)/\partial T_2 = 0 \qquad \textbf{(5.4)}$$

Where P_1 and P_2 represent the power obtained from the steam produced in the first and second flash stage. The solutions that satisfy equations 5.2.2a are provided below:

$T_1^{opt} = (T_o T_{in}^2)^{1/3}$ Note that the temperature should be in an absolute scale, either degrees Rankine or Kelvin

$T_1^{opt} = [(37.7 + 273) \cdot (315.5 + 273)^2]^{1/3}$

$T_1^{opt} = 475$ K (202.6 °C, 396.8 °F) Optimal flash temperature for stage 1

And

$T_2^{opt} = [T_o T_1^{opt}]^{1/2}$

$T_2^{opt} = [(37.7 + 273) \cdot (475)]^{1/2}$

$T_2^{opt} = 384$ K (111 °C, 232 °F) Optimal flash temperature for stage 2

The second flash specifications are then used to arrive at the gaseous and liquid phase separations as shown by the calculations below and it is then seen if the ensuing exhaust streams satisfy the needs of the fish farm, failing which other values close to the optimal flash temperatures are used and the process described repeated; as such this is an iterative process.

The flash process is assumed to be isenthalpic; a mass and enthalpy balance, solved simultaneously then give the gaseous and liquid mass flows:

$$m_{total} = m_{gas} + m_{liq} \qquad \textbf{(5.5)}$$

and

$$m_{total} \cdot H_l(T_{in}) = m_{gas} \cdot H_v(T_1^{opt}) + m_{liq} \cdot H_l(T_1^{opt}) \quad \textbf{(5.6)}$$

where m_{total} is the mass flow of the fluid from the well head, 70.8 lb/s

m_{gas} & m_{liq} are the gas and liquid flow rates respectively, lb/s

$H_l(T_{in})$ is the specific enthalpy of the stream in at 600 °F and 1550 Psia, 618 Btu/lb

$H_v(T_1^{opt})$, $H_l(T_1^{opt})$ are the specific enthalpy of the gas and liquid streams that exit the separator at 396.8 °F and 240 Psia and are 1200 Btu/lb and 372 Btu/lb respectively

Substituting values and solving simultaneously:

m_{gas}	=	21 lb/s	or	9.54 Kg/s	
m_{liq}	=	49.8 lb/s	or	22.6 Kg/s	**(5.7)**

The first flash stage converts some 30 % of the geothermal wellhead fluid into steam, this is fed into a condensing turbine to produce power. The hot water from this first stage may be flashed further to produce additional steam, this stream becomes the feed into the second separator that for an overall optimal power output should flashed at 232.7 °F. A similar calculation as in the above example is carried out for the second flash stage, the results of the issuing streams from the second stage are then:

m_{gas2}	=	8.91 lb/s	or	4.05 kg/s	
m_{liq2}	=	30.2 lb/s	or	18.6 kg/s	**(5.8)**

An exit pressure of 20.5 psia (1.4 bar), results from the first isenthalpic flash steps producing saturated steam that is fed into the second stage of a condensing multistage turbine that produces a liquid effluent just below atmospheric pressure. The key parameter to be varied now is the exhaust conditions at the turbine; this determines on the one hand the power output from the turbine and on the other the available heat for the fish farm.

The outlet pressure is easy to choose: atmospheric exhaust ensures a high power output from the turbine (the system can also operate at negative or back pressures which would yield more power from the turbine, however the cost implications and the variance with the EGS model that does not consider negative pressure conditions as potential solutions makes this exercise redundant). Likewise, the lower the outlet temperature, the more power generated from the turbine; there are however two constraints on the setting of this temperature, first the exhaust rejection temperature can not be less than the ambient temperature which varies seasonally, second if this rejection temperature is too low, the needs of the fish farm may not be met.

The approach would then require the choice of a temperature, the satisfaction of the two constraints (and iteration if this temperature was not adequate) and then the calculation of the power output from the turbine at this temperature. It is assumed that we have the capability of controlling our exhaust temperature to suite ambient temperatures. For the purposes of the power calculations, since the variance in temperature is small at about 20 ^{o}C with an average of 22.5 ^{o}C, this average is used to make power calculations (special care should be taken to make sure that in the winter month where exhaust temperatures are lowest at 12 ^{o}C and heat requirements are highest in the farm, these needs are met). In warmer months it is common practice to use a cooling pool to get the geothermal fluid to the right temperature before it enters the tanks; this is seemingly a waste of energy, however it is the most economically viable solution when dealing with a small variable load. In the summer months when heating is not required, the exhaust stream may also be shunted to a bottoming cycle to produce electricity. However, due to rather low exhaust temperature this will likely prove to be inefficient and expensive.

The streams that heat the farm are then the hot liquid from the second separator at 111 °C and the condensed fluid from the turbines at 22.5 °C. The set-point for the tank temperature being 25 °C this then yields the following net energy transfer to the tanks. Heat from the fluid from separator:

$$m_{liq2} \cdot C_p \cdot \Delta T_1 = 18.58 \text{ kg/s} \cdot 4200 \text{ J/Kg °C} \cdot (111 \text{ °C} - 25 \text{ °C}) = 6.71 \text{ MW} \quad \textbf{(5.9)}$$

Heat from the condensed turbine fluid:

$$(m_{gas} + m_{gas2}) \cdot C_p \cdot \Delta T_1 = (4.05 + 9.56) \cdot 4200 \cdot (22.5 \text{ °C} - 25 \text{ °C}) = -0.143 \text{ MW} \quad \textbf{(5.10)}$$

At first it may not be obvious why we introduce a stream with a negative thermal load contribution to the fish tanks: the need for a minimum water throughput to maintain the health of the aquaculture makes this necessary. In the coldest month in January when the ambient temperature and hence the turbine exhaust temperature is 12 °C (to maximize the turbine power), this results in a negative thermal load stream of about 0.743 MW being released from the tanks. The resulting net energy inputs into the fish tank based on the average and coldest month are then 6.57 MW and 5.97 MW respectively. Both these values exceed the 5.4 MW peak requirement of the fish farm, so the heat requirements of aquaculture load are met.

Since it is not possible for the turbine rejection temperature to be below the ambient temperature, this also becomes the optimal operating temperature for the power plant (i.e. 22.5 °C on average). There are several methods of calculating the power output from the plant, the most straightforward is reproduced here, based on appendix 'A' from Milora and Tester (1976), the power for the first stage P_1 is given by:

$$m_{gas} \cdot (C_p / H_{fg}) \cdot (T_{in} - T_1^{opt}) \cdot \eta_t [C_p \cdot (T_1^{opt} - T_o) - T_o \cdot C_p \cdot \ln (T_1^{opt} / T_o) + H_{fg}(1 - T_o/T_1^{opt})] \quad \textbf{(5.11)}$$

H_{fg} is the heat of vaporization from liquid to gas at the flash conditions at 829 Btu/lb (1928 KJ/kg). Note that temperature values need to be given in absolute terms: degrees Rankine or Kelvin. The turbine efficiency for the first stage is represented by η_t, and can be obtained from Figure 3.4. Since the efficiency is a function of the turbine power as well as pressure, we need a first an initial average guess at this power, this gives the approximate horsepower of the turbine and hence a more accurate efficiency reading. Initially η_t is set to unity, which then gives us an order of magnitude value of P_1 and this together with a turbine inlet pressure of 188 psig(12.9 bar) yields an efficiency of 70 %.[1] Using this efficiency value:

$$P_1 = 2.47 \quad MW \qquad \textbf{(5.12)}$$

The power generated from the steam second flash separator fed into the second turbine stage is given by the term below:

$$P_2 = m_{gas2} \cdot C_p \cdot \eta_{t2} [\, 1 - (C_p / H_{fg2}) \cdot (\, T_{in} - T_1^{opt}) \,] \cdot [(T_2^{opt} - T_o)/(T_2^{opt})] \cdot [T_1^{opt} - T_2^{opt}] \qquad \textbf{(5.13)}$$

$$P_2' = 0.466 \text{ MW}$$

The efficiency for the second turbine stage is difficult to determine due to the operation of this stage at about 20 psia (1.4bar) (no curves for such a low pressure), furthermore with the first pass calculation of power, with η_{t2} set at unity, giving a value of 0.67 MW, this power rating is also off the graph. However, while it is true that efficiency drops with the reduction in the turbine power rating for steam, it does increase with a drop in pressure in this region as the Figure 3.4 in Chapter 3 suggests.

[1] An initial value of 3.5 MW, which translates to 4,700 hp yields an efficiency of 71 % on the 200 psig curve. The power is then multiplied by this efficiency and a new horsepower rate obtained, this value is then employed in finding a second efficiency reading (about 70 %) and the iterative cycle is carried out until there is very little change in efficiency readings in each iteration which happens at around 69 % efficiency.

The second stage efficiency was assumed to be similar to that of the first turbine stage ie 70 %. This results in an output of 0.466 MW from the second turbine stage. Note that the heat of vaporization H_{fg} varies with temperature and this value depends on the flash conditions: in this case H_{fg2} is equal to 959 Btu/lb. (2,230 kJ/kg)

5.2.3 Cost Savings From Fish Farm Cogeneration

The usual mode of heat supply for fish tanks in the aquaculture industry is achieved through the use of cheap feed-water boilers. These units are fossil fuel operated employing natural gas, propane or oil. In some rare cases (ornamental fish farming) the use of electric heating elements maybe preferable because of the small scale of the operation and the easy control of an electric heating system, albeit this would be less energy efficient and more expensive.

In this case we shall consider a simple oil-fired boiler. These are available in many forms and power ratings a selection of which can be seen online on the Nationwide Boiler Inc. (www.nationwideboiler.com) or Parker Boilers (www.parkerboiler.com). A water tube boiler with an output capacity of 8000 hp of power can be assumed to have an overall fuel efficiency of 75 % (ASME). Note that the actual cost of the boiler is thought to be minimal (about $7,000) as it operates under atmospheric conditions and would only need to heat the fluid some 15 ^{o}C at most, requiring a very small unit (short residence times).

Diesel fuel ("industrial No.2") is one of the cheaper sources of fossil energy and retails for about USD 40.00 per barrel (42 US gallons/barrel (bbl). At 5.2 million Btu per barrel (Perry *et al*, 1984) (5.486 GJ /bbl) and the aforementioned efficiency we would require:

Heating cost = $\frac{\text{(Yearly fish farm heating requirement) x (Price per barrel)}}{\text{(energy per barrel of oil) x (boiler efficiency)}}$

Heating cost per year = $(64{,}292 \times 10^9) \times (\$40/\text{bl}) / [(5.486 \times 10^9) \times (75\%)]$

= **USD 625,000 (2001 dollars)** **(5.14)**

In order to be able to incorporate this cost into the EGS model's (described in the next section) operation cost, it must be converted into 1997 dollars. This is achieved by using the PPI Commodities indices for 1997 and 2001 from Table 4.3.

1997 Fuel displacement value = $625,000 x 64.5/89.2

= **USD 452,000 (1997 Dollars)** **(5.15)**

NEXT PAGE

Figure 5.2 Design Schematic of a Dual-Flash 600 ^{o}F Geothermal Power Plant

GEOTHERMAL DOUBLE STEAM FLASH- 600F SOURCE

5.2.4 EGS Modeling and Optimization

The foregoing calculations are based on a specific inlet temperature for geothermal fluid and the power optimization of that resource. In reality, there is large range of solutions as many possible operation temperatures based on drilled rock depth exist. To find an optimum in this space of solutions the use of a computer model that uses constraints based on power and economics is required. The locus of an optimum lies in balancing the costs of drilling, that increase with depth; and power plant costs that tend to decrease with the temperature grade of the resource and hence depth.[2]

EGS Modeling is a computer-based simulator developed by the MIT Energy Laboratory. It is used in the technical and economic analysis of geothermal power systems and can optimize (given user inputs) as well as simulate such systems. Input parameters include: reservoir characteristics such as temperature gradient, depth, engineering parameters that deal with flow rate, well diameter and well pattern. Other parameters deal with macro and micro financial and economics of the simulation.

Optimization runs are carried out for 3 different grades of HDR resource termed as *High*, *Medium* and *Low*, corresponding to temperature gradients of 80, 50 and 30 °C/km respectively. Variation in draw-down rates are also investigated in these runs by the investigation of two particular scenarios: no draw-down (i.e. no temperature decline in the reservoir with operation); and a draw-down corresponding to roughly 4 % drop of the reservoir temperature in the first ten years; this corresponds to a drawdown parameter of 0.00006 kg/m^2-s. The detailed output of these runs is provided in the appendix of this thesis. Table 5.2 shows the system inputs for these runs:

[2] Beyond a certain optimal power plant temperature, the costs of the power plant increases with increased geothermal fluid temperature.

IMPERIAL VALLEY HDR FACILITY	
Power Plant Capacity Factor (%)	90
System Configuration	Doublet
Injector and Producer Well Casing ID (in)	7
Thermal Gradient (^{o}C/km)	30, 50, 80
Drawdown Parameter (kg/m^2-s)	0.00006
Reservoir Impedance (GPa-s/m^3)	1.57
Water Loss Rate (%)	2
Production Well Flow Rate (kg/s)	32.2
Water Reinjection Temperature (^{o}C)	22.5
Pump Efficiency (%)	80
Drilling and Completion Technology Level	Commercially Mature
Project Life (years)	20
Fixed Charge Rate (%)	15
Accrued Financing During Constr. (%)	9

Table 5.2 EGS Simulator design parameters for Fish Farm Cogeneration

5.2.4 Results and Analysis

To appreciate the analysis fully we will examine both economic and thermodynamic aspects of the simulation runs.

Economics

The busbar cost of the electric power produced is used as the yardstick for the evaluation of various scenarios. In order to account for the benefits of cogeneration design of the fish farm, the displacement cost of the fuel to heat the fish tanks is deducted from the maintenance cost of the power plant and inserted directly into the EGS model; this then gives rise to a new busbar cost which is slightly lower than the case with no cogeneration.

Busbar costs calculated by the model are in 1997 dollars, to bring this to the present day dollar, the PPI for power generation in the Pacific US is used. The indices for 1997 and 2001 are 114.0 and 114.8 respectively; we would then multiply 1997 busbar costs by 1.007 to arrive at 2001 costs. The MIT Composite Plant Cost index for the same period are 495.4 and 527.4 that yields a factor of 1.06. These ratios compares well, so we used an average value of 1.03 in the simulation. Table 5.3 below shows results:

Temperature Gradient °C / km	Drawdown Parameter kg/m^2-s	Well Depth km	Net Power MW	Electricity Busbar Cost, cent/kWh (2001)	Electricity Busbar Cost, Cogeneration cent/kWh (2001)
30	0	7.8	3.00	69.3	67.4
50	0	6.3	6.26	21.0	20.0
80	0	3.9	5.70	12.6	11.4
30	0.00006	7.8	3.06	85.5	83.2
50	0.00006	6.3	6.26	25.2	24.1
80	0.00006	3.9	5.70	15.2	13.8

Table 5.3 EGS Simulator Results with and without Fish Farm Cogeneration

The breakeven electricity prices in the table are fairly high. This can be attributed to the small power plant producing well under 10 MW and hence suffering from diseconomies of scale as described in Chapter 4. It is interesting to note that optimal economics does not equate the highest power output as is shown by the 50 °C/km. Note that the optimal well depth drops drastically with the increased temperature gradient; this shows in a word the economic difficulties faced in viable use of low-grade HDR resources globally. Figure 5.3 shows the economic results in terms of busbar costs for the 3 grades and in different reserve performance levels.

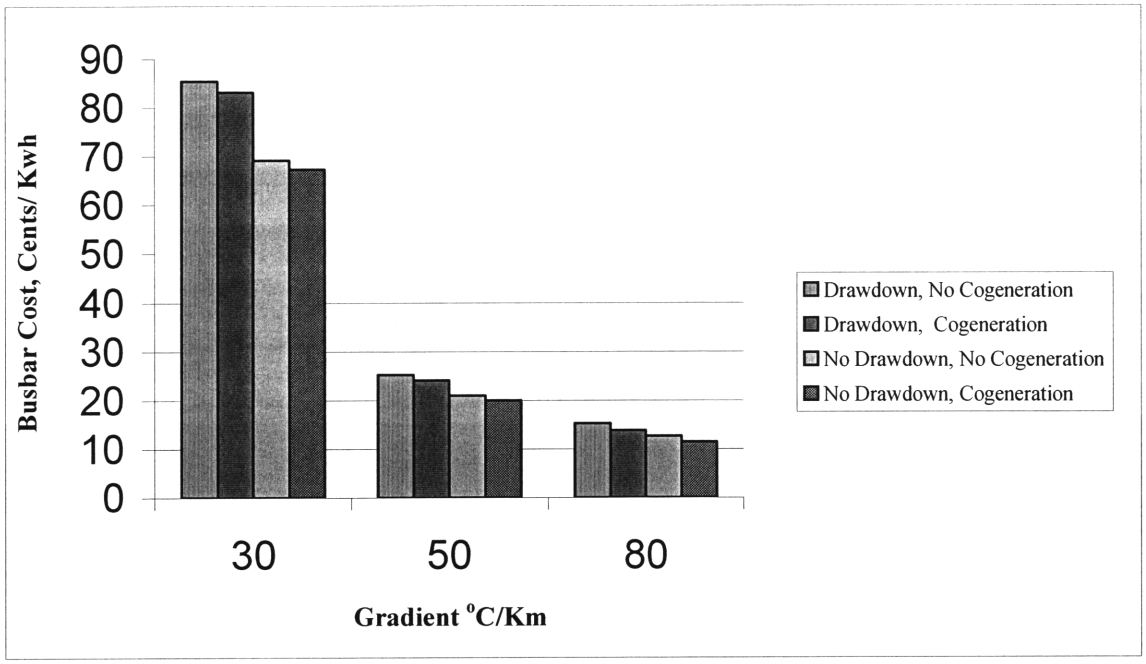

Figure 5.3 Electricity Busbar Costs for Fish Farm Cogeneration Case

Figure 5.3 shows that there is little advantage to the cogenerative feature in supplementing and lowering electricity busbar costs. The average heating need is no more 2.07 MW_t per month; while this is in the same order of magnitude as the electrical power produced, the cost of fuel displaced and heat provided by that is miniscule in comparison to the cost of electricity production. Hence, the offset from cogenerration makes little difference to the busbar electricity price.

The biggest difference is exhibited by the drawdown effect of the reservoir being most pronounced in the 30 °C/km case even given that the drawdown rate is very modest with a drawdown parameter of 6×10^{-5} kg/m^2s.

Thermodynamics

The thermodynamic efficiency of power production is normally measured by one of two techniques. First the utilization efficiency, η_u, is a measure of power or work efficiency given the constraints of the second law of thermodynamics i.e. it is the actual power obtained in comparison to the maximum power attainable (theoretically given the 2nd law limits). Hence:

$$\eta_u = P_{net} / P_{max} \quad \textbf{(5.16)}$$

P is equal by the availability change ΔB multiplied by the mass flow rate of geofluid. The availability change given by $\Delta B = \Delta H - T_o \Delta S$ that measures the change in enthalpy and entropy from the geofluid at the well head to a specified ambient or 'dead-state' condition, T_o. Availability values are calculated and reported as output by the EGS model. Alternatively, they can be calculated by hand using thermodynamic properties of saturated water at T_{gf} and T_o

The second efficiency that is particularly useful for cogeneration cycles is aptly called the "cycle conversion efficiency", η_c. This is a measure of total work and heat utilized versus the total heat available. η_c in the strictest sense normally considers only the mechanical output; however in order to consider the advantage of cogeneration, the heat output may also be added to the work done to arrive at an overall cycle efficiency.

$$\eta_c = P_{net} / Q'_H \quad \textbf{(5.17)}$$

Note that Q'_H is heat rate and is equal to the mass flow rate of geofluid at the wellhead multiplied by ΔH under the limits of change mentioned above. As such, η_c will obviously yield a lower efficiency than η_u for heat engines and turbines or any system where work from heat is obtained, but has the advantage of showing the effect of obtaining additional cogenerative energy from the system in the form of heat or further work, i.e. the average heating need of the farm, 2.07 MW is added to the electrical power produced to obtain P_{net} in this case. Table 5.4 shows these efficiencies for the HDR –Fish farm cogeneration

scheme. Note that η_u only shows the efficiency is expressed for power production, whereas η_c the cycle efficiency is expressed for power production with and without cogeneration.

Temperature Gradient °C / km	Optimum Geofluid Temperature °C	Net Power MW	Utilization Efficiency η_u	Cycle Efficiency Without cogen η_c	Cycle Efficiency With cogen η_c
30	212	3.00	52.4 %	11.8%	20.7%
50	279	6.26	60.8%	18.9%	25.2%
80	257	5.7	59.5%	19.1%	26.8%

Table 5.4 Thermodynamic Efficiencies for Fish Farm Cogeneration Case

As expected, the higher-grade resource had a higher utilization efficiency. It is interesting to note that the EGS economic optimization for the 80 °C/km gradient resource yielded a temperature substantially lower than that of the 50 °C/km gradient resource, consistent with the fact that the optimal economic condition occurs at a relatively shallow depth.

Cycle efficiencies, albeit very low, all benefited from cogeneration; in particular the efficiency of the low-grade resource benefited most, almost doubling. While this is encouraging from a technical point of view, it had little impact on the economics of the process as energy types have different prices. The cases with drawdown have similar utilization and cycle efficiencies at the start of production however wellheat geofluid temperatures and availabilities were not available after a long period of operation to specify efficiencies. Typically, efficiencies would drop with a decrease in reservoir temperature and wellheat temperatures from the levels provided above.

Finally, it should be born in mind that these results, apart from depending on the resource and economic factors assumed vary greatly with environmental conditions, particularly the ambient temperature.

5.3 PULP AND PAPER MILL IN NEWZEALAND

Pulp and paper is the second most energy intensive product industry in the world averaging some 21 MJ per dollar of product manufactured. In the US, about 12 % of the total manufacturing energy is drawn by pulp and paper mills. Furthermore, paper is one of the few products for which per-capita demand has not saturated in the United States, having grown by an average of 1.7 % from 1960 to 1990 and is projected to continue demand growth at 0.6 % per annum per capita until 2040 (Nilsson, Larson, Gilbreath, Guptta, 1995).

Pulp mills are complex and large, the economies of scale have meant the closing of old facilities replaced by new larger and more energy efficient units. Plants today employ 40 % less steam and 5 % less electricity compared to schemes from the early eighties. The largest single commodity used in a pulp mill is wood, with energy being a close second at 17 % by cost; however, much of the spent pulp and liquor is used in biomass cogenerative steam production that is not counted towards the energy purchase needs, so in actuality energy is the most used commodity in a mill.

The energy use in a pulp mill is basically supplied in two modes: electricity and steam. Electricity is used in high yield mechanical pulping processes (little development has happened in this area because of its cost), pumping, air-handling, control systems and lighting. The use of steam and direct heating is much larger in comparison and is employed in drying and black liquor concentration in evaporators and of course pulping in solution with chemical additives.

The electricity-to-heat production ratio of conventional back-pressure steam turbine systems ranges from 1 / 6 to 1 / 4. This ratio is appropriately matched for the pulp and paper industry use. Furthermore, new energy efficiency projects compete with other new schemes in a pulp mill and unless the new energy technology has a shorter payback period; under these conditions, it will get shelved in favor of other faster payback projects: a common trend in the eighties and early nineties. Today, with the recent rise in

fuel prices, energy efficiency is beginning to become the watchword for industry. With the era of utility deregulation, the pulp mill has started becoming the archetype of the user- operator; many experts feel that within two decades mills will gain as much from selling excess energy to the grid as they would from the pulp business.

During the last 20 years the US DOE has funded a variety of R&D projects aimed at improved drying techniques, energy efficiency and black liquor gasification for power production; it is thought that the latter technique, when viable, will drastically reduce the need for the purchase of energy by mills. There is also pressure on the industry that has a reputation for pollution, to clean and lessen its gaseous and aqueous discharge, under guidelines from the EPA. (Nilsson, Larson, Gilbreath, Guptta, 1995)

This case study addresses whether HDR geothermal is suitable for supplying energy pulp and paper industry. Key issues include the nature of future fuel markets, the stringency of forthcoming environmental measures and the development of the next generation of more efficient cogenerative-biomass technologies; it should be possible to see if an HDR solution falls in the ballpark of possible implementable energy efficiency technologies being undertaken by pulp mills of today.

5.3.1 The Electrical and Geothermal Industries in New Zealand

Up until the late eighties, New Zealand's power was supplied by utilities managed by the central government. A new public owned body known as the Electricity Corporation of New Zealand (ECNZ), under private management, took on supply of power reducing costs substantially. Local companies found it hard to compete with ECNZ and two acts in 1996 and later in 1998 unbundled and deregulated the electricity market giving birth to a host of energy companies, among them Contact Energy that inherited geothermal power generating assets in Wairakei and Ohaaki. The Wairakei field has been in operation since 1942, its output however is reducing by some 4 % per year. Kawerau, another productive

field and the subject of this case study is located just west of the Bay of Plenty in Eastern New Zealand as shown by the map below:

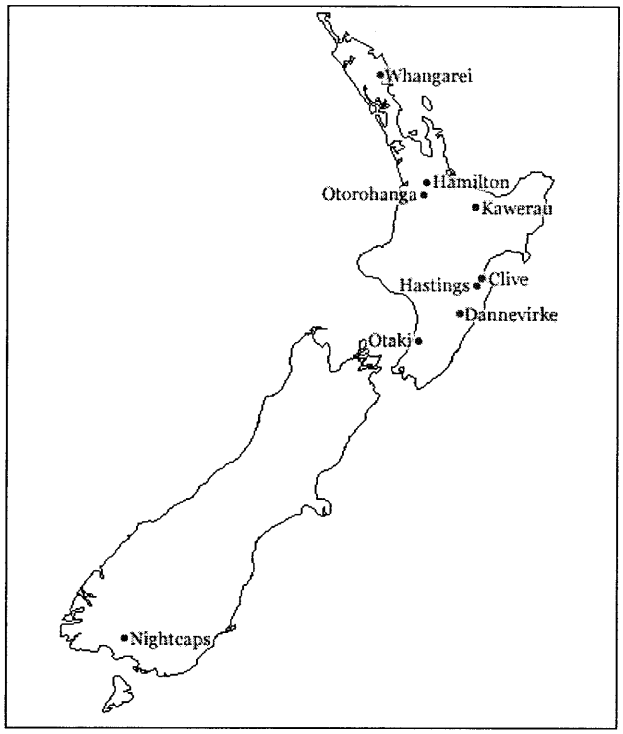

Figure 5.4 Map of New Zealand showing Kawerau

While the general elections of 1999 resulted in the instatement of the center-left government and the indefinite deferment of the electricity privatization process, there has been an encouraging addition to the nations installed renewable energy generating capacity: 154 MW of geothermal, 39 MW of wind and 8 MW of landfill biogass in the last 5 years.

Geothermal power production accounts for 15 % of New Zealand's total power output. High-grade liquid dominated fields in Wairakei, Ohaaki and Kawerau amongst a half a dozen different sites have been very economically harnessed for generation, the projects costing no more than $ 1000 /kW_e (1995 Dollars). In New Zealand, a variety of direct-use applications using geothermal heating exist, the largest of these is a 210 MW_t industrial process heating operation with a capacity factor of 83 % will be similar to our

pulp and paper case study; Malaysian prawn farming and alpha-alpha drying are other direct use applications exhibiting much lower capacity factors and power requirements.

5.3.2 Steam Requirements at the Fletcher Paper Mill, Kawerau, NZ

The Fletcher paper mill is a kraft pulp mill located in Kawerau has a huge and complex energy demand. The electrical needs of the plant are some 180 MW and are partially produced by the burning of black liquors and waste wood ("hog") in boilers that produce 400 ^{o}C steam at 45 barg, this also meets some 75 % of the steam demand. The remainder of the steam is obtained from the Kawerau geothermal field, a hydrothermal resource, that produces some about 270 tonnes/hr of hot water. Steam requirements in the plant vary, but are required at three different pressures: 45 barg for power generation, 10.3 and 3.4 barg as process heat. The 45 barg steam exists the steam turbines at 10.3 and 3.4 barg. The geothermal fluid is split from the well and used used partially in heat exchangers and another portion flashed to feed a turbine, both effluents are then used for evaporation and drying operations (Hoston, Everett, 2000).

This scenario can almost be duplicated using an HDR scheme, replacing the hydrothermal resource with a HDR reservoir. Some minor changes need to be made: the additional flow from the well feeding the heat exchangers will be diverted to a flashing drum and fed straight into the power turbine /cogeneration scheme. This is done for a couple of reasons: first, the real geothermal utilization operation procedure at the Fletcher Plant would be classified as two parallel, independent processes making use of the same well to draw geofluid i.e. the turbogenerator and for the process heat exchangers. This arrangement is different than many cogeneration systems as the units are not in series. Second, although there would be no more than 95 t/hr going through the turbine at Fletcher, 270 t/hr would be coming out of the well; this would require some creative modeling on the EGS system, a possibility by running each scenario differently and transferring required information, it would however be very difficult to model if there was drawdown on the system: the different flow rates would result in different cooling

rates of the reservoir and would be difficult to resolve for power generation at the lower flow rate when in actuality, the throughput is much higher.

Another challenge is posed by the plant's process steam requirements: the optimized depths and wellhead temperatures for the three grades of HDR normally studied are such that their optimal flashing temperatures would be below the 147 °C and 3.4 barg, a temperature requirement for steam provided to the cogenerative load. While there are many cascade options for generating steam at a variety of pressures (examples are partial exhaust turbines and multi-stage flashing) the problem is addressed by flashing the hot water will be flashed at 3.4 barg, the gaseous portion will then be fed directly into the pulp mill as process steam; the separated hot water will then be fed to a power plant to produce electricity. This design is different from others considered as the power plant can be considered as a bottoming cycle; as such, it will probably be quite inefficient and expensive.

5.3.3 EGS Modeling and Optimization

Further simplifications are needed to model tis case using the EGS simulator. First, optimal depths using the different grades of HDR resource are determined for each case (note that this is more or less invariant to exhaust conditions). These optimal depths will yield geofluid at particular temperatures that are then assumed to be flashed at 3.4 barg (yielding 147 °C steam). The steam from this process is used in the pulp mill and its cogenerative savings value calculated. The hot water flow rate is calculated from the flash process specification, an EGS simulation is carried out using this flow rate and the original optimized depth; the temperature gradient would then need to be adjusted so as to allow for a wellhead temperature of 147 °C which is essentially that of the hot water exhaust from the drum. The well depth and operation temperature being the same, this will effectively reproduce the thermodynamics of the scenario in mind as all depths and temperatures are correct. We also have to input the capital and operating cost for the original run into this new, lower flow-rate scenario to create the correct busbar cost of

electricity production. This final touch however, requires the subtraction of the cogenerative savings from the initial model showing the full flow, effectively varying the capital input for the plant (the savings are too great to only deduct from the annual operating expenses only, a NPV is calculated and deducted from capital input). The simulation will be run using 13.6 °C turbine exit, which represents the average annual ambient temperature in Kawerau, NZ.

While there were no published seasonal temperature data for Kawerau, data from 3 very close neighboring towns are provided on the next page. A mean temperature of 13.6 °C will be used as the basis for water heating from ambient conditions.

	Jan	*Feb*	*Mar*	*Apr*	*May*	*Jun*	*Jul*	*Aug*	*Sep*	*Oct*	*Nov*	*Dec*	Yearly avg
Hamilton	18.3	18.6	17.1	14.5	11.6	9.4	8.7	9.8	11.5	13.1	15.0	16.9	**13.6**
Taumarunui	18.3	18.4	16.4	13.3	10.2	8.0	7.4	8.6	10.7	12.7	14.8	16.8	**13.0**
Gisborne	19.2	18.8	17.4	14.8	12.0	9.9	9.3	10.2	11.8	13.8	15.9	17.9	**14.3**

Table 5.5 Mean Air Temperatures in °C for New Zealand's East Coast from 1961-1998

Source: www.weatherunderground.com

So much for the power calculations, what affect if any, would this manipulation of the simulator have on the busbar electricity price produced? Since the design of the well, flashing drums, turbine and all other equipment is essentially the same (only the exit condition varies), then it would be correct to assume that the costs for the two schemes would be comparable if not very close. Furthermore, there would be little economy of scale, with both schemes with different exhaust conditions producing the same order of magnitude power (preliminary results show 5 MW and 10 MW for the different exhaust conditions), then it would be safe to assume that the only economic drawback in the release of steam at pressure would be dictated by the thermodynamics of the process and hence the reduced amount of power produced.

Again, optimization runs are carried out for 3 different grades of HDR resource termed as *High*, *Medium* and *Low*, corresponding to temperature gradients of 80, 50 and 30 ^{o}C/km respectively for the analysis of this thesis (note these gradients would be site specific, but for the purposes of comparison and analysis in this thesis, exact values are used). The system is kept as a doublet, the flow rate of 270 tonnes/hr corresponds to 75 Kg/s, note that this flow rate will be different for the cogenerative runs depending on the amount of steam separated from the flow stream and diverted to the pulping process. The water reinjection temperature which is the same as the turbine exhaust (the system being a closed loop) condition and the average annual temperature is set to 13.6 ^{o}C; other variable are entered as the table on the following page indicates:

FLETCHER PULP MILL , KAWERAU	
Power Plant Capacity Factor (%)	90
System Configuration	Doublet
Injector and Producer Well Casing ID (in)	7
Thermal Gradient (^{o}C/km)	30, 50, 80
Drawdown Parameter (kg/m^2-s)	0.00006
Reservoir Impedance (GPa-s/m^3)	1.57
Water Loss Rate (%)	2
Production Well Flow Rate (kg/s)	57-75
Water Reinjection Temperature (^{o}C)	13.6
Pump Efficiency (%)	80
Drilling and Completion Technology Level	Commercially Mature
Project Life (years)	20
Fixed Charge Rate (%)	15
Accrued Financing During Constr. (%)	9

Table 5.6 EGS Simulator design parameters for Pulp & Paper Cogeneration

5.3.4 Cost Savings From Pulp & Paper Steam Cogeneration

The plant might lose considerable power generation potential because of its large demand for steam given the flow rates of this case study. (Note that additional geothermal wells maybe drilled in parallel to supplement production, however, this will not be explored further in this thesis). How much would this steam be worth?

To answer this question, I will attempt to calculate the amortized cost of steam at pressure if it was to be produced on-site at the pulp mill. Boilers operating under pressure would institute the capital cost of such a steam-generating facility and the fuel to heat the boilers would constitute the operating cost. However, as the calculation on the next page shows, the cost of the boiler at about ¼ of a million dollars amortized over 20 years is small compared to the fuel cost to run the boiler (nevertheless, this piece of equipment could be sized and priced accurately using information in Perry's Chemical Engineering Handbook).

The streams that exit the flash drum are part steam and part hot water. The exact composition can be determined using enthalpy balances around the flashing separator for each data point. From the EGS model, for the 30°C/km data point for example the wellhead temperature is 205 °C (For 50°C/km, 258 °C and for 80°C/km, 215 °C). The flash temperature for each data point is invariant at 147 °C. Calculation details are provided in the Appendix:

$$
\begin{aligned}
m_{gas30} &= 8.87 \text{ kg/s} \\
m_{liq30} &= 66.1 \text{ kg/s} \\
m_{gas50} &= 17.8 \text{ kg/s} \\
m_{liq50} &= 57.2 \text{ kg/s} \\
m_{gas80} &= 9.93 \text{ kg/s} \\
m_{liq80} &= 65.07 \text{ kg/s}
\end{aligned}
\qquad \textbf{(5.18)}
$$

In the absence of cogeneration, a boiler would be needed to provide flows differing enthalpy steam. The efficiency for a 40,000 hp unit boiler using No. 2 Fuel is about 80 %. A barrel of oil harbors 5.486 GJ of energy, considering an 90 % capacity factor for the pulp mill is then to heat the steam to saturation at 3.4 barg, the number of barrels per year is then:

$$\frac{\text{(Flow rate)x(number of hrs/ year) x(Capacity Factor)x(energy required per Kg of water)}}{\text{(Heating value of a barrel No.2) x (boiler efficiency)}}$$

$$= (31932)x(8760)x(0.9)x(2.69\ MJ)/(5486\ MJ)x(0.80) \qquad \textbf{(5.18)}$$

Reservoir Grade °C/km	Oil Equivalent bbl/yr	Equivalent Fuel Cost 2001 USD
30	154,305	$ 6,172,000
50	309,653	$ 12,386,000
80	172,745	$ 6,910,000

Table 5.6.1 Annual Fuel Savings Equivalent for Pulp & Paper Mill using Cogeneration
(N.B. Using estimate of $40 per barrel retail)

The above value in the table are in 2001 dollars, in order to be able to deduct this saving from the EGS model capital costs (too large to offset just operating expenses), we have to turn it into 1997 dollars by using the PPI Commodities indices for No. 2 oil in 1997 and 2001 as before. It should be noted that this cogenerative saving would be accrued over a year, while the costs are born at the start of the project; and 9 % during construction as per out EGS model input (this is brought forward to year 0 on the output report of the EGS simulator). To account for this it may be prudent to discount the cogenerative savings another half a year, but as before, all costs and revenues for the same year are summed without further monthly discounting.

1997 Fuel requirement value per annum = $ 6,172,000 x 64.5/89.2 **(5.19)**

= USD 4,463,000 (1997 Dollars)

Other annual savings in 1997 dollars are $8,956,000 and $ 4,997,000. The Net Present Value of this annuity for the next 20 years in 1997 USD using a discount rate of 15 % is:

$$\text{NPV savings} = 4.463M[1-1/(1+0.15)^{20}]/0.15 = \$\ 27{,}935{,}000\ (1997\ \$) \quad \textbf{(5.20)}$$

To these values is added the cost of a boiler at USD 250,000 adjusted to 1997 Dollars using the MIT Composite Plant Cost Index that yields a multiplicand of 1/ 1.065, yielding a capital cost of USD 235,000. The 1997 Capital saving values for the 20 year life of the project are provided below:

Reservoir Grade °C/km	Total NPV Savings 1997 USD
30	$ 28,170,000
50	$ 56,294,000
80	$ 31,513,000

Table 5.6.2 NPV Fuel Savings Equivalent for Pulp & Paper Mill using Cogeneration
(N.B. Using estimate of $40 per barrel retail and 15 % discount rate)

5.3.5 Results and Analysis

Results are provided in terms of busbar electricity prices in. cents/ kWh_e; a negative busbar indicates that the savings from the use of cogeneration as opposed to burning oil and using a boiler are such that they more than pay for the electricity: in other words a sum is made for the daily operation of the scheme. This is also presented in another form as free electricity plus annual savings (revenue of USD 823,00 per annum for example, see table below). In the fish farm case study, the exhaust conditions were the same in both the cogenerative and straight power plant operation; in the case of the pulp mill however, these are drastically different. In order to appreciate the full economic and technical impact of utilizing energy from a geofluid stream, the "no-cogeneration" case would allow for an ambient exhaust condition, while the "cogeneration case" would vent steam at 3.4 barg. While the first scenario leaves the pulp mill without steam, it allows for a study of power conversion and use of energy with the power-generating unit being the main focus as opposed to the pulp mill.

To model the bottoming power cycle and the cogenerative cost benefits on the EGS simulator, the system is first optimized for depth using the full 75 kg/s flow. This flow is flashed at 147 °C to produce process steam for the pulp and paper plant. The hot water being at the same temperature, is fed into the electricity plant. In order to model this, the original optimal depth is entered into the simulator but the temperature gradient is iterated to allow for a wellhead temperature of 147 °C; the appropriate flow rate is also entered. The cogenerative savings net present value (from 20 years of operation) is deducted from operating expenses and capital costs of this simulation and the results entered directly into the EGS model. The well depth, flow rate, geofluid tempereature and capital and operating expenses having been calculated and entered, this then gives rise to a cogenerative electricity price.

The net capital expense for the three cases to be employed in the EGS model in millions are: $ 83.03, -$ 2.07, -$ 7.862. These negative values indicate more savings than capital costs; as they can not be entered into the EGS simulator as negative capital costs, they would need to be annualized for the next 20 years and deducted further from annual operating expense. The annualized values to be deducted from operating expense are then USD 331,000 and USD 1,256,000 for the 50 and 80 °C/km resource grades respectively.

Temperature Gradient °C / km	Drawdown Parameter kg/m^2-s	Well Depth km	Net Power MW	Electricity Busbar Cost, cent/kWh (2001)	Net Power with Cogen MW	Electricity Busbar Cost, Cogeneration cent/kWh (2001)
30	0	7.8	7.51	25.13	1.07	171
50	0	6.3	14.43	10.8	1.16	1.53
80	0	3.9	11.65	7.3	1.25	-8.35*

Table 5.7 EGS Simulator Results with and without Pulp & Paper Cogeneration

* The surplus of $ 823 K per annum was divided by the number of KWhs produced per year at 90 % availability: this gives "negative busbar cost". Or it would be equally correct to contend that the electricity bus bar cost was 0.0 cent/KWh (ie free) with an annual surplus of $ 823 K (1997).

It is clear by comparing net power outputs for the same case with and without cogeneration that a considerable amount of high grade heat that could produce electricity is being used to produce direct steam, leaving a very low efficiency and output electrical system. While the higher resource grades scenarios offset the cost of their poor electricity production by producing steam and requiring shallow wells, the low temperature-gradient scenario produced very little steam and was further hampered by deep drilling requirements resulting in an exorbitant electricity busbar cost. The problem was further compounded by the very low power production metric that only produce a few kWh of electricity which further worsens the value of the economic investment.

The cases with drawdown were omitted in this case study; a drop in temperature in the geofluid would affect the flashing parameters yielding a different steam output every year and hence a different savings scenario for each of the twenty years making such calculations long and tedious. With drawdown, the already unfavorable economic forecast of the low-grade system would be much worse, while the mid and high-grade scenarios would still show good viability in the cases with cogeneration. Figure 5.5 provides the results with and without cogeneration.

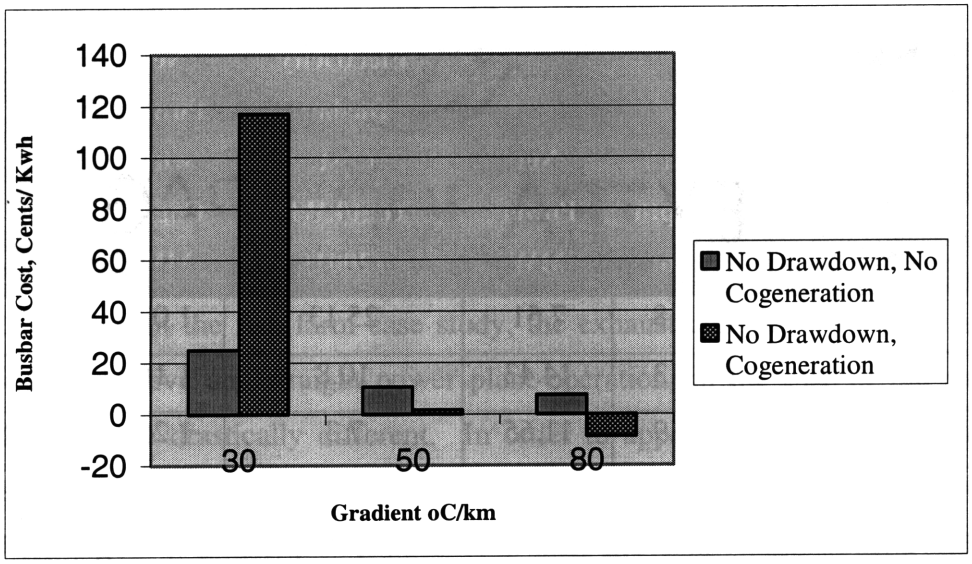

Figure 5.5 Electricity Busbar Costs for Pulp & Paper Cogeneration Case

One can not help but notice the low-grade system's extreme cost in the diagram, when cogeneration is implemented. This data point is somewhat of anomaly as this system is neither a good steam producer nor an economically sound geothermal venture to produce electricity exhibiting a well of 7.8 kilometer depth. Its non-cogenerative option, produces a good amount of electricity which results in a more acceptable busbar cost, whereas the cogenrative design yields neither adequate steam or power. To further understand the systems, a look at their thermodynamic performance is helpful.

Thermodynamics

The bottoming power cycles all had an input temperature of 147 ^{o}C and an equal atmospheric exhaust condition. The utilization efficiency for all three cases that exhibited different flow throughputs was calculated to be about 32 %. This is quite low in comparison to the utilization efficiencies achieved for the fishfarm, but understandable due to the low temperature power conversion cycle. In order for the cycle efficiencies with and without cogeneration to be considered and compared, for the non-cogenerative scenario, the resource availability at initial geofluid temperatures were considered (not 147 ^{o}C) in power generation with the exhaust at 13.6 ^{o}C. This is then compared to the cogeneration cycle utility that involves the direct-steam topping cycle and the power converting bottoming cycle; this would be the only meaningful comparison. Note that the steam that feeds the pulp mill after the flash drum is assessed based on its heat content and added to the power generation metric from the bottoming cycle, these are then divided by the availability of the geofluid prior to the entrance into the flash drum multiplied by the flow rate at that point (75 Kg/s). To better understand this, cycle efficiencies for the 30 ^{o}C/Km data point are calculated below:

Power generated from source with no cogeneration:	6.51 MW
Enthalpy from 212^{o}C to dead-state (both saturated liq.):	846 KJ/Kg x 75 Kg/s
	63.45 MW

$$\eta_c = 6.51 / 63.45$$
$$= 10.26\ \% \quad \textbf{(5.21)}$$

For the cogenerative case:

Power generated in bottoming cycle: 1.07 MW

Heat supplied via steam to plant: 846 KJ/Kg x 8.87 Kg/s

7.51 MW

Total Power from cycle: 8.58 MW **(5.22)**

The Cycle efficiency for the cogenerative case:

$$\eta_c = 8.58 / 63.45$$
$$= 13.52\ \% \quad \textbf{(5.23)}$$

Temperature Gradient °C / Km	Geofluid Temperature °C	Utilization Efficiency Bottoming Cycle η_u	Cycle Efficiency Bottoming Cycle η_u	Complete Cycle Efficiency η_c	Cogeneration Cycle Efficiency η_c
30	212	32.0 %	1.7 %	10.2%	13.5%
50	279	32.0 %	1.6%	16.4%	25.3%
80	257	32.0 %	1.6%	14.7%	14.8%

Table 5.8 Thermodynamic Efficiencies for Pulp & Paper Cogeneration Case

The utilization and bottoming cycle efficiencies being very low are expected given the inefficiencies of a low-temperature power conversion cycle; the higher quality portion of the resource being initially used to produce steam. The typical range for geothermal power cycle efficiencies is 10-25 %, the bottoming cycle (power cycle) efficiencies are much lower in this case. The electrical power generation for the cogeneration designs

was no more than roughly 1 MW as compared to 7.5, 20.9 and 10.5 MW of thermal energy harnessed for the 30, 50 and 80 ^{o}C/Km grades. In this light, its not difficult to see that the highest temperature system producing the most steam turns out to be the most efficient, albeit not the economically the cheapest option. Comparing the last two columns, that of cycle efficiencies with and without cogeneration, the marked difference was in the mid temperature gradient that yielded the highest temperature geofluid; the cogeneration design adding some 10 % further efficiency. While for the 80 ^{o}C/km no increased efficiency was noted in using cogeneration, this design reduced the busbar electricity cost substantially.

Finally, the reader would have gathered that the bleeding of steam prior to power generation requires additional makeup water; the condensing and recycling of process steam would be necessary in this case. The HDR cogeneration scheme is not then strictly a closed loop. Another advantage of an HDR system not discussed here is the possible treatment of polluted aqueous exhaust streams of a pulp mill. Rather than implementing costly recovery processes, the waste fluid may be pumped into the HDR reservoir where a lot of the impurities would separate, hot water yielding clean steam would then emerge from the out-well for power generation and heating.

5.4 DISTRICT HEATING IN MACEDONIA

District heating systems distribute steam or hot water to multiple buildings or sites. This heat can be provided from a variety of sources, including geothermal, cogeneration plants, waste heat from industry, and purpose-built heating plants.

Apart from Roman spas, the first known use of geothermal energy for district heating was in France in the Fourteenth Century where a small village used geothermal wells to heat their homes. In the U.S., the first steam district heating system was deployed at the US Naval Academy in 1853. Today there are some 30,000 district heating schemes in the US alone, including the large system in Boise, Idaho. Today, many commercial ventures provide District heating in various places in the world, the largest of these are indicated by their annual output below:

CITY	PJ	GWh
St. Petersburg	237	66,000
Moscow	150	42,000
Prague	54	15,000
Seoul (est.)	36	10,000
Berlin	33	9,247
New York City	28	7,800
Paris	17.6	5,100
Göteborg	12	3,500
Reykjavík	11	3,200
Indianapolis	5.8	1,625
Philadelphia	4	1,100
Detroit	3.1	870

Table 5.9 Annual Energy Consumption of the Largest District Heating Systems
Source: Pierce, M. A., University of Rochester, NY, June 2001 www.energy.rochester.edu/dh/

The distribution system in district heating schemes account for the most of the capital investment. Long pipe sections of variable diameter need to be insulated and often placed underground to minimize heat losses and obstructions with infrastructure; this can

account for anywhere from 35 to 75 percent of the total initial cost (Dimitrov, 2000). Another aspect of disaqiltrict heating is its intermittent use with the change of season, with load factors just below 50% in most instances. In very cold climates such as the Bulgarian Black Sea operations of Varna, load factors can reach 60 %.

The subject of this particular study is the expanding district heating system in Kocani, Macedonia. The Republic of Macedonia, born recently from the disintegration of Yugoslavia is a developing country of about 2.1 million inhabitants and an area of approximately 26,000 Km^2. Its energy supply consists mainly of fossil fuel and hydroelectric power, of which 50 % of the former has to be imported. The development of alternative domestic energy sources have received considerable attention in recent years, giving rise to the increased use of geothermal energy in the displacement of fossil-fuel boilers in district heating schemes.

5.4.1 The Geothermal Field at Kocani and District Heating Requirements[3]

The Kocani geothermal field has been in operation since 1982. Although it is not a high enthalpy system, new boreholes can increase flow rates to as much as 450 l/s. The distribution system of this particular scheme involves 1.7 km of primary steel piping from the main station and some 3 km of secondary piping from substations to end users. This cost is estimated to range between USD 50-650 / kW_t[4],(Histrov, Nikolova, Bojadgieva, 2000) it includes the cost of heat exchangers but this cost is obviously very dependent on the local layout and environmental conditions. The layout of such a scheme is appreciably complex involving many pipes, valves and pumps, the details of which are beyond the scope of this thesis.

---

[3] The calculations of this case study are based on the data obtained from Dimitrov in " Geothermal District heating Schemes in the Republic of Macedonia", WGC 2000.

[4] "Utilization of Geothermal Waters for Space Heating in Bulgaria", Hristo Hristov, Nadya Nikolova, Klara Bojadgieva, WGC 2000. Note that the cost range of District Heating systems estimated to be USD 150-900 (including drilling and well completion), was multiplied by the percentage of costs associated by piping and heat exchange equipment from Dimitrov in " Geothermal District heating Schemes in the Republic of Macedonia", WGC 2000.

Heat transfer to each unit happens via counter-current flow plate heat exchangers; the rates of heat flow are individually controlled by flow valves. Geofluid use in these units results in scaling and long-term corrosion. This affects both the rate of heat transfer and can give rise to substantial maintenance costs; thankfully, this is a much lesser problem in the HDR scheme to be modeled in an analogous fashion here. In HDR systems the geofluid tends to be clean chemically and less subject to corrosion and fouling problems. A storage tank is used as a buffer to smooth out the variable flow requirements of the system.

The input temperature to the district heating system is kept constant at 78 ^{o}C. This may appear to be somewhat high for space heating use, but the higher temperature reduces the heat exchange area requirement and lowers capital costs. Surprisingly, the geofluid in the Kocani scheme used to be expelled to the environment in the early eighties and not re-injected. This tactic may reduce capital and pumping costs further, it does however require that the exhausted fluid be benign. The HDR design to be implemented is a closed loop system with complete reinjection. Flow rates to the scheme vary between 100 and 250 L/s depending on seasonal needs and an average shall be used in the design phase.

The Kocani geothermal project has developed over the years to include several direct heating applications. A greenhouse and rice drying plant have been supplemented with space heating and other industrial uses. These direct uses all have their own particular capacity or load factors. Because these operating conditions were not available for the Macedonia case, however, the use of data from a published paper at the World Geothermal Congress, 2000 in Japan were used for the study (Lund, Boyd, 2000)[5]. The table on the next page shows the maximum thermal loads of these applications, their capacity factors and hence their annual energy usage.

[5] Capacity factors for the various applications obtained from: " Geothermal Direst-Use in the United States and Update: 1995-1999", John Lund, Tonya Boyd, Geo-Heat Center, Oregon Institute of Technology, WGC 2000

APPLICATION	INSTALLED THERMAL POWER MW_t	CAPACITY FACTOR	ANNUAL ENERGY USE TJ
Space Heating	19.19	0.33	199.7
Agricultural Drying	1.36	0.49	21.0
Greenhouses	52.90	0.30	500.5
Industrial Process Heat	6.86	0.35	75.7
Other Uses	2.11	0.2	13.3
TOTAL	**82.42**	**0.34 (avg)**	**810.2**

Table 5.10 Thermal Power Requirements of Kocani District Heating

Source: See Footnote 9

There is a distinction between the district heating requirements listed above and the space heating needs as outlined in Table 5.11; the former includes several drying and industrial uses, while the latter involves itself only with the heating of space. The load factors for the various district heating operations being know and comparable to that of space heating, it was thought that they may be included as an amalgamate in a separate calculation in addition to load calculations based purely on space heating. This former amalgamate may be viewed as a larger space heating operation and shall be referred to as "District Heating", while the smaller operation involving only the buildings shall be known as "Space Heating". Figure 5.6 shows a schematic of the Kocani geothermal scheme.

Table 5.11 provides a breakdown of the space heating network's end users (identified by the numeral "6" in Figure 5.6)

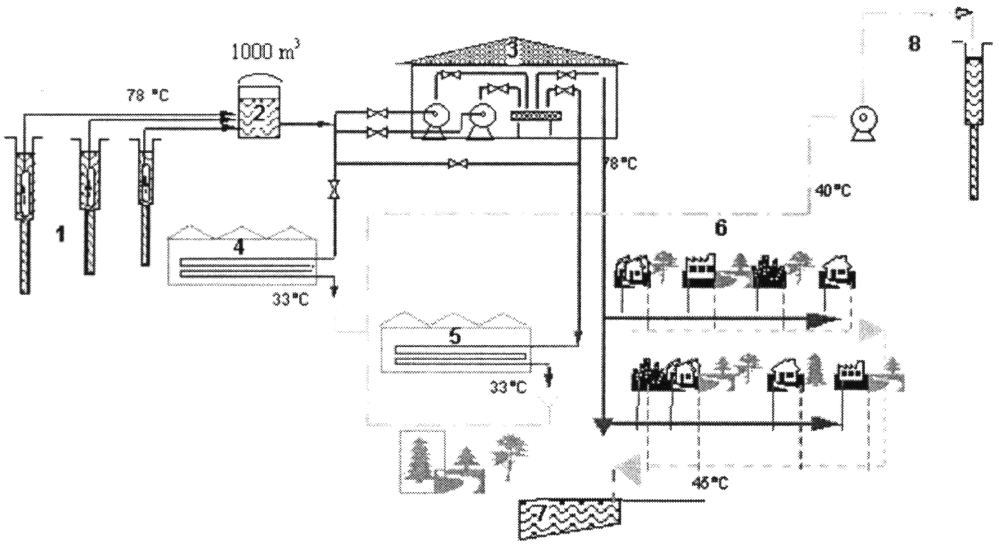

1. Geothermal wells; 2. Sedimentation basin; 3. Circulation pumps; 4. Geothermal complex "Mosa Pijade"; 5. Geothermal complex "Kocansko Pole"; 6. District heating; 7. Swimming pool; 8. Reinjection

Figure 5.6 Diagram of Kocani Geothermal District Heating Scheme

CONSUMER	THERMAL POWER kW_t
School "Kiril I Metodij"	930
Court	146
School "Mosa Pijade"	320
Police Department	252
Administrative Buildings (3)	907
PTT (unknown use)	380
Medical Center	4,000
Shopping Center	836
Block of Houses "A", "B" & on "Tito" and "Vlahov" streets short of Shopping Center	4,676
New Anticipated	6,739
TOTAL	**19,190**

Table 5.11 Thermal Power Requirements of Subunits of Kocani Space Heating
Source: See Footnote 9

5.4.2 Cost Savings From District Heating Cogeneration

Prior to quantifying the value of the sensible heat distributed by the district heating system, it should be born in mind that the scenario being analyzed is one of geothermal heating replacing fossil fuel heating practices; the case in point in Macedonia. As such, there would be no need to calculate the capital cost of the piping network that would have been previously under operation using fossil fuel boilers. The cost of drilling and pumping is more or less covered by the HDR design scheme that will be created by the EGS Simulator.

In the cases above, the yearly energy use is already provided. Assuming use of No.2 oil for heating, the equivalent number of barrels of oil needed to meet the demand of the District Heating and Space Heating schemes are calculated below. A boiler efficiency of 80 % was employed and a barrel of oil is estimated to produce 5.486 GJ of combustible energy:

$$\frac{\text{(Total annual energy used)}}{\text{(Heating value of a barrel No.2) x (boiler efficiency)}} \qquad \textbf{(5.23)}$$

Project	Oil Equivalent Per annum bbl/yr	Equivalent Fuel Cost per annum 2001 USD	Total Savings NPV 1997 USD
District Heating	184,606	$ 7,384,000	$ 33,425,000
Space Heating	309,653	$ 1,820,000	$ 8,237,000

Table 5.11.1 Fuel Savings Equivalent for District and Space Heating using Cogeneration
(N.B. Using estimate of $40 per barrel retail)

5.4.3 EGS Modeling and Optimization

One last piece of information is required to model the Kocani scheme as an HDR operation: namely, the flow rate. Although the article in question provides a range of flow rates and the maximum heat load, flow rates are not provided. An average can be calculated from the exhaust conditions provided in the schematic drawing of the project and the annual heat used by the different segments of the district heating scheme.

Considering the Space Heating scheme alone first:

$$\text{Thermal Power x Capacity Factor} = F \cdot \rho \cdot C_p \cdot \Delta T$$

$$19.19 \text{ x } 0.33\text{x}1000 = \text{F. } 4.2\ (78\text{-}45)$$

$$F = 45.7 \text{ L/s}$$

Similarly, for the whole scheme (District Heating), an average thermal power of 25.61 MW_t results. Considering the exit temperature of 40 °C. This flow rate is then 161 L/s. This would then be used to set up our input table, however, the EGS simulator allows a maximum flow rate of 150 kg/s and this will be the value to use, bearing in mind that the turbine exit (water re-injection temperature) is 78 °C.

The seasonal nature of district heating needs is sometimes dealt with by putting the hot power plant effluent to alternate uses such as a binary bottoming cycle. The economic advantages of such an expensive plant with an availability of 50 % and below (half year operation) for the sake of energy efficiency are not being considered in this thesis.

It is also important to obtain an average annual ambient temperature for Kocani. This will allow us to determine condensing turbine exhaust conditions (also the re-injection temperature) for a non-cogenerative power plant design used as a comparison.

KOCANI DISTRICT HEATING	
Power Plant Capacity Factor (%)	90
System Configuration	Doublet
Injector and Producer Well Casing ID (in)	7
Thermal Gradient (^{o}C/Km)	30, 50, 80
Drawdown Parameter (Kg/m^{2}-s)	0.00006
Reservoir Impedance (GPa-s/m^{3})	1.57
Water Loss Rate (%)	2
Production Well Flow Rate (Kg/s)	150, 45.7
Water Reinjection Temperature (^{o}C)	12.4, 78
Pump Efficiency (%)	80
Drilling and Completion Technology Level	Commercially Mature
Project Life (years)	20
Fixed Charge Rate (%)	15
Accrued Financing During Constr. (%)	9

Table 5.12 EGS design parameters for District & Space Heating Cogeneration

5.4.4 Results and Analysis

The power output and busbar electricity cost for the space and district heating schemes are provided in detail in Tables 5.13 and 5.14 respectively. As expected, because the magnitude of the cogenerative operation of the district heating scheme is substantially larger than that of the space heating, a larger impact on busbar electricity prices resulted. The higher flow rate required in the district heating scheme was also an added benefit in lowering busbar costs relative to the space heating scheme; this can be attributed to the economies of scale experienced. There was little benefit in cogeneration in lower grade resources.

Temperatue Gradient °C / km	Drawdown Parameter kg/m^2-s	Well Depth km	Net Electric Power MW	Net electric Power with Cogen design MW	Electricity Busbar Cost No Cogen cent/kWh (2001)	Electricity Busbar Cost with Cogeneration cent/kWh (2001)
30	0	7.81	4.35	3.94	49.9	50.5
50	0	6.30	8.86	8.39	15.7	14.4
80	0	3.94	7.31	6.86	9.76	7.86
30	6×10^{-5}	7.89, 7.99	4.49-2.60	4.27-2.91	58.4	63.0
50	6×10^{-5}	6.30	8.86-5.91	8.40-6.12	17.8	15.8
80	6×10^{-5}	3.94	7.31-4.75	6.86-4.91	11.2	8.74

Table 5.13 EGS Simulator Results with and without Space Heating Cogeneration

Temperature Gradient °C / km	Drawdown Parameter kg/m^2-s	Well Depth km	Net Electric Power MW	Net Electric Power with Cogen design MW	Electricity Busbar Cost No Cogen cent/kWh (2001)	Electricity Busbar Cost with Cogeneration cent/kWh (2001)
30	0	8.85, 9.03	12.21	11.36	33.3	32.9
50	0	6.30	22.88	21.01	9.18	6.00
80	0	3.94	19.53	17.84	6.43	2.88
30	6×10^{-5}	9.06	13.5-5.04	12.32-5.84	43.3	41.3
50	6×10^{-5}	6.30	22.9-12.8	21.01-13.23	10.4	6.93
80	6×10^{-5}	3.94	19.5-10.9	17.84-11.41	7.63	3.31

Table 5.14 EGS Simulator Results with and without District Heating Cogeneration

The well depths in parenthesis are indicative of slightly modified optimal well depth for cogeneration and drawdown variations of design. With drawdown for example and a high flow rate, a deeper well yielded a slightly improved busbar cost. The breakeven electricity prices were notably lower for the 50 and 80 ^{o}C/km. Figures 5.7 and 5. illustrate this more clearly. A comparison between the two schemes also point to the benefits of a larger cogenerative load and economies of scale in power production. Also noteworthy is the rate of decline of busbar cost with an increase in temperature gradient being geometric in nature.

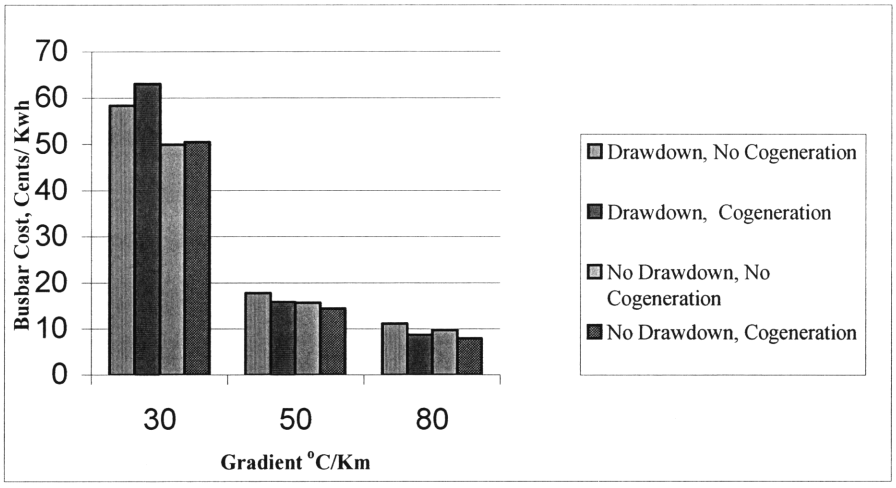

Figure 5.7 Electricity Busbar Costs for Space Heating Cogeneration Case

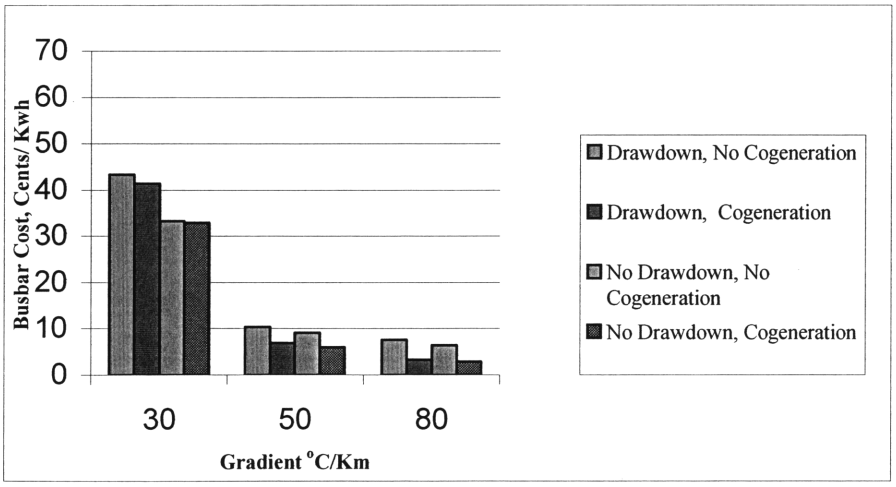

Figure 5.8 Electricity Busbar Costs for District Heating Cogeneration Case

Thermodynamics

As before, utilization efficiencies may be calculated for the non-cogenerative cases using availability data from the EGS simulator. Cycle efficiencies are arrived at by considering electrical power produced added to the sensible heat (in cogeneration cycle efficiency calculation) used and divided by the total heat supplied. The utilization efficiency for all three cases that exhibited different flow throughputs was calculated to be 32 %. This is quite low in comparison to the utilization efficiencies achieved for the fish farm, but understandable due to the low temperature power conversion cycle. The utilization efficiencies without cogeneration were healthy, however, the all important cycle efficiencies received a comparatively huge boost from the magnitude of cogeneration sensible heat used, tripling in the case of the lowgrade resource and more than doubling in the other District Heating cases; while the gains in the Space Heating cycle efficiencies from cogeneration were more modest, they were never the less sizable.

Temperature Gradient °C / Km	Geofluid Temperature °C	Utilization Efficiency η_u	Cycle Efficiency η_c	CogenCycle Efficiency η_c
30	212	52.7%	11.8%	20.7%
50	279	60.8 %	18.9%	25.2%
80	257	59.5 %	19.1%	26.8%

Table 5.15 Thermodynamic Efficiencies for Space Heating Cogeneration Case

Temperature Gradient °C / Km	Geofluid Temperature °C	Utilization Efficiency η_u	Cycle Efficiency η_c	CogenCycle Efficiency η_c
30	244	58.2%	11.2%	42.4%
50	279	60.8 %	16.4%	38.9%
80	257	59.5 %	14.9%	39.7%

Table 5.16 Thermodynamic Efficiencies for District Heating Cogeneration Case

The comparison between the efficiencies of the two heating shows the effects of a much larger heating cogenerative load, the District Heating system being some 4 times the size of the Space Heating scheme.

5.5 MULTIPLE CASE ANALYSIS

The merits of cogeneration design in Enhanced Geothermal Systems can be seen on a case by case basis in the previous analysis. It is however important that a generalized effect of such design be investigated. The following is a simple attempt to investigate this phenomenon (if any) by placing the previous set of data in sets and looking for possible trends.

Having gone through the individual case analysis, there seems to be a definite inverse relationship between the overall busbar cost of power and the magnitude of the cogenerative load. This seems intuitively plausible as the much more efficient use of direct heat versus the production of electricity in a low temperature system is a source of great financial operating-subsidy. The figure below looks at electricity busbar cost vs cogenerative thermal load in MW:

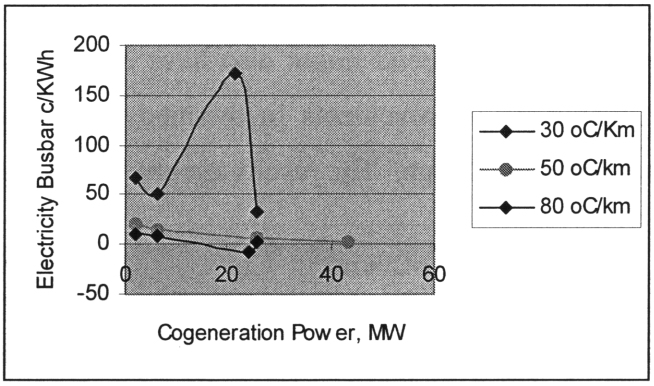

Figure 5.9 Graph of Busbar vs Cogenerative Power Showing Outlier

The plot above shows a general trend. Removing the outlier point in the 30 ^{o}C/Km series which represents the very inefficient pulp and paper steam and power production point, the graph on the next page results. The family of curves thus produced are noteworthy for two aspects: first, as anticipated, the inverse relationship between busbar cost and

cogeneration load is illustrated by "half-life" shaped curve for each resource-grade. Secondly, the difference vertical distance between the different resource-grade curves show the nonlinear effect of temperature gradient on electricity busbar cost; there is substantial difference between the 30 °C/Km series and the 50 and 80 °C/Km series, the latter two being much closer to each other, a testimony to the reduced marginal reduction of busbar cost with increased resource temperature gradient in this case.

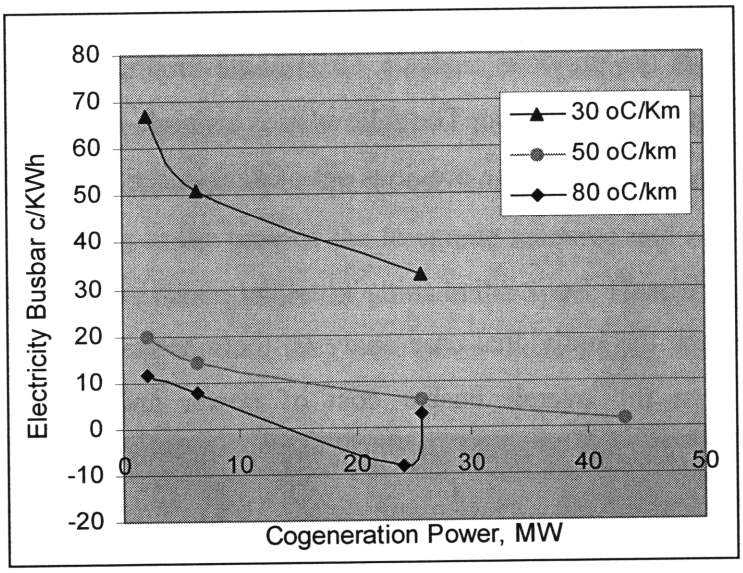

Figure 5.10 Graph of Busbar vs Cogenerative Power for all Cases Studied

Plots of busbar cost versus the ratio of thermal and electric powers were less conclusive, although a general trend might also have been anticipated in this case. Also of interest would be improvements in thermodynamic cycle efficiencies by introduction of cogenerative design. The results are provided graphically:

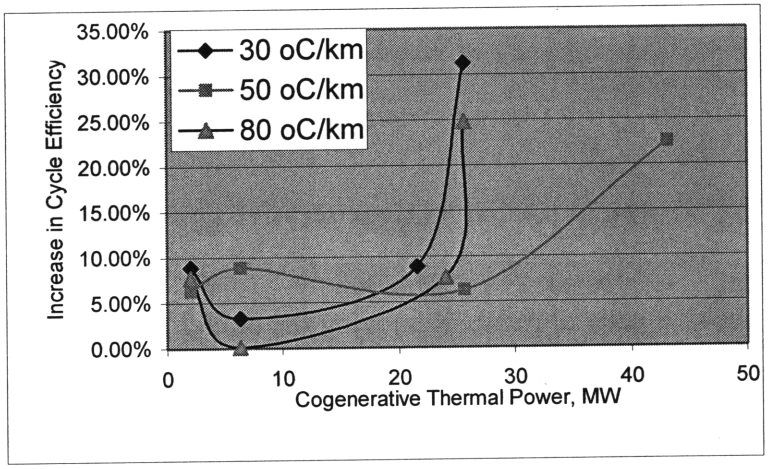

Figure 5.11 Increase in Cycle Efficiency vs Cogenerative Power for Cases

All cases showed improved cycle efficiency with the implementation of cogenerative design (they are all above the x-axis). If a linear "best-fit" line was drawn for each series of data points (using the "least square errors" method) as a means of , a line passing through the origin with a positive slope would result in each case. This would indicate that cycle efficiencies are proportional to thermal cogenerative power; furthermore, the slopes would also be inversely proportional to the temperature gradient of the resource: the low-temperature resources benefiting most in increased efficiency from cogeneration.

CHAPTER 6
CONCLUSION AND RECOMMENDATIONS

The economic benefits from the use of cogeneration in HDR electricity production were very much dependent on the particular nature of the direct heat load. In fish farming for example, the gains were modest, whereas in pulp and paper and district heating the economic benefits could be termed as substantial and moderate respectively. According UNESCAP[1] (2002), the heat to electrical power ratios for extraction-condensing steam turbines should be in the range of 2-10. The case studies here also employing a condensing steam turbine, exhibited a much broader heat-to-power ratio: 0.36-37 (see Chapter 6 notes in the appendix to this thesis). Apart from generally accepted design constraints, the question arises: at what point is the design primarily direct use entity with minimal electric power production and when would it be considered a cogenerative scheme?

While it is unlikely that cogeneration design alone would be enough to bring HDR energy use into mainstream energy generation techniques; it is a step in the right direction in improving energy efficiency where geothermal energy tends to lag fossil fuel electricity production. It is the opinion of this writer that niche use of HDR technology with cogeneration in off-grid electricity production or by industrial user operators with specific direct heat needs is very likely in the near future. There are also geopolitical and environmental benefits in the further development of EGS energy to supplement and displace fossil fuel energy supply.

Future research in cogeneration and HDR power systems would do well to look more carefully at the design aspect of the schemes, where greater efficiencies are possible by use of other well configurations such as the triplet and star formations that improve flow rates and increase power outputs. Additional wells would also be of further use in design

[1] United Nations Economic and Social Commission for Asia and the Pacific

of high-demand direct use topping cycles such as pulp and paper. These need to be better optimized; in the pulp and paper case study in chapter 5, the direct use application got priority much to the detriment of the electrical power generation.

Lastly, more elaborate cogeneration design for seasonal variations could be considered. The heating application if unused in the warmer months may be shunted in favor of binary-fluid power cycle. The higher capital cost associated with such a design would need to be justified by the increased availability of the system. A total of four case studies (two in district heating design) each with 3 different resource grades of temperature gradient were used to draw conclusions in this thesis; with more case studies employing direct heat of varying enthalpies, it should be possible to come up with an empirical relationship between electrical busbar cost for HDR power systems and other parametesr that could possibly included flow rate and ratio of electrical power to cogenerative output for example.

REFERENCES

1. Tester, J.W., D.W. Brown, R.M. Potter (1989) *Hot dry rock geothermal energy – a new agenda for the 21st century.* Los Alamos National Laboratory Report LA-11514-MS, Los Alamos, New Mexico, U.S.A.

2. Brown. D., (1995). *The U.S. hot dry rock program: 20 years of experience in reservoir testing.* Proceedings from the World Geothermal Congress 1995, 2607-2611

3. Edwards, L.M. *et al*, (1982), *Handbook of geothermal energy.* Gulf Publishing Company, Chapter 1, p. 1

4. Edwards, L.M. (1982), *Handbook of Geothermal Energy.* Houston: Gulf Pub. Co. c1982, Chapter 2, p. 47

5. Kitsou, O., 2000, *Power generation from geothermal resources: challenges and opportunities.* MIT Master's thesis.

6. Tanenbaum, 1999, *Geothermal Resource: A Hot Prospect for Energy Production,* http://www.physics.pomona.edu

7. Arpasi, M., J. Lorberer, S. Pap, Hungarian Geothermal Association, 2000, *High Pressure and Temperature (Geopressured) Reservoirs in Hungry.* Proceedings from the World Geothermal Congress 2000.

8. Tester, J.W. and Howard J. Herzog *Economic Predictions for Heat Mining: A Review and Analysis of Hot Dry Rock (HDR) Geothermal Energy Technolgy.* MIT Energy Laboratory. Final report for the US DOE, July 1990. p. 3

9. Armstead H.C.H, J.W. Tester, 1987 *Heat Mining* London: E.& F.N. Spon 1987, Chapter 2, p.9

10. Zenke, J., P. Seibit, F. Kabus (2000). *Increasing of the efficiency of the Neubrandenburg Geothermal Heating Plant through surplus heat storage in the Summer.* Proceedings from the World Geothermal Congress 2000.

11. The World Commission on the Environment and Development, (1987) *The Report of The World Commission on the Environment and Development, 96th Plenary Meeting*, December 1987

12. Watson, R.T. & Core Writing Team (2001), *Climate Change 2001: Synthesis Report* IPCC, Geneva, 2001

13. Herzog, H. J. Ed., (1988) *Proceedings of the Stakeholder's Workshop on Carbon Sequestration*, June 1998.

14. Armstead H.C.H, J.W. Tester, 1987 *Heat Mining* London: E.& F.N. Spon 1987, p. 394

15. Edwards, L.M. *et al*, (1982), *Handbook of geothermal energy*. Gulf Publishing Company, Chapter 5, p 222

16. Watts, P., CEO Shell U.S.A (2002) *Shell & sustainability*. Address, MIT November, 2002

17. Jotaki, H. (2000) *High-Angle Directional Drilling at Takagami Geothermal Field* WGC 2000

18. Armstead H.C.H, J.W. Tester, 1987 *Heat Mining* London: E.& F.N. Spon 1987, Chapter 7, pp. 99-104

19. [1]Tester, Brown, [2]Potter (1989) *Hot Dry Rock Geothermal Energy- A New Energy Agenda for the 21st Century*, [1]MIT, [2]Los Alamos National Laboratory: July 1989

20. Tester, J.W., J.M, Edwards, Chilingar, Rieke III, Fertl,(1984) *Handbook of Geothermal Energy* 1984, Chp 10 p. 474

21. [1]Gunerhan, [2]Coury, *Upstream Reboiler Design and Testing for Removal of Noncondensable Gases from Geothermal Steam at Kizildere Geothermal Power Plant, Turkey* , [1]Solar Energy Institute, Turkey. [2]Coury & Associates, USA June 2000.

22. Gawlik, K., Kelly S., (2000) *Development and Field Testing of Polymer-based Heat Exchanger Coatings*. National Renewable Energy Laboratory, World Geothermal Congress (WCG), Japan, 2000.

23. Kolin I., Koscak-Kolin S., Golub M. (2000) *Geothermal Electricity Production by Means of the Low Temperature Difference Stirling Engine*. Faculty of Mining , Geology and Petroleum Engineering, Croatia, World Geothermal Congress (WCG), Japan, 2000

24. Megel, T, (2000) *Production Capacity and Sustainability of Geothermal Doublets*, Proceedings World Geothermal Congress, Tohoku , Japan 2000

25. Armstead H.C.H, J.W. Tester, 1987 *Heat Mining* London: E.& F.N. Spon 1987, pp. 409

26. Armstead H.C.H, J.W. Tester, 1987 *Heat Mining* London: E.& F.N. Spon 1987, pp 438.

27. AmeriCulture, Inc., Executive Summary quoting the FAO of the United Nations, 2000

28. Mock, Tester, Wright (1997) *Geothermal Energy From the Earth: an Environmentally Sustainable Resource* 1997.

29. Milora, S.L., Tester, J.W. (1976), Geothermal energy as a source of electric power, MIT Press, 1976. Appendix A

30. American Society of Mechanical Engineers, www.asme.org , approximate boiler efficiency, 2001

31. Perry H. et al, (1984) *Perry's Chemical Engineers' Handbook*, McGraw-Hill, 1984, Section 9-36

32. Nilsson, L.J., Larson E. D., Gilbreath, K., Guptta A., (1995) *Energy Efficiency and the Pulp and Paper Industry*, 1995, American Council for Energy-Efficient Economy

33. Hoston G., G.Everett, (2000) *Energy Model for an Industrial Plant Using Geothermal Steam in New Zealand*, WGC June 10, 2000.

34. Hristov, H., Nikolova, N., Bojadgieva, K., (2000) *Utilization of Geothermal Waters for Space Heating in Bulgaria*, World Geothermal Congress, 2000.

35. Dimitrov, (2000) *Geothermal District heating Schemes in the Republic of Macedonia*, World Geothermal Congress, 2000.

36. Lund, J, Boyd, T (2000) *Geothermal Direst-Use in the United States and Update: 1995-1999*, Geo-Heat Center, Oregon Institute of Technology, WGC 2000.

37 United Nations Economic and Social Commission for Asia and the Pacific (2002) *Guidebook on cogeneration as a means of pollution control and energy efficiency in Asia* http://www.unescap.org/enrd/energy/co-gen/part1c106.htm

APPENDIX

Chapter 4

Various Costing Indices not normalized to 1965

YEAR	CE PLANT COST INDEX	M&S EQUIPMENT COST INDEX	NELSON REFINERY COST INDEX	ENR GENERAL COST INDEX
1989	355.4	895.1	1195.9	4615
1990	357.6	915.1	1225.7	4732
1991	361.3	930.6	1252.9	4835
1992	358.2	943.1	1277.3	4985
1993	359.2	964.2	1310.8	5210
1994	368.1	993.4	1349.7	5408
1995	381.1	1027.5	1392.1	5471
1996	381.7	1039.1	1418.9	5620
1997	386.5	1056.8	1449.2	5825
1998	389.5	1061.9	1477.6	5920
1999	390.6	1068.3	1497.2	6060
2000	394.1	1089	1542.7	6221
2001	394.3	1093.9	1579.7	6342
2002	391.5	1092	1616.1	6502

Chapter 5

Fish Farming: 30 °C/ km Resource, No Draw Down

*** SUMMARY OF RESULTS *NO Cogeneration****

Electricity breakeven price (cents/kWh)	68.80 (1997 $), **69.3 (2001 $)**
System configuration:	DOUBLET
Gradient (deg.C/Km)	30.0
Well depth (km)	7.80
Flowrate per production well (kg/s)	32.2
Reservoir volume per well-pair (M m^3)	146.6

Variable name	Initial guess	Lower bound	Upper bound	Optimized value
DEPTH	4.500	1.000	10.500	7.796

*** SUMMARY OF RESULTS *Cogeneration* ***

Electricity breakeven price (cents/kWh)	66.91 (1997 $) **67.4 (2001 $)**
System configuration:	DOUBLET
Gradient (deg.C/Km)	30.0
Well depth (km)	7.75
Flowrate per production well (kg/s)	32.2
Reservoir volume per well-pair (M m^3)	146.6

Variable name	Initial guess	Lower bound	Upper bound	Optimized value
DEPTH	4.500	1.000	10.500	7.750

ECONOMIC PARAMETERS

Fixed Annual Charge Rate Method	
Fixed annual charge rate (%)	15.0
Accrued financing during construction (%)	9.0
Project life (years)	20.0
Capacity factor (%)	90.0

ENGINEERING PARAMETERS

Well depth (km)	7.80
Well deviation from vertical (degrees)	0.0
Wellbore length (km)	7.80
Water loss rate (%)	0.00
System configuration:	DOUBLET
Pump efficiency (%)	80.0
Injection temperature (deg. C)	22.5
Production Well Temperature Drop (deg.C)	15.0
Flowrate per production well (kg/s)	32.2

Injection well casing ID (inches)	7.0
Production well casing ID (inches)	7.0

RESOURCE CHARATERISTICS

Maximum reservoir temperature (deg C)	330.0
Number of segments	1
Gradient (deg.C/Km)	30.0

RESERVOIR PARAMETERS

The drawdown parameter model is used	
Circular fractures with known diameter are used	
Area of the fracture (M m^2)	0.102
Well separation (m)	360.0
The reservoir volume per well-pair is calculated	
The fracture separation and the number of fractures per well-pair are input variables	
Reservoir volume per well-pair (M m^3)	146.6
Fracture separation (m)	60.0
Number of fractures per well-pair	25.0
Impedance per fracture (GPa/m^3/s)	1.57
Well bottom temperature (deg. C)	248.9
Reservoir top temperature (deg. C)	205.7

CAPITAL COSTS (K$)

Drilling and completion costs	58727.85
Stimulation costs	3866.45
Surface power plant costs	3547.70
Fluid distribution costs	717.12
Exploration costs	31439.83
Total capital costs	98298.95
Annualized capital costs	16071.88

OPERATING AND MAINTENANCE COSTS (K$/yr)

Wellfield maintenance costs	363.55	***($ 0 with cogeneration)***
Power plant maintenance costs	183.26	***($ 94 K with cogeneration)***
Water costs	0.00	
Total operating and maintenance costs	546.82	***($ 94 K with cogeneration)***

POWER GENERATION RESULTS

Initial geofluid availability (MWe/kg/s)	0.180
Initial practical availability (MWe/kg/s)	0.095
Initial net power generation(MWe/kg/s)	0.095
Overall geofluid pressure drop (psia)	-869.
Injection well pressure drop (psia)	163.
Reservoir pressure drop (psia)	293.
Production well pressure drop (psia)	191.
Buoyancy correction (psia)	1517.

Pumping power/ Net installed power (%) 0.0

****
POWER GENERATION PROFILE
****

YEAR	THERMAL DRAWDOWN	GEOFLUID TEMPERATURE (degrees Celsius)	PUMP POWER (MW)	NET POWER (MW)	FIRST LAW EFFICIENCY (%)
0	1.0000	212.29	0.0000	3.0640	11.7424
1	1.0000	212.29	0.0000	3.0640	11.7424
2	1.0000	212.29	0.0000	3.0640	11.7424
3	1.0000	212.29	0.0000	3.0640	11.7424
4	1.0000	212.29	0.0000	3.0640	11.7424
5	1.0000	212.29	0.0000	3.0640	11.7424
6	1.0000	212.29	0.0000	3.0640	11.7424
7	1.0000	212.29	0.0000	3.0640	11.7424
8	1.0000	212.29	0.0000	3.0640	11.7424
9	1.0000	212.29	0.0000	3.0640	11.7424
10	1.0000	212.29	0.0000	3.0640	11.7424

****
* HEAT EXTRACTION PROFILE *
****

YEAR	THERMO POWER (MJ/Kg)	HEAT EXTRACTED (10^15 J/Kg)	RESERVOIR HEAT CONTENT (10^15 J)	PERCENTAGE OF TOTAL HEAT MINED (%)
0	0.810	0.7406	85.10	0.00
1	0.810	0.7406	84.36	0.87
2	0.810	0.7406	83.62	1.74
3	0.810	0.7406	82.88	2.61
4	0.810	0.7406	82.14	3.48
5	0.810	0.7406	81.39	4.35
6	0.810	0.7406	80.65	5.22
7	0.810	0.7406	79.91	6.09
8	0.810	0.7406	79.17	6.96
9	0.810	0.7406	78.43	7.83
10	0.810	0.7406	77.69	8.70

Fish Farming: 50 °C/ km Resource, No Draw Down

*** SUMMARY OF RESULTS *NO Cogeneration* ***

Electricity breakeven price (cents/kWh)			20.86 (1997 $), **21.0 (2001 $)**	
System configuration:			DOUBLET	
Gradient (deg.C/Km)			50.0	
Well depth (km)			6.30	
Flowrate per production well (kg/s)			32.2	
Reservoir volume per well-pair (M m^3)			146.6	
Variable name	Initial guess	Lower bound	Upper bound	Optimized value
DEPTH	4.500	1.000	6.300	6.300

*** SUMMARY OF RESULTS *Cogeneration* ***

Electricity breakeven price (cents/kWh)			19.94 (1997 $), **20.0 (2001 $)**	
System configuration:			DOUBLET	
Gradient (deg.C/Km)			50.0	
Well depth (km)			6.30	
Flowrate per production well (kg/s)			32.2	
Reservoir volume per well-pair (M m^3)			146.6	
Variable name	Initial guess	Lower bound	Upper bound	Optimized value
DEPTH	4.500	1.000	6.300	6.300

ECONOMIC PARAMETERS

Fixed Annual Charge Rate Method	
Fixed annual charge rate (%)	15.0
Accrued financing during construction (%)	9.0
Project life (years)	20.0
Capacity factor (%)	90.0

ENGINEERING PARAMETERS

Well depth (km)	6.30
Well deviation from vertical (degrees)	0.0
Wellbore length (km)	6.30
Water loss rate (%)	0.00
System configuration:	DOUBLET
Pump efficiency (%)	80.0
Injection temperature (deg. C)	22.5
Production Well Temperature Drop (deg.C)	15.0
Flowrate per production well (kg/s)	32.2
Injection well casing ID (inches)	7.0
Production well casing ID (inches)	7.0

RESOURCE CHARATERISTICS

Maximum reservoir temperature (deg C)	330.0
Number of segments	1
Gradient (deg.C/Km)	50.0

RESERVOIR PARAMETERS

The drawdown parameter model is used	
Circular fractures with known diameter are used	
Area of the fracture (M m^2)	0.102
Well separation (m)	360.0
The reservoir volume per well-pair is calculated	
The fracture separation and the number of	
fractures per well-pair are input variables	
Reservoir volume per well-pair (M m^3)	146.6
Fracture separation (m)	60.0
Number of fractures per well-pair	25.0
Impedance per fracture (GPa/m^3/s)	1.57
Well bottom temperature (deg. C)	330.0
Reservoir top temperature (deg. C)	258.0

CAPITAL COSTS (K$)

Drilling and completion costs	30486.37
Stimulation costs	3866.45
Surface power plant costs	5350.98
Fluid distribution costs	1466.02
Exploration costs	17319.09
Total capital costs	58488.90
Annualized capital costs	9562.94

OPERATING AND MAINTENANCE COSTS (K$/yr)

Wellfield maintenance costs	363.55	***($ 0 with Cogeneration)***
Power plant maintenance costs	374.65	***($ 286.2 K with Cogeneration)***
Water costs	0.00	
Total operating and maintenance costs	738.20	***($ 286.2 K with Cogeneration)***

POWER GENERATION RESULTS

Initial geofluid availability (MWe/kg/s)	0.320
Initial practical availability (MWe/kg/s)	0.195
Initial net power generation(MWe/kg/s)	0.195
Overall geofluid pressure drop (psia)	-1394.
Injection well pressure drop (psia)	129.
Reservoir pressure drop (psia)	293.
Production well pressure drop (psia)	169.
Buoyancy correction (psia)	1985.
Pumping power/ Net installed power (%)	0.0

****
POWER GENERATION PROFILE
****

YEAR	THERMAL DRAWDOWN	GEOFLUID TEMPERATURE (degrees Celsius)	PUMP POWER (MW)	NET POWER (MW)	FIRST LAW EFFICIENCY (%)
0	1.0000	279.00	0.0000	6.2638	17.0716
1	1.0000	279.00	0.0000	6.2638	17.0716
2	1.0000	279.00	0.0000	6.2638	17.0716
3	1.0000	279.00	0.0000	6.2638	17.0716
4	1.0000	279.00	0.0000	6.2638	17.0716
5	1.0000	279.00	0.0000	6.2638	17.0716
6	1.0000	279.00	0.0000	6.2638	17.0716
7	1.0000	279.00	0.0000	6.2638	17.0716
8	1.0000	279.00	0.0000	6.2638	17.0716
9	1.0000	279.00	0.0000	6.2638	17.0716
10	1.0000	279.00	0.0000	6.2638	17.0716

****
* HEAT EXTRACTION PROFILE *
****

YEAR	THERMO POWER (MJ/Kg)	HEAT EXTRACTED (10^15 J/Kg)	RESERVOIR HEAT CONTENT (10^15 J)	PERCENTAGE OF TOTAL HEAT MINED (%)
0	1.139	1.0414	112.82	0.00
1	1.139	1.0414	111.78	0.92
2	1.139	1.0414	110.74	1.85
3	1.139	1.0414	109.69	2.77
4	1.139	1.0414	108.65	3.69
5	1.139	1.0414	107.61	4.62
6	1.139	1.0414	106.57	5.54
7	1.139	1.0414	105.53	6.46
8	1.139	1.0414	104.49	7.38
9	1.139	1.0414	103.45	8.31
10	1.139	1.0414	102.40	9.23

Fish Farming: 80 °C/ km Resource, No Draw Down

*** SUMMARY OF RESULTS *NO Cogeneration* ***

Electricity breakeven price (cents/kWh)	12.46 (1997 $), **12.55 (2001 $)**			
System configuration:	DOUBLET			
Gradient (deg.C/Km)	80.0			
Well depth (km)	3.94			
Flowrate per production well (kg/s)	32.2			
Reservoir volume per well-pair (M m^3)	146.6			
Variable name	Initial guess	Lower bound	Upper bound	Optimized value
DEPTH	3.000	1.000	3.937	3.937

*** SUMMARY OF RESULTS *Cogeneration**

Electricity breakeven price (cents/kWh)	11.35, **11.43 (2001 $)**			
System configuration:	DOUBLET			
Gradient (deg.C/Km)	80.0			
Well depth (km)	3.94			
Flowrate per production well (kg/s)	32.2			
Reservoir volume per well-pair (M m^3)	146.6			
Variable name	Initial guess	Lower bound	Upper bound	Optimized value
DEPTH	3.000	1.000	3.937	3.937

ECONOMIC PARAMETERS

Fixed Annual Charge Rate Method	
Fixed annual charge rate (%)	15.0
Accrued financing during construction (%)	9.0
Project life (years)	20.0
Capacity factor (%)	90.0

ENGINEERING PARAMETERS

Well depth (km)	3.94
Well deviation from vertical (degrees)	0.0
Wellbore length (km)	3.94
Water loss rate (%)	2.00
System configuration:	DOUBLET
Pump efficiency (%)	80.0
Injection temperature (deg. C)	22.5
Production Well Temperature Drop (deg.C)	15.0
Flowrate per production well (kg/s)	32.2
Injection well casing ID (inches)	7.0
Production well casing ID (inches)	7.0

RESOURCE CHARATERISTICS

Maximum reservoir temperature (deg C)	330.0
Number of segments	1
Gradient (deg.C/Km)	80.0

RESERVOIR PARAMETERS

The drawdown parameter model is used	
Circular fractures with known diameter are used	
Area of the fracture (M m^2)	0.102
Well separation (m)	360.0
The reservoir volume per well-pair is calculated	
The fracture separation and the number of fractures per well-pair are input variables	
Reservoir volume per well-pair (M m^3)	146.6
Fracture separation (m)	60.0
Number of fractures per well-pair	25.0
Impedance per fracture (GPa/m^3/s)	1.57
Well bottom temperature (deg. C)	330.0
Reservoir top temperature (deg. C)	214.8

CAPITAL COSTS (K$)

Drilling and completion costs	9875.91
Stimulation costs	3866.45
Surface power plant costs	4927.66
Fluid distribution costs	1210.73
Exploration costs	7013.86
Total capital costs	26894.60
Annualized capital costs	4397.27

OPERATING AND MAINTENANCE COSTS (K$/yr)

Wellfield maintenance costs	363.55 ***($ 0 with cogeneration)***
Power plant maintenance costs	309.41 ***($ 220.96 K with cogeneration)***
Water costs	9.80
Total operating and maintenance costs	682.76 ***($ 231.76 K with cogeneration)***

POWER GENERATION RESULTS

Initial geofluid availability (MWe/kg/s)	0.270
Initial practical availability (MWe/kg/s)	0.161
Initial net power generation(MWe/kg/s)	0.161
Overall geofluid pressure drop (psia)	-515.
Injection well pressure drop (psia)	77.
Reservoir pressure drop (psia)	293.
Production well pressure drop (psia)	93.

Buoyancy correction (psia) 979.
Pumping power/ Net installed power (%) 0.0

****
POWER GENERATION PROFILE
****

YEAR	THERMAL DRAWDOWN	GEOFLUID TEMPERATURE (degrees Celsius)	PUMP POWER (MW)	NET POWER (MW)	FIRST LAW EFFICIENCY (%)
0	1.0000	257.40	0.0000	5.1730	15.6346
1	1.0000	257.40	0.0000	5.1730	15.6346
2	1.0000	257.40	0.0000	5.1730	15.6346
3	1.0000	257.40	0.0000	5.1730	15.6346
4	1.0000	257.40	0.0000	5.1730	15.6346
5	1.0000	257.40	0.0000	5.1730	15.6346
6	1.0000	257.40	0.0000	5.1730	15.6346
7	1.0000	257.40	0.0000	5.1730	15.6346
8	1.0000	257.40	0.0000	5.1730	15.6346
9	1.0000	257.40	0.0000	5.1730	15.6346
10	1.0000	257.40	0.0000	5.1730	15.6346

****
* HEAT EXTRACTION PROFILE *
****

YEAR OF MINED	THERMO POWER (MJ/Kg)	HEAT EXTRACTED (10^15 J/Kg)	RESERVOIR HEAT CONTENT (10^15 J)	PERCENTAGE TOTAL HEAT (%)
0	1.028	0.9391	103.84	0.00
1	1.028	0.9391	102.90	0.90
2	1.028	0.9391	101.96	1.81
3	1.028	0.9391	101.03	2.71
4	1.028	0.9391	100.09	3.62
5	1.028	0.9391	99.15	4.52
6	1.028	0.9391	98.21	5.43
7	1.028	0.9391	97.27	6.33
8	1.028	0.9391	96.33	7.23
9	1.028	0.9391	95.39	8.14
10	1.028	0.9391	94.45	9.04

Separation Calculations around Pulp Mill: 30 °C/ km Resource, Flashed at 147 °C

$m_{total} = m_{gas} + m_{liq}$

and

$m_{total} \cdot H_l(T_{in}) = m_{gas} \cdot H_v + m_{liq} \cdot H_l$

m_{gas30} = 75 (870 - 619)/2123 = 8.87 Kg/s 0r 31,032 Kg/ hr

m_{liq} = 66.13 Kg/s

Separation Calculations around Pulp Mill: 50 °C/ km Resource, Flashed at 147 °C

$m_{total} = m_{gas} + m_{liq}$

and

$m_{total} \cdot H_l(T_{in}) = m_{gas} \cdot H_v + m_{liq} \cdot H_l$

m_{gas30} = 75 (1124 - 619)/2123 = 17.8 Kg/s

m_{liq} = 57.2 Kg/s

Separation Calculations around Pulp Mill: 80 °C/ km Resource, Flashed at 147 °C

$m_{total} = m_{gas} + m_{liq}$

and

$m_{total} \cdot H_l(T_{in}) = m_{gas} \cdot H_v + m_{liq} \cdot H_l$

m_{gas30} = 75 (900 - 619)/2123 = 9..93 Kg/s

m_{liq} = 65.07 Kg/s

Pulp Mill: 30 °C/ km Resource, No Draw Down, Cogeneration

Net Total Capital Cost	=	Gross Capital Cost	–	Cogenerative Savings NPV
$ 27.6 M	=	$ 95.1 M	-	$ 67.5 M

Enter $ 27.6 M as total Capital Cost

Pulp Mill: 50 °C/ km Resource, No Draw Down, Cogeneration

Net Total Capital Cost	=	Gross Capital Cost	–	Cogenerative Savings NPV
- $ 10.25 M	=	$ M 57.244	-	$ 67.5 M

The $ 10.25 M Capital gain is amortized over 20 years and deducted from the yearly operating expense:

A	=	$10.25M \times 0.15/[1 - 1/(1.15)^{20}]$
A	=	$ 1.637 M

Net Total Annual O. Cost	=	Gross Annual O. Cost	–	Remaining Saving Annuities
- $ 0.959 M	=	$ 0.678 M	-	$ 1.637 M

This savings is then divided by the total KWh per year produced considering the 90 % capacity factor to give the effective busbar cost. (a negative number in this case).

District and Space Heating Energy Demand

$$\frac{\text{(Total annual energy used)}}{\text{(Heating value of a barrel No.2) x (boiler efficiency)}} \qquad \textbf{(5.23)}$$

For District Heating:

=	(810.2 TJ)/(5.486 GJ)x(0.80)
=	184,606 barrels for District Heating
@ $40/barrel:	$ 7,384,000 (2001 Dollars)
	$ 5,340,000 (1997 Dollars) per annum

For Space Heating:

=	(199.7 TJ)/(5.486 GJ)x(0.80)
=	45,502 barrels for Space Heating
@ $40/barrel	$ 1,820,000 (2001 Dollars)
	$ 1,316,000 (1997 Dollars) per annum

A Net present Value of the savings caused by these 20 annuities is needed to offset data in the EGS Model. These are calculated as follows:

NPV savings for district Heating = $5.34M[1-1/(1+0.15)^{20}]/0.15$

= **$ 33,425,000 (1997 Dollars)**

NPV savings for Space Heating = $1.316M[1-1/(1+0.15)^{20}]/0.15$

= **$ 8,237,000 (1997 Dollars)**

Chapter 6

Gradient	MW_{th}	MWe	MW_{th}/MW_e	Busbar Cost	Increase in Cycle Efficiency
30	2.04	3	0.68	67	8.90%
30	6.33	3.94	1.61	51	3.30%
30	21.5	1.07	20.09	171	8.90%
30	25.61	11.36	2.25	33	31.20%
50	2.04	6.26	0.33	20	6.30%
50	6.33	8.39	0.75	14.4	8.90%
50	25.61	21.01	1.22	6	6.30%
50	43.1	1.16	37.16	1.53	22.50%
80	2.04	5.7	0.36	11.4	7.70%
80	6.33	6.86	0.92	7.86	0.10%
80	24	1.25	19.20	-8.35	7.70%
80	25.61	17.84	1.44	2.88	24.80%

Table showing range of heat to electric power ratios for cases studies